NREL
NATIONAL RENEWABLE ENERGY LABORATORY

Voltage Impacts of Utility-Scale Distributed Wind

A. Allen
National Renewable Energy Laboratory

NREL is a national laboratory of the U.S. Department of Energy
Office of Energy Efficiency & Renewable Energy
Operated by the Alliance for Sustainable Energy, LLC

This report is available at no cost from the National Renewable Energy Laboratory (NREL) at www.nrel.gov/publications.

Technical Report
NREL/TP-5D00-61825
September 2014

Contract No. DE-AC36-08GO28308

NREL
NATIONAL RENEWABLE ENERGY LABORATORY

Voltage Impacts of Utility-Scale Distributed Wind

A. Allen
National Renewable Energy Laboratory

Prepared under Task Nos. WE11.0835 and WE14.8D01

NREL is a national laboratory of the U.S. Department of Energy
Office of Energy Efficiency & Renewable Energy
Operated by the Alliance for Sustainable Energy, LLC

This report is available at no cost from the National Renewable Energy Laboratory (NREL) at www.nrel.gov/publications.

National Renewable Energy Laboratory
15013 Denver West Parkway
Golden, CO 80401
303-275-3000 • www.nrel.gov

Technical Report
NREL/TP-5D00-61825
September 2014

Contract No. DE-AC36-08GO28308

NOTICE

This report is available at no cost from the National Renewable Energy Laboratory (NREL) at www.nrel.gov/publications.

Available electronically at http://www.osti.gov/scitech

Available for a processing fee to U.S. Department of Energy and its contractors, in paper, from:

U.S. Department of Energy
Office of Scientific and Technical Information
P.O. Box 62
Oak Ridge, TN 37831-0062
phone: 865.576.8401
fax: 865.576.5728
email: mailto:reports@adonis.osti.gov

Available for sale to the public, in paper, from:

U.S. Department of Commerce
National Technical Information Service
5285 Port Royal Road
Springfield, VA 22161
phone: 800.553.6847
fax: 703.605.6900
email: orders@ntis.fedworld.gov
online ordering: http://www.ntis.gov/help/ordermethods.aspx

Cover Photos: (left to right) photo by Pat Corkery, NREL 16416, photo from SunEdison, NREL 17423, photo by Pat Corkery, NREL 16560, photo by Dennis Schroeder, NREL 17613, photo by Dean Armstrong, NREL 17436, photo by Pat Corkery, NREL 17721.

NREL prints on paper that contains recycled content.

List of Acronyms

ANSI	American National Standards Institute
DG	distributed generation
PV	photovoltaic
RSS	residual sum of squares
WTG	wind turbine generator

Abstract

Although most utility-scale wind turbines in the United States are added at the transmission level in large wind power plants, distributed wind power offers an alternative that could increase the overall wind power penetration without the need for additional transmission. This report examines the distribution feeder-level voltage issues that can arise when adding utility-scale wind turbines to the distribution system. Four of the Pacific Northwest National Laboratory taxonomy feeders were examined in detail to study the voltage issues associated with adding wind turbines at different distances from the sub-station. General rules relating feeder resistance up to the point of turbine interconnection to the expected maximum voltage change levels were developed. Additional analysis examined line and transformer overvoltage conditions.

Table of Contents

List of Figures ..... **vi**
List of Tables ..... **x**
1 Introduction **1**
2 Technical Background **4**
2.1 Software and Feeder Information 4
2.2 Taxonomy Feeder Bus Coordinates 4
2.3 Wind Turbine Details 4
2.4 Feeder Hosting Capacity 5
3 Taxonomy Feeder Analysis Results **6**
3.1 Taxonomy Feeder Selection 6
3.2 Results for Feeder R1-12.47-2 7
3.2.1 Circuit Load Description 7
3.2.2 Circuit Voltage-Regulation Devices 9
3.2.3 Wind Turbine Location Impact—Steady-State Analysis 11
3.2.4 Conclusions for Feeder R1-12.47-2 35
3.3 Results for Feeder R1-12.47-1 35
3.3.1 Circuit Load Description 36
3.3.2 Circuit Voltage-Regulation Devices 37
3.3.3 Wind Turbine Location Impact—Steady-State Analysis 38
3.3.4 Conclusions for Feeder R1-12.47-1 53
3.4 Results for Feeder R4-12.47-1 54
3.4.1 Circuit Load Description 54
3.4.2 Circuit Voltage-Regulation Devices 56
3.4.3 Wind Turbine Location Impact—Steady-State Analysis 57
3.4.4 Conclusions for Feeder R4-12.47-1 69
3.5 Results for Feeder R5-12.47-3 70
3.5.1 Circuit Load Description 70
3.5.2 Circuit Voltage-Regulation Devices 73
3.5.3 Wind Turbine Location Impact—Steady-State Analysis 73
3.5.4 Conclusions for Feeder R5-12.47-3 86
4 Overall Observations: Combining Results From All Feeders **88**
4.1 Overvoltage Limits 88
4.2 Line and Transformer Ratings 91
5 Conclusions **93**
References **95**
Appendix A **99**
Appendix B **113**

List of Figures

Figure 1. Feeder R1-12.47-2. Phase A load distribution 8
Figure 2. Feeder R1-12.47-2. Phase B load distribution 8
Figure 3. Feeder R1-12.47-2. Phase C load distribution 9
Figure 4. Feeder R1-12.47-2. Substation and capacitor bank locations 10
Figure 5. Possible wind turbine connections for feeder R1-12.47-2 11
Figure 6. Feeder R1-12.47-2. Heat map of Phase A per-unit bus voltages with 0 kW of wind power 13
Figure 7. Feeder R1-12.47-2. Heat map of Phase A per-unit bus voltages with 3,000 kW of wind power connected to Bus 17 14
Figure 8. Feeder R1-12.47-2. Heat map of Phase A per-unit bus voltages with 3,000 kW of wind power connected to Bus 183 14
Figure 9. Feeder R1-12.47-2. Phase A voltage profiles without wind and with 3,000 kW of wind power connected to Bus 17 15
Figure 10. Feeder R1-12.47-2. Phase A voltage profiles without wind and with 3,000 kW of wind power connected to Bus 183 15
Figure 11. Feeder R1-12.47-2. Heat map of Phase A change in bus voltage with 3,000 kW of wind power connected to Bus 17 16
Figure 12. Feeder R1-12.47-2. Heat map of Phase A change in bus voltage with 3,000 kW of wind power connected to Bus 183 16
Figure 13. Feeder R1-12.47-2. Heat map of Phase A per-unit bus voltages with 33% of full load and with 0 kW of wind power 17
Figure 14. Feeder R1-12.47-2. Heat map of Phase A per-unit bus voltages with 33% of full-load and with 3,000 kW of wind power 18
Figure 15. Feeder R1-12.47-2. Heat map of Phase A per-unit bus voltages with 33% of full load and with 3,000 kW of wind power 18
Figure 16. Feeder R1-12.47-2. Phase A voltage profiles with 33% of full load without wind and with 3,000 kW of wind power connected to Bus 17 18
Figure 17. Feeder R1-12.47-2. Phase A voltage profiles with 33% of full load without wind and with 3,000 kW of wind power connected to Bus 183 19
Figure 18. Feeder R1-12.47-2. Heat map of Phase A change in bus voltage with 33% of full load and with 3,000 kW of wind power connected to Bus 17 20
Figure 19. Feeder R1-12.47-2. Heat map of Phase A change in bus voltage with 33% of full load and with 3,000 kW of wind power connected to Bus 183 20
Figure 20. Feeder R1-12.47-2. Relationship between maximum change in voltage and distance in km 22
Figure 21. Feeder R1-12.47-2. Relationship between maximum change in voltage and impedance 23
Figure 22. Bus 163, which experiences the maximum voltage change, and the wind turbine locations that cause it—Phase A 25
Figure 23. Bus 183, which experiences the maximum voltage change, and the wind turbine locations that cause it—Phase A 25
Figure 24. Bus 110, which experiences the maximum voltage change, and the wind turbine locations that cause it—Phase B 26
Figure 25. Bus 292, which experiences the maximum voltage change, and the wind turbine locations that cause it—Phase B 26
Figure 26. Bus 248, which experiences the maximum voltage change, and the wind turbine locations that cause it—Phase C 27
Figure 27. Feeder R1-12.47-2. Relationship between max change in voltage and impedance to WTG 28
Figure 28. Maximum wind power that can be tolerated for wind turbine resistance to the substation when only overvoltage limits are considered 30
Figure 29. Line rating exceeded for Phase A 31
Figure 30. Line rating exceeded for Phase B 31
Figure 31. Line rating exceeded for Phase C 31

Figure 32. Line rating not exceeded for Phase A 32
Figure 33. Line rating not exceeded for Phase B 32
Figure 34. Line rating not exceeded for Phase C 32
Figure 35. Transformer MVA ratings for Phase A 33
Figure 36. Transformer MVA ratings for Phase B 33
Figure 37. Transformer MVA ratings for Phase C 33
Figure 38. Tap position for different wind power levels during full load 34
Figure 39. Tap position for different wind power levels during 33% of full load 34
Figure 40. Feeder R1-12.47-1. Phase A load distribution 36
Figure 41. Feeder R1-12.47-1. Phase B load distribution 36
Figure 42. Feeder R1-12.47-1. Phase C load distribution 37
Figure 43. Feeder R1-12.47-1. Substation and capacitor bank locations 38
Figure 44. Possible wind turbine connections for feeder R1-12.47-1 39
Figure 45. Feeder R1-12.47-1. Phase A voltage profiles without wind and with 4,500 kW of wind power connected to Bus 3 40
Figure 46. Feeder R1-12.47-1. Phase A voltage profiles without wind and with 4,500 kW of wind power connected to Bus 594 40
Figure 47. Feeder R1-12.47-1. Heat map of Phase A change in bus voltage with 4,500 kW of wind power connected to Bus 3 41
Figure 48. Feeder R1-12.47-1 Heat map of Phase A change in bus voltage with 4,500 kW of wind power connected to Bus 594 41
Figure 49. Feeder R1-12.47-1 with capacitor bank switches closed. Phase A voltage profiles without wind and with 4,500 kW of wind power connected to Bus 3 42
Figure 50. Feeder R1-12.47-1 with capacitor bank switches closed. Phase A voltage profiles without wind and with 4,500 kW of wind power connected to Bus 594 42
Figure 51. Feeder R1-12.47-1 with control mode set to “static.” Phase A voltage profiles without wind and with 4,500 kW of wind power connected to Bus 3 43
Figure 52. Feeder R1-12.47-1 with control mode set to “static.” Phase A voltage profiles without wind and with 4,500 kW of wind power connected to Bus 594 43
Figure 53. Feeder R1-12.47-1 with control mode set to “static.” Phase B voltage profiles without wind and with 4,500 kW of wind power connected to Bus 3 43
Figure 54. Feeder R1-12.47-1 with control mode set to “static.” Phase B voltage profiles without wind and with 4,500 kW of wind power connected to Bus 594 43
Figure 55. Feeder R1-12.47-1 with control mode set to “static.” Phase C voltage profiles without wind and with 4,500 kW of wind power connected to Bus 3 44
Figure 56. Feeder R1-12.47-1 with control mode set to “static.” Phase C voltage profiles without wind and with 4,500 kW of wind power connected to Bus 594 44
Figure 57. Feeder R1-12.47-1 with control mode set to “static” and low load. Phase A voltage profiles without wind and with 4,500 kW of wind power connected to Bus 3 44
Figure 58. Feeder R1-12.47-1 with control mode set to “static” and low load. Phase A voltage profiles without wind and with 4,500 kW of wind power connected to Bus 594 44
Figure 59. Relationship between Phase C max change in voltage and phase resistance to WTG with 6,000 kW of wind power and 66% load 45
Figure 60. Relationship between Phase A max change in voltage and phase resistance to WTG with 3,000 kW of wind power and 33% load 45
Figure 61. Maximum wind power that can be tolerated for wind turbine resistance to substation when only overvoltage limits are considered 47
Figure 62. Maximum wind power at a bus that does not exceed overvoltage limits 49
Figure 63. Maximum wind power at a bus that does not exceed line ratings for Phase A 50
Figure 64. Maximum wind power at a bus that does not exceed line ratings for Phase B 50
Figure 65. Maximum wind power at a bus that does not exceed line ratings for Phase C 51
Figure 66. Transformer MVA ratings and apparent power for Phase A 52
Figure 67. Transformer MVA ratings and apparent power for Phase B 52
Figure 68. Transformer MVA ratings and apparent power for Phase C 52
Figure 69. Maximum wind power for each wind turbine location that does not exceed line ratings, substation regulator transformer ratings, and overvoltage limits 53

Figure 70. Feeder R4-12.47-1. Phase A load distribution 55
Figure 71. Feeder R4-12.47-1. Phase B load distribution 55
Figure 72. Feeder R4-12.47-1. Phase C load distribution 56
Figure 73. Feeder R4-12.47-1. Substation and capacitor bank locations 57
Figure 74. Possible wind turbine connections for feeder R4-12.47-1 58
Figure 75. Feeder R4-12.47-1. Phase A voltage profiles without wind and with 4,500 kW of wind power connected to Bus 381 59
Figure 76. Feeder R4-12.47-1. Phase A voltage profiles without wind and with 4,500 kW of wind power connected to Bus 46 59
Figure 77. Feeder R4-12.47-1. Heat map of Phase A change in bus voltage with 4,500 kW of wind power connected to Bus 381 60
Figure 78. Feeder R4-12.47-1. Heat map of Phase A change in bus voltage with 4,500 kW of wind power connected to Bus 46 60
Figure 79. Feeder R4-12.47-1. Phase A voltage profiles with 33% of full load without wind and with 4,500 kW of wind power connected to Bus 381 61
Figure 80. Feeder R4-12.47-1. Phase A voltage profiles with 33% of full load without wind and with 4,500 kW of wind power connected to Bus 46 61
Figure 81. Feeder R4-12.47-1. Heat map of Phase A change in bus voltage with 33% of full load with 4,500 kW of wind power connected to Bus 381 61
Figure 82. Feeder R4-12.47-1. Heat map of Phase A change in bus voltage with 33% of full load with 4,500 kW of wind power connected to Bus 46 61
Figure 83. Relationship between Phase A max change in voltage and phase resistance to WTG with 6,000 kW of wind power and 100% load 62
Figure 84. Relationship between Phase B max change in voltage and phase resistance to WTG with 3,000 kW of wind power and 100% load 62
Figure 85. Maximum wind power that can be tolerated for wind turbine resistance to substation when only overvoltage limits are considered 63
Figure 86. Maximum wind power at a bus that does not exceed overvoltage limits 64
Figure 87. Maximum wind power at each bus that does not exceed line ratings for Phase A 65
Figure 88. Maximum wind power at each bus that does not exceed line ratings for Phase B 65
Figure 89. Maximum wind power at each bus that does not exceed line ratings for Phase C 66
Figure 90. Transformer MVA ratings and apparent powerr flows for Phase A 67
Figure 91. Transformer MVA ratings and apparent powerr flows for Phase B 67
Figure 92. Transformer MVA ratings and apparent powerr flows for Phase C 67
Figure 93. Maximum wind power for each wind turbine location that does not exceed line ratings, substation regulator transformer ratings, and overvoltage limits 68
Figure 94. Magnified view of the maximum wind power for each wind turbine location that does not exceed line ratings, substation regulator transformer ratings, and overvoltage limits 69
Figure 95. Feeder R5-12.47-3. Phase A load distribution 71
Figure 96. Feeder R5-12.47-3. Phase B load distribution 71
Figure 97. Feeder R5-12.47-3. Phase C load distribution 72
Figure 98. Location of regulators and capacitor banks for feeder R5-12.47-3 73
Figure 99. Possible wind turbine connections for feeder R5-12.47-3 74
Figure 100. Feeder R5-12.47-3. Phase B voltage profiles without wind and with 4,500 kW of wind power connected to Bus 907 75
Figure 101. Feeder R5-12.47-3. Phase B voltage profiles without wind and with 4,500 kW of wind power connected to Bus 1,054 75
Figure 102. Feeder R5-12.47-3. Heat map of Phase B change in bus voltage with 4,500 kW of wind power connected to Bus 907 76
Figure 103. Feeder R5-12.47-3. Heat map of Phase B change in bus voltage with 4,500 kW of wind power connected to Bus 1,054 76
Figure 104. Feeder R5-12.47-3. Phase B voltage profiles with 33% of full load without wind and with 4,500 kW of wind power connected to Bus 907 77
Figure 105. Feeder R5-12.47-3. Phase B voltage profiles with 33% of full load without wind and with 4,500 kW of wind power connected to Bus 1,054 77

Figure 106. Feeder R5-12.47-3. Heat map of Phase B change in bus voltage with 33% of full load and with 4,500 kW of wind power connected to Bus 907 78
Figure 107. Feeder R5-12.47-3. Heat map of Phase B change in bus voltage with 33% of full load and with 4,500 kW of wind power connected to Bus 1,054 78
Figure 108. Relationship between Phase B max change in voltage and phase resistance to WTG with 33% load and 1,500 kW of wind power 79
Figure 109. Relationship between Phase B max change in voltage and phase resistance to WTG with 33% load and 4,500 kW of wind power 79
Figure 110. Maximum wind power that can be tolerated for wind turbine resistance to substation when only overvoltage limits are considered 80
Figure 111. Maximum wind power at a bus that does not exceed overvoltage limits 81
Figure 112. Maximum wind power at a bus that does not exceed line ratings for Phase A 82
Figure 113. Maximum wind power at a bus that does not exceed line ratings for Phase B 82
Figure 114. Maximum wind power at a bus that does not exceed line ratings for Phase C 83
Figure 115. Locations of voltage regulators in feeder R5-12.47-3 84
Figure 116. Transformer 1 MVA ratings for Phase A 85
Figure 117. Transformer 2 MVA ratings for Phase A 85
Figure 118. Transformer 3 MVA ratings for Phase A 85
Figure 119. Transformer 4 MVA ratings for Phase A 85
Figure 121. Feeder R5-12.47-3. Maximum amount of wind power that can be tolerated at each bus without exceeding overvoltage limits, line ratings, and regulator transformer ratings 86
Figure 122. Summary of the relationship between resistance and max wind power when only overvoltage is considered 88
Figure 123. Exponential curve fit to the relationship between resistance and max wind power when only overvoltage is considered 89
Figure 124. Intersection of different megawatt wind power output levels and the exponential equation describing the relationship between the resistance between the WTG and the substation and the maximum wind power that can be interconnected to the feeder when only overvoltage limits are considered 90
Figure 125. Intersection of different megawatt wind power output levels and the exponential equation describing the relationship between the resistance between the WTG and the substation and the maximum wind power that can be interconnected to the feeder when only overvoltage limits are considered 91
Figure 126. Relationship between the resistance from the WTG bus to the feeder substation and the maximum wind power that can be placed at that bus; no generalization possible 92
Figure 127. Feeder R1-12.47-2. Heat map of Phase B per-unit bus voltages with 0 kW of wind power 99
Figure 128. Feeder R1-12.47-2. Heat map of Phase B per-unit bus voltages with 3,000 kW of wind power connected to Bus 17 100
Figure 129. Feeder R1-12.47-2. Heat map of Phase B per-unit bus voltages with 3,000 kW of wind power connected to Bus 183 100
Figure 130. Feeder R1-12.47-2. Phase B voltage profiles without wind and with 3,000 kW of wind power connected to Bus 17 100
Figure 131. Feeder R1-12.47-2. Phase B voltage profiles without wind and with 3,000 kW of wind power connected to Bus 183 100
Figure 132. Feeder R1-12.47-2. Heat map of Phase B change in bus voltage with 3,000 kW of wind power connected to Bus 17 101
Figure 133. Feeder R1-12.47-2. Heat map of Phase B change in bus voltage with 3,000 kW of wind power connected to Bus 183 101
Figure 134. Feeder R1-12.47-2. Heat map of Phase C per-unit bus voltages with 0 kW of wind power 102
Figure 135. Feeder R1-12.47-2. Heat map of Phase C per-unit bus voltages with 3,000 kW of wind power connected to Bus 17 103
Figure 136. Feeder R1-12.47-2. Heat map of Phase C per-unit bus voltages with 3,000 kW of wind power connected to Bus 183 103

Figure 137. Feeder R1-12.47-2. Phase C voltage profiles without wind and with 3,000 kW of wind power connected to Bus 17 103
Figure 138. Feeder R1-12.47-2. Phase C voltage profiles without wind and with 3,000 kW of wind power connected to Bus 17 103
Figure 139. Feeder R1-12.47-2. Heat map of Phase C change in bus voltage with 3,000 kW of wind power connected to Bus 17 104
Figure 140. Feeder R1-12.47-2. Heat map of Phase C change in bus voltage with 3,000 kW of wind power connected to Bus 183 105
Figure 141. Feeder R1-12.47-2. Heat map of Phase B per-unit bus voltages with 33% of full load and 0 kW of wind power 106
Figure 142. Feeder R1-12.47-2. Heat map of Phase B per-unit bus voltages with 33% of full load and 3,000 kW of wind power connected to Bus 17 107
Figure 143. Feeder R1-12.47-2. Heat map of Phase B per-unit bus voltages with 33% of full load 3,000 kW of wind power connected to Bus 183 107
Figure 144. Feeder R1-12.47-2. Phase B voltage profiles with 33% of full load without wind and 3,000 kW of wind power connected to Bus 17 107
Figure 145. Feeder R1-12.47-2. Phase B voltage profiles with 33% of full load without wind and 3,000 kW of wind power connected to Bus 183 107
Figure 146. Feeder R1-12.47-2. Heat map of Phase B change in bus voltage with 33% of full load and 3,000 kW of wind power connected to Bus 17 108
Figure 147. Feeder R1-12.47-2. Heat map of Phase B change in bus voltage with 33% of full load and 3,000 kW of wind power connected to Bus 183 108
Figure 148. Feeder R1-12.47-2. Heat map of Phase C per-unit bus voltages with 33% of full load and 0 kW of wind power 109
Figure 149. Feeder R1-12.47-2. Heat map of Phase C per-unit bus voltages with 33% of full load and 3,000 kW of wind power connected to Bus 17 110
Figure 150. Feeder R1-12.47-2. Heat map of Phase C per-unit bus voltages with 33% of full load and 3,000 kW of wind power connected to Bus 183 110
Figure 151. Feeder R1-12.47-2. Phase C voltage profiles with 33% of full load without wind and with 3,000 kW of wind power connected to Bus 17 110
Figure 152. Feeder R1-12.47-2. Phase C voltage profiles with 33% of full load without wind and with 3,000 kW of wind power connected to Bus 183 110
Figure 153. Feeder R1-12.47-2. Heat map of Phase C change in bus voltage with 33% of full load and 3,000 kW of wind power connected to Bus 17 111
Figure 154. Feeder R1-12.47-2. Heat map of Phase C change in bus voltage with 33% of full load and 3,000 kW of wind power connected to Bus 183 112

List of Tables

Table 1. Summary of the Examined Taxonomy Feeders* 7
Table 2. Real and Reactive Power of Each Phase Through the Substation 8
Table 3. Maximum Per-Unit Voltages Anywhere on the Feeder with Different Amounts of Wind Power 21
Table 4. Correlation Coefficients r_1 and r_2 for Different Wind and Load Scenarios 23
Table 5. Relationship Between Max Change in Voltage and Impedance to WTG for Varying Amounts of Load and Wind Power 28
Table 6. Maximum Wind Power That Can Be Tolerated for Wind Turbine Resistance to the Substation When Only Overvoltage Limits Are Considered 30
Table 7. Total Real and Reactive Power for Each Phase 36
Table 8. Relationship Between Max Change in Voltage and Phase Resistance to WTG for Varying Amounts of Load and Wind Power 46
Table 9. Maximum Wind Power at a Bus That Does Not Exceed Overvoltage Limits 47
Table 10. Real and Reactive Power for Each Phase Through the Substation 54
Table 11. Relationship Between Max Change in Voltage and Phase Resistance to WTG for Varying Amounts of Load and Wind Power 62
Table 12. Penetration for Each Level of Wind Power When Feeder R4-12.47-1 Is at Full Load 69

Table 13. Real and Reactive Power for the Feeder When Capacitor Banks Are Switched Open and When Regulator Controls Are Turned Off 72
Table 14. Relationship Between Max Change in Voltage and Phase Resistance to WTG for Varying Amounts of Load and Wind Power 79
Table 15. Maximum Resistance Between the WTG and the Substation That a Radial Distribution Feeder Can Tolerate Without Exceeding Overvoltage Limits for Each Megawatt Wind Power Output Level 91
Table 16. Maximum Wind Power for Buses in Feeder R4-12.47-1 113
Table 17. Maximum Wind Power for Buses in Feeder R5-12.47-3 114

1 Introduction

The need for transmission lines to connect remote wind power plants to major load centers is a barrier to increasing the wind power penetration level in North American interconnections. By adding utility-sized megawatt-scale wind turbines to existing distribution networks, the amount of wind power supplied to consumers can be increased without the associated political difficulties and additional cost of building transmission lines. The focus of this work is to assess the limitations on the amount of wind power that can be added to the distribution system without adversely impacting distribution system operations. Although this report gauges the amount of wind power that can be installed within a distribution circuit, the impacts of distributed wind on bulk system operations has been studied in a companion report [1]. The focus of the research presented in this report is to determine where and the number of megawatt-scale wind turbine generators (WTGs) that can be placed within a distribution system without causing sustained overvoltage conditions or exceeding equipment ratings. Similar impact studies and distribution analyses have been performed but instead examined the impact of rooftop photovoltaic (PV) on feeder voltage profiles [2-7]. However, distributed wind differs from rooftop photovoltaic in terms of scale and distribution of the resource. Traditionally, the power available from a distribution-connected wind power plant is fed in at one bus in the distribution circuit, compared to the many locations of distributed rooftop solar power. Other case studies have examined a specific distribution circuit and did not provide general results. The research presented here aims to provide general guidelines for use on a wide array of distribution circuits.

The integration of distributed wind presents some unique issues. Unlike distributed PV, distributed wind is typically concentrated at one location in a feeder. Also, the installations under study in this report are multi-megawatt wind power plants that differ vastly in size and behavior from the multi-kilowatt PV installations more typically installed in a distribution system. This single point of injection for megawatts of power leads to some unique challenges that distribution planners may not foresee. Also, distributed wind has been studied less, because many of the best wind resources in the United States are located far from large population centers [7]. However, many rural areas in the United States have sufficient wind resources to make distributed wind a potential generation option.

Considerable work has been done on the integration of distributed generation (DG) in general [8-12], including work on planning [13] and cost-effectiveness [14]. Reference [8] provided an overview of both the positive and negative impacts that (DG) has on radial distribution systems. The paper focuses on issues of distribution voltage quality, reduction in power loss, and reliability when DG is introduced to an existing system. Reference [9] studied the positive and negative impacts DG has on system reliability and on power quality by using an example feeder and different power quality indices defined in the paper. The paper also described the negative impact DG has on overcurrent protection coordination. Other reliability indices are also suggested to better show the positive impacts DG can have on the frequency and duration of system interruption. The work in [10] considered impacts on reliability and power quality when DG is connected to a medium-voltage system. The impacts are measured using several indices for different network configurations when considering DG, and they can be used to determine the location of the most beneficial DG sites within a feeder. Reference [11] provided a checklist to help engineers quickly evaluate potential DG projects.

There is also a body of prior work in the field of integrating distributed wind into the distribution system in various countries. Some worldwide experiences with real feeders are worthy of note [15-18]. Reference [15] is a German case study that investigated the impact on voltage that occurs when an additional wind turbine is added to an actual medium-voltage distribution network with existing wind turbines. A range of system voltages were identified when one year of measured wind data and simulated low-voltage household load profiles were included in the simulation. Three case studies were included in [17] to examine the system impacts of distribution-connected wind turbines. The cases were completed for National Grid feeders located in the northeastern part of the United States. In [18], case studies within Turkey were examined. Conclusions from this work suggested that multiple wind turbines at a single location could be considered a single plant; hence, the same approach has been taken in this report. Additionally, numerous system studies have been performed on distributed wind integration using simulated test feeders (though some of these have been targeted toward controlling other devices rather than wind turbines) [19, 20]. In this report, simulated test feeders based on taxonomy feeders made available by the Pacific Northwest National Laboratory [21] have been studied.

There are also specific studies that look at one aspect of distributed wind integration, such as impacts on system protection [22, 23]. In this report, quasi-steady-state voltage impacts have been predominantly considered; however, current and transient voltages can also be primary limiting factors. Power quality impacts of DG (wind, PV, and others) have received attention [24-26]. Studies on faults have also been conducted for systems with DG [27-29]. These papers have been mostly concerned with voltage sag during a fault event; however, in this report the main concern is steady-state voltage rise. Voltage rise as a result of DG has been studied before and has been identified as an issue for the integration of DG [30-35]. In [32], real distribution system data was used to show that the introduction of embedded generation to a weak feeder will cause the voltage to rise above the allowable range. The paper also examined using embedded generation to control voltage. Reference [35] considered how varying system conditions—such as conductor size, wind power output, and voltage compensation techniques—impact feeder voltages. The paper also showed that an extremely weak and a lightly loaded feeder with smaller conductor sizes creates difficult conditions to control voltage magnitude on the feeder. The research in [30, 31, 33, 34] also recognize the impact DG has on voltage rise in distribution feeders and provided a variety of solutions to mitigate voltage rise.

However, none of these papers provided a generalized quantitative rule describing system conditions that impact voltage rise. The research presented in this report describes the measurement and estimation of voltage rise and provides a general quantitative rule for the placement of distributed wind turbines within a feeder based on American National Standards Institute (ANSI) voltage rise limits. The rule presents a straightforward relation between the amount of wind power that can be connected to a radial distribution system at a particular bus and the resistance between that bus and the substation, assuming that steady-state voltage is the limiting factor. A novel feature of the work presented in this report is that we consider Type 3 (doubly-fed induction generator) and Type 4 (full-power-converter) wind turbines for inclusion in the distribution feeders; however, we currently consider only a unity power factor. These machines are typically used for transmission-connected wind power plants. These machines offer more flexibility with respect to power factor control than the Type 1 (fixed-speed, directly connected) and Type 2 (variable-rotor-resistance) machines that have been included in

distribution systems in the past. Additionally, in this work we study the single-point injection of power rather than the injection of power by wind turbines at multiple locations along a feeder.

Megawatt-scale wind turbines connected to the distribution circuit are generally located away from heavily-populated areas; therefore the impact that megawatt-scale wind turbines will have on rural distribution feeders in particular is studied. Characteristics of rural distribution feeders differ from more-heavily-populated and -loaded urban and suburban areas. Rural distribution feeders tend to be radial, have longer feeder lengths, and are relatively lightly loaded; therefore, the steps taken to determine general guidelines require that limits be established for a few select distribution feeders located in rural areas. Common limits that occur in these feeders are used to provide general guidelines for the placement and amount of wind power that can be connected to a distribution circuit. The distribution feeders studied come from 24 Pacific Northwest National Laboratory distribution taxonomy feeders available in GridLAB-D.

2 Technical Background

2.1 Software and Feeder Information

Open Distribution System Software (OpenDSS) [36] and MATLAB [37] were used to conduct the research presented in this report. OpenDSS is an electric power distribution system simulator used extensively for distributed resource integration studies. The COM interface [38] is used to run OpenDSS commands using MATLAB and allows for looping and automation. It is more efficient to run hundreds of simulations sequentially in batch mode using the COM interface than it is to execute the OpenDSS script in the stand-alone graphical user interface. For example, for each loop iteration a wind turbine can be placed at a selected bus within the distribution circuit, the circuit power flow solution solved, and the voltage information extracted. For the next loop iteration, the same process is repeated with the wind turbine located at a different bus, and so on, until all desired wind turbine locations have been analyzed.

The analysis described is applied to a variety of feeders from the 24 Pacific Northwest National Laboratory distribution taxonomy feeders [21] available in GridLAB-D [39]. However, the taxonomy feeders were first converted to OpenDSS format. A software tool that converts the electrical distribution system model data from GridLAB-D format to OpenDSS format was created for this project and will soon be publically available for download. The software is structured such that properties for each instance of a GridLAB-D object are collected for all objects in the taxonomy feeder file and then operated on via syntax or mathematical conversions to create a corresponding OpenDSS element, associated DSS file, and master circuit file. For example, many GridLAB-D power system objects have exact equivalents in OpenDSS, such as power delivery elements (overhead and underground lines and transformers) and power conversion elements (loads, generators, and capacitor banks). Other objects in GridLAB-D, such as triplex loads and split-phase transformers, are not unique elements in OpenDSS and had to be created using the load and transformer elements. The converted models were run and the results were validated against the GridLAB-D model power flows. The voltage profiles, total loads from each phase, and line impedances from each model were compared, and the converted OpenDSS feeders were found to accurately represent the GridLAB-D models.

2.2 Taxonomy Feeder Bus Coordinates

The taxonomy feeders [21] did not include bus coordinates used to visualize the layout of the feeders. The bus coordinates were taken from [40], which provided an arbitrary spatial layout. A MATLAB subroutine was written to extract the coordinates (located in DOT files that contain the “Attributed DOT Format” text) and rewritten to a text file containing the bus name, the x-coordinate of the bus, and the y-coordinate of the bus. This text file format is used by OpenDSS to define bus x, y coordinates. Plots of the circuits within the report were generated using subroutines written in MATLAB.

2.3 Wind Turbine Details

Four typical WTG model types are used for power flow representations of wind power plants, as described in [41]. The Western Electricity Coordinating Council standard Type 1 and Type 2 models, also known as fixed-speed and variable-slip WTGs, respectively, represent WTGs with capacitor bank controls to supply reactive power to the WTG. Western Electricity Coordinating Council standard Type 3 and Type 4 WTGs, also known as doubly-fed asynchronous and full-

power-converter generators, respectively, have power electronic controls that allow for power factor control or voltage control at the terminals. In this paper, a combined Type 3/Type 4 WTG model was used, because most megawatt-scale modern WTGs are either Type 3 or Type 4. For the research presented here, the active power factor controls for the generator models representing the Type 3/Type 4 WTGs were set so that the power factor at the WTG terminals was held at unity (i.e., the power factor is equal to 1.0). The three-phase rating of the wind turbine used is 1.5 MW.

Possible WTG locations considered for all distribution circuits studied in this report are selected based on two conditions: the first is that the wind turbine must be connected to a bus that is connected to three-phase lines, and the second is that the wind turbine must be at least 0.1 km from the substation. All buses in the circuit that meet these conditions are studied as possible wind turbine locations.

2.4 Feeder Hosting Capacity

The hosting capacity of the circuit will be determined by a variety of factors, including transient voltage issues, current limitations, and protection and coordination issues. The central factor considered in this report is sustained overvoltage. When generation is added to distribution circuits, the voltage magnitude can increase for end users and could result in sustained overvoltages that exceed overvoltage limits. The national standards for utilization voltage ratings are described in the American National Standard for Electric Power System and Equipment—Voltage Ratings (60 Hertz) (ANSI C84.1-2011) [42] and establish voltage tolerances for end users. From the standard, the Range A utilization voltage is used as the overvoltage limit. For this voltage range, 125 V on a 120-V base is permitted and is an approximate 0.042 per-unit increase from nominal voltage. For the current research, the hosting capacity for distribution circuits will limit wind power so that voltage rise does not exceed this rating.

Equipment ratings are other factors that are considered when determining the location and maximum amount of wind power that can be connected to each distribution feeder. The equipment ratings that are considered are the line ratings for overhead and underground lines and voltage-regulating transformer MVA ratings. The ratings are for continuous operation and do not consider momentary overcurrents caused by system conditions such as faults.

3 Taxonomy Feeder Analysis Results

This report describes the analysis as applied to all of the taxonomy feeders under study. For the analysis, the solution mode for OpenDSS is set to snapshot. Static or single steady-state snapshot mode calculates voltages and currents at every point in the distribution system based on a specified loading condition [43], i.e., time series data such as load profiles are not used in snapshot solution mode. This provides a conservative view of hosting capacity, because adding load will serve to increase the hosting capacity. In this mode, a single power flow solution at the selected load level is calculated, and the voltages from all buses in the circuit are extracted. An initial base case is run before a wind turbine is placed on the distribution circuit. For this initial power flow solution, the circuit characteristic data are extracted and the bus voltages are saved. The circuit characteristics do not change between each case except for the addition of a wind turbine or wind turbines.

The next step is to place a wind turbine at each of the selected wind turbine locations and to find the power flow solutions for each location. As described earlier in Section 2.3, the COM interface using MATLAB is used. After a wind turbine is placed at a three-phase bus within the circuit, the power flow solution is found and the bus voltages, power, and current are recorded. This is done for every possible wind turbine location. The bus voltages for the base case with no wind turbines can now be compared to bus voltages at different wind turbine locations. In the analysis, the wind power output is set to multiples of 1.5 MW, and the controls for all voltage-regulating devices are turned off. The capacitor bank controls are turned off and the capacitor banks are switched open so that sustained system conditions could be studied under different load and wind power conditions. When overvoltage conditions are studied, low-load conditions (33% of peak load) are used to create a worst-case scenario. During low-load conditions, the voltage drop would be low and capacitor banks would already be in their open state. Setting the capacitor banks open ensures consistency throughout the entire study. The voltage-regulator controls are also turned off for changes in voltage calculations. Changes in feeder bus voltages may be exaggerated if the tap position of the voltage regulator is different among cases without wind and with wind. Another reason for not including voltage-regulator controls is that the taxonomy feeder data did not include line-drop compensation, which would allow for better regulation of bus voltages.

The analyzed feeders were selected based on shared feeder characteristics and on feeder characteristics that are representative of feeders to which wind turbines would be connected. An overview of the taxonomy feeders analyzed and the feeder characteristics are given in Section 3.1. The results of the analysis for each of the taxonomy feeders are presented in Sections 3.1 to 3.4.

3.1 Taxonomy Feeder Selection

The Pacific Northwest National Laboratory created 24 taxonomy feeders that represent typical radial distribution feeders found in 5 different climate regions located within the contiguous United States. The representative feeders for each of the climate regions were selected based on common characteristics obtained from actual distribution feeder data. The feeder data was taken from 575 feeder models from 17 utilities. A detailed description of how the taxonomy feeder classification was accomplished can be found in [21].

It is likely that wind turbines connected to distribution feeders will be located in rural regions; therefore, the feeders that were first analyzed are feeders described as either containing a rural area or representing a rural area. Seven feeders fit this description. A summary of these feeders is given in Table 1, along with the feeder climate region, voltage level, and load size in megawatts according to the taxonomy report. The majority of the taxonomy feeders are at a voltage level of 12.47 kV; however, because some of the representative feeders serve a lightly populated region that covers a wide geographical area, the voltage level is higher (either at 34.5 kV or 24.9 kV) [21].

Table 1. Summary of the Examined Taxonomy Feeders*

Feeder	Climate Region	Feeder Voltage (kV)	Load MW [22]	Description
R1-12.47-2	**1**	**12.47**	**2.83**	**Moderate suburban and light rural**
R1-12.47-1	**1**	**12.47**	**7.15**	**Moderate suburban and rural**
R1-25.00-1	1	24.9	2.1	Light rural
R2-35.00-1	2	34.5	8.9	Light rural
R4-12.47-1	**4**	**12.47**	**5.5**	**Heavy urban with rural spur**
R4-25.00-1	4	24.9	0.95	Light rural
R5-12.47-3	**5**	**12.47**	**9.2**	**Moderate rural**

*Results of the analysis are presented for the feeders shown in bold.

Feeder R1-25.00-1 was the first higher voltage feeder examined. The feeder consists of many underground cables, and the reactive power supplied by these cables boosts the voltage levels, especially during low-load conditions, because the reactive power supplied by these cables stays the same whether the system is at full load or lightly loaded. In the case of this feeder, the voltage rise is especially pronounced in phases A and C. As a result, the power factor at the substation for Phase A is -0.5, and for Phase C it is -0.3 (strongly capacitive); whereas for Phase B it is -0.96 (mildly capacitive). For Phase C, the phase with the most extreme capacitive power factor, the voltage rise exceeds ANSI overvoltage limits even without wind in the system; therefore, wind cannot be added. Thus, this feeder has not been included in the analysis for deriving general rules. Similar conditions were observed for feeders R2-35.00-1 and R4-25.00-1; therefore, the feeders that are used in the overall results section are at a voltage level of 12.47 kV. Results for each of the feeders shown in bold in Table 1 are provided in the sections below.

3.2 Results for Feeder R1-12.47-2

The first taxonomy feeder that is analyzed is feeder R1-12.47-2. The taxonomy feeder is located in a mix of suburban and rural populated areas and consists of approximately 70% overhead lines and 30% underground lines [44]. The following sections provide circuit details and steady-state analysis results for feeder R1-12.47-2.

3.2.1 Circuit Load Description

This section describes the load for feeder R1-12.47-2. Table 2 below shows the real, reactive, and apparent power through the substation bus for each phase. From [42], the feeder is located in a moderately populated suburban and lightly populated rural area. The total circuit loading is low because of the sparse rural loading, and it has 272 customers.

Table 2. Real and Reactive Power of Each Phase Through the Substation

Phase	kW	kVar	kVA
Phase A	874.22	22.50	874.51
Phase B	817.82	15.81	817.97
Phase C	1,163.08	36.08	1,163.64
Total	2,855.12	74.39	2,856.09

The rural load is fed through a long primary circuit in which the majority of the load is located far from the substation, as shown in Figure 1 to Figure 3. The solid lines represent the three-phase primary circuit, and the dashed line represents single- or two-phase laterals. Load distributions for each phase are also shown in Figure 1 to Figure 3. The substation location is indicated in Figure 1 to Figure 3.

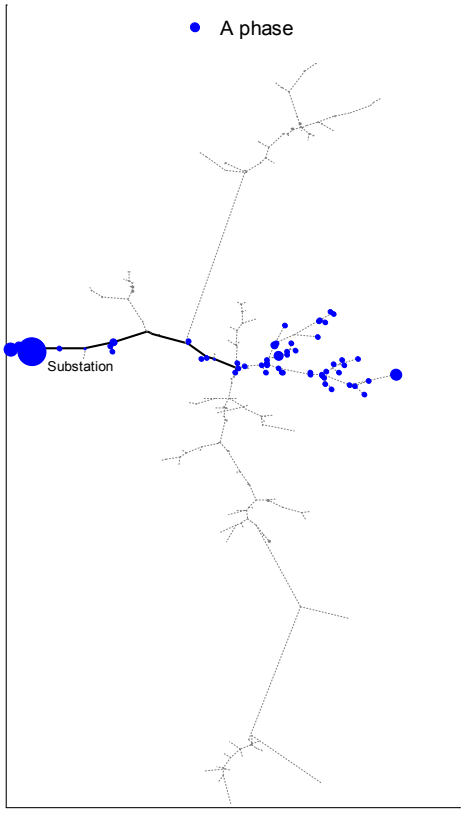

Figure 1.
Feeder R1-12.47-2. Phase A load distribution

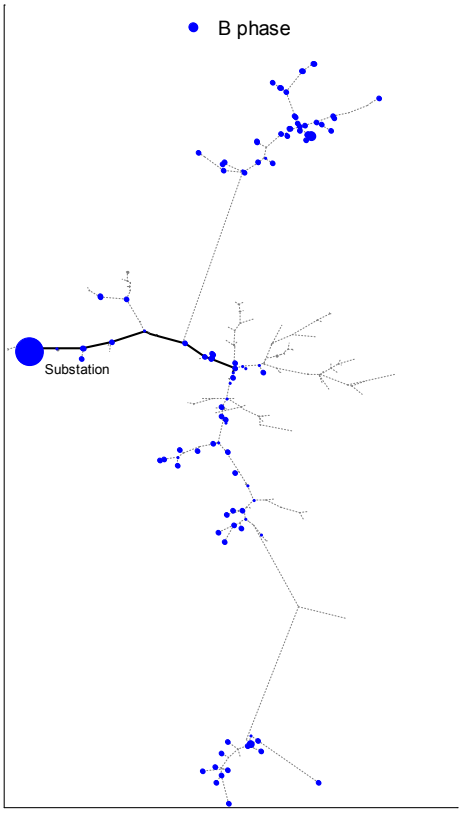

Figure 2.
Feeder R1-12.47-2. Phase B load distribution

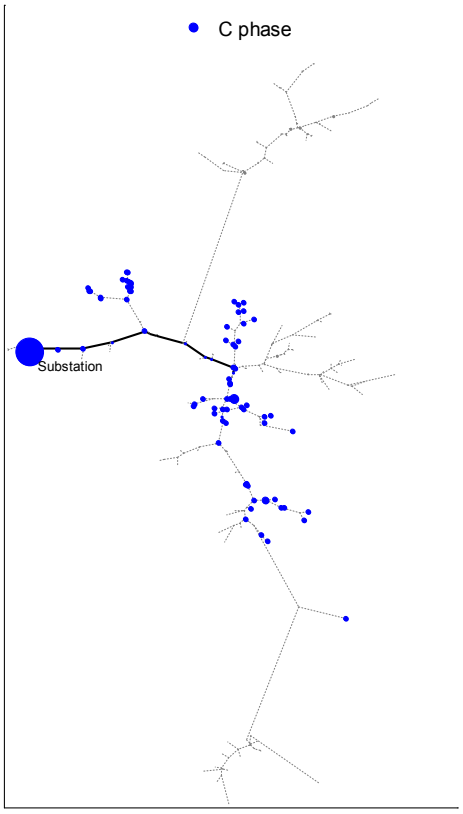

Figure 3.
Feeder R1-12.47-2. Phase C load distribution

To create low-load conditions, all loads attached to the circuit will be uniformly scaled to a fraction (33%) of the total load. This is done using the *LoadMulti* command in OpenDSS.

3.2.2 Circuit Voltage-Regulation Devices

The circuit has one capacitor bank and one step-voltage regulator located at the substation. The locations of these devices are shown in Figure 4. The capacitor bank is switched to its open position for all of the analysis, because overvoltage rather than undervoltage is being examined.

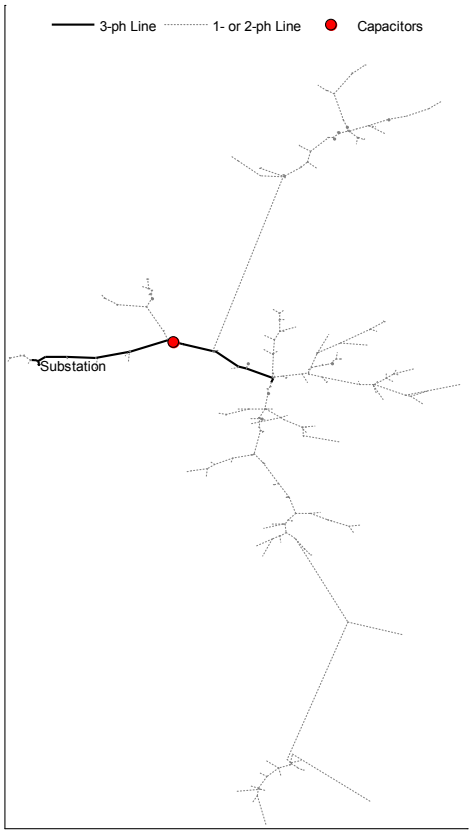

Figure 4.
Feeder R1-12.47-2. Substation and capacitor bank locations

The step-voltage-regulator controls provided do not implement line-drop compensation and only utilize the voltage across the controlled winding. This type of voltage regulation does not change with varying load. Therefore, the only influence the system has on tap changes is the change in voltage at the bus of the controlled winding. Because this regulator is located near the substation, the monitored voltage does not change and the variation in load and wind power outputs do not have an influence. By including line-drop compensation, the current through the substation is monitored and the regulator taps are adjusted according to the current. The controls for a line-drop compensator (which would need input from a current transformer as well as impedance settings) were not included in the original GridLab-D (.glm) file. Therefore, regulator controls with line-drop compensation are added to the circuit. The new regulator controls are given below:

```
New regcontrol.feeder_reg_cfg transformer=R1-12-47-2_reg_1 winding=2
vreg=123.0 band=3.0 ptratio=60 CTprim=200 R=2 X=0 delay=5
```

The values for CTprim, R, and X are selected from another circuit and may be changed in the future. For now, these new controls are used in the analysis.

3.2.3 Wind Turbine Location Impact—Steady-State Analysis

Steady-state analysis or snapshot mode is used for the analysis in this section. The impacts that wind power from each possible wind turbine location have on the bus voltages, current flows, and power flows are examined. If these values exceed ANSI C84.1-2011 Range A, then either the number of wind turbines must be reduced or the location of a wind turbine must be altered.

Figure 5 shows each of the possible wind turbine locations for the circuit and the bus number for feeder R1-12.47-2. The method used to describe the selection of possible wind turbine locations is described in Section 2.3.

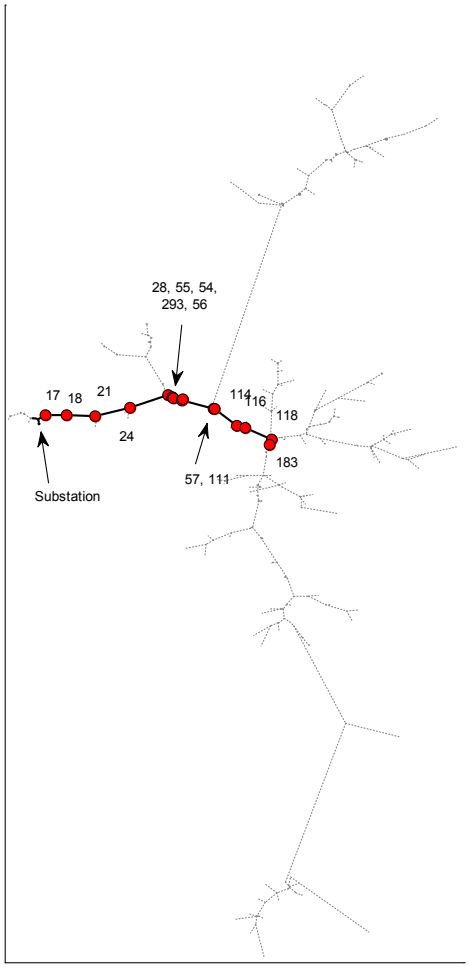

Figure 5.
Possible wind turbine connections for feeder R1-12.47-2

Two different scenarios are studied for this circuit. In both cases, the controls for all voltage-regulation devices are turned off. The capacitor banks are left open, and all voltage regulators are set to tap position 0. For the first case, the load is left at full load; for the second case, the load is

dropped to 33% of full load. The low-load level of 33% was selected based on the lowest normalized value taken from an example distribution system load profile.

3.2.3.1 Steady-State Analysis I—Overvoltage Limits

The steady-state voltage analysis compares the voltages at every bus in the circuit to two scenarios: before wind turbines are added to the circuit and after wind turbines are added to the circuit. The changes that occur to bus voltages are shown below. Because the distribution feeder consists of three phases with some single-phase laterals, the bus voltages are separated by phase. The changes in Phase A voltages are shown below. Phases B and Phase C voltages are shown in the appendix.

Figure 6 shows the per-unit bus voltages for Phase A during full-load and zero wind power conditions. Each Phase A bus voltage is displayed on the circuit; the color indicates its per-unit voltage according to the color bar on the right. In this figure, the voltage is higher near the substation and drops along the feeder the farther the bus is from the substation.

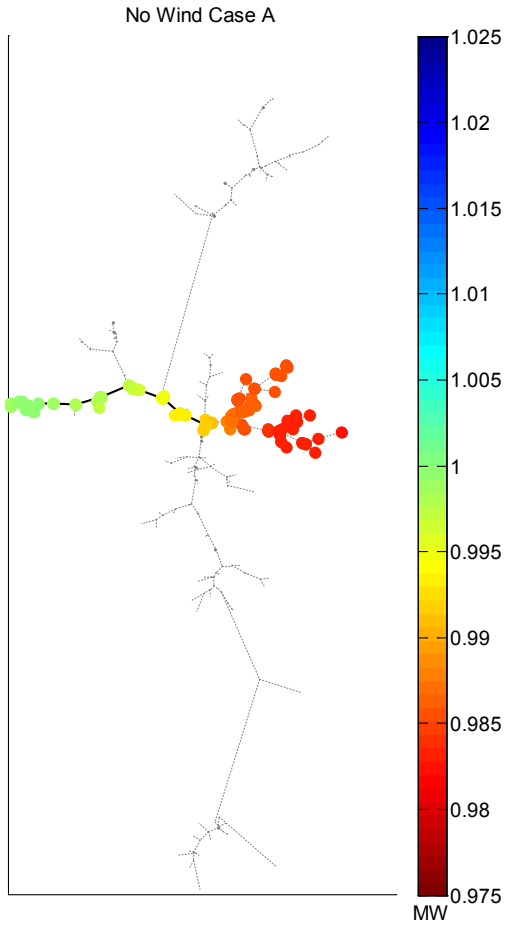

Figure 6.
Feeder R1-12.47-2. Heat map of Phase A per-unit bus voltages with 0 kW of wind power

Next, the bus voltages are calculated for each possible wind turbine location indicated in Figure 5. The wind turbine locations that caused the largest change in voltage and the smallest change in voltage are identified. The largest change occurs when wind turbines are added to Bus 183, and the smallest changed occurs when wind turbines are added to Bus 17. Figure 7 and Figure 8 show Phase A bus voltages when two 1.5-MW wind turbines are added to the feeder at these buses. Figure 7 shows the wind turbines connected to Bus 17, located near the substation. Figure 8 shows the wind turbines connected to Bus 183, located farthest from the substation. The voltage profile for each case is shown in Figure 9 and Figure 10. The voltage profiles for the cases with wind turbines connected to Bus 17 and with wind turbines connected to Bus 183 (shown in black) are compared to the voltage profile when no wind turbines are connected to the feeder (shown in blue). The larger change in voltage occurs when the wind turbines are located farthest from the substation at Bus 183, as shown in Figure 10.

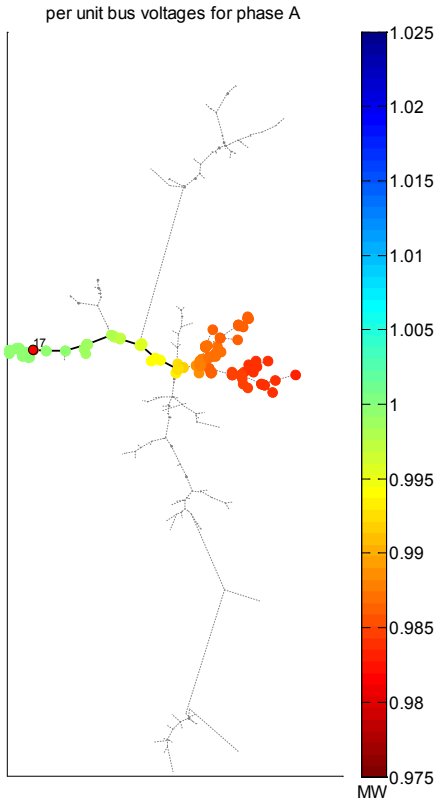

Figure 7.
Feeder R1-12.47-2. Heat map of Phase A per-unit bus voltages with 3,000 kW of wind power connected to Bus 17

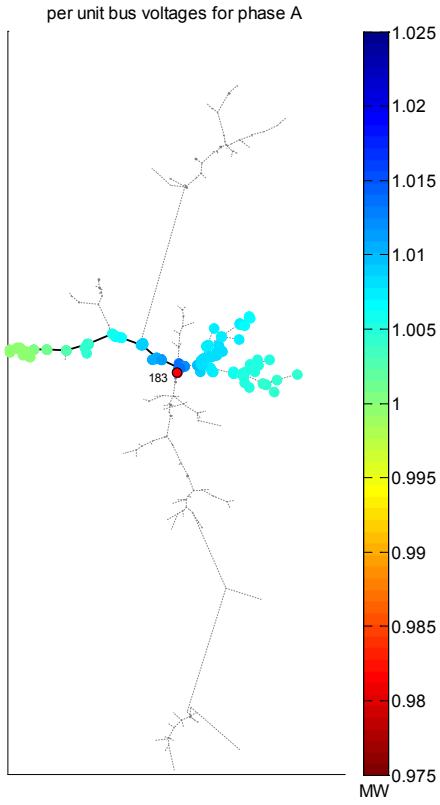

Figure 8.
Feeder R1-12.47-2. Heat map of Phase A per-unit bus voltages with 3,000 kW of wind power connected to Bus 183

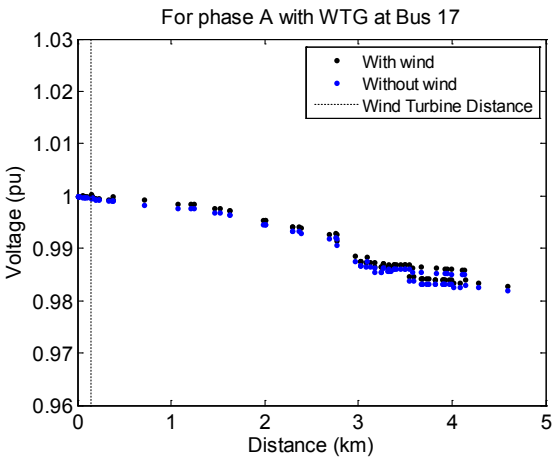

Figure 9.
Feeder R1-12.47-2. Phase A voltage profiles without wind and with 3,000 kW of wind power connected to Bus 17

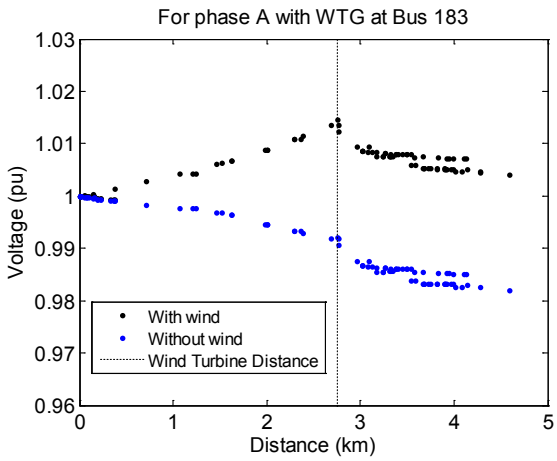

Figure 10.
Feeder R1-12.47-2. Phase A voltage profiles without wind and with 3,000 kW of wind power connected to Bus 183

The next step is to examine the change in voltage that occurs at each bus in the feeder when a wind turbine or turbines are connected to the feeder. The percent change in voltage for each bus is calculated using the equation below.

$$\Delta V_{BusX} = (V_{WindBusX} - V_{noWindBusX})/(V_{noWindBusX}) * 100$$

In the equation, ΔV_{BusX} is the percent change in voltage for Bus X, $V_{WindBusX}$ is the voltage at Bus X when a wind turbine or wind turbines are connected to the circuit, and $V_{noWindBusX}$ is the voltage at Bus X before a wind turbine or wind turbines are connected to the circuit. The percent change in voltage is calculated for all buses in the circuit.

The percent change in voltage when wind turbines are added to Bus 17 is shown in the heat map in Figure 11, and the change in voltage when wind turbines are added to Bus 183 is shown in the heat map in Figure 12. The figures again show that the voltage change is greater when the wind turbines are located farther from the substation. Figure 12 also shows that the greatest change in voltage occurs downstream from the wind turbine location at Bus 183, or along the single-phase laterals. Similar patterns occurred in Phase B and Phase C voltages.

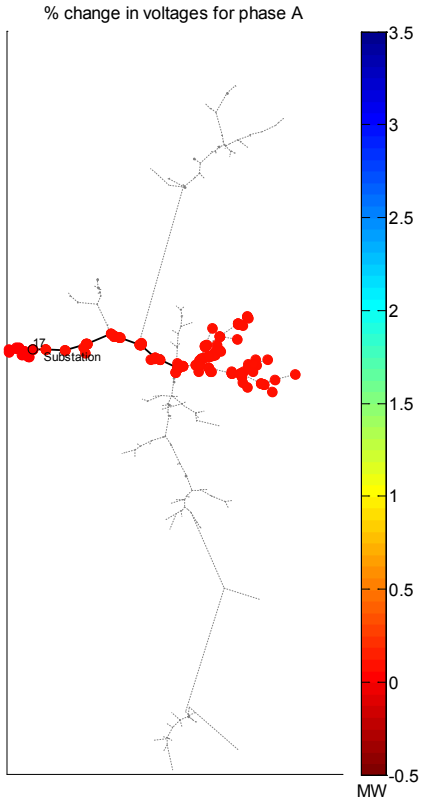

Figure 11.
Feeder R1-12.47-2. Heat map of Phase A change in bus voltage with 3,000 kW of wind power connected to Bus 17

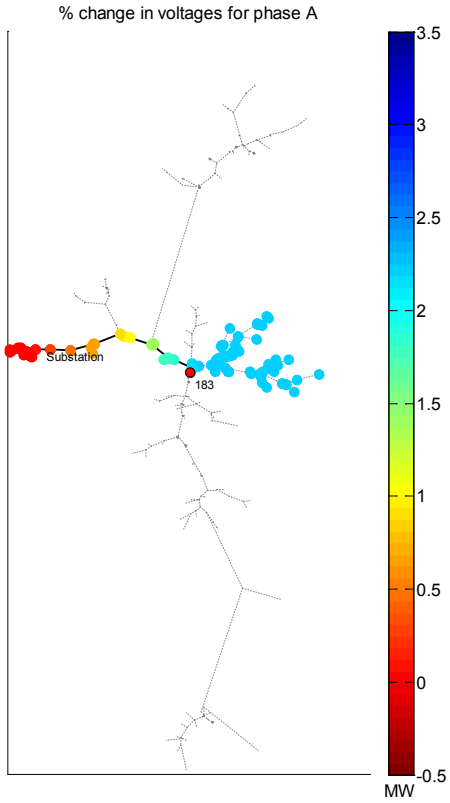

Figure 12.
Feeder R1-12.47-2. Heat map of Phase A change in bus voltage with 3,000 kW of wind power connected to Bus 183

The same analysis is applied when the load is uniformly reduced to 33% of full load. Figure 13 shows the Phase A per-unit bus voltages without wind turbines connected to the feeder. The per-unit voltage is much higher when the load is reduced, and there is less voltage drop across the feeders and laterals. When the load is reduced, the voltage at the end of the laterals is at 0.995 per unit, compared to below 0.98 per unit with full load. Wind turbines are now added to the circuit to test if bus voltages will increases above the full-load cases.

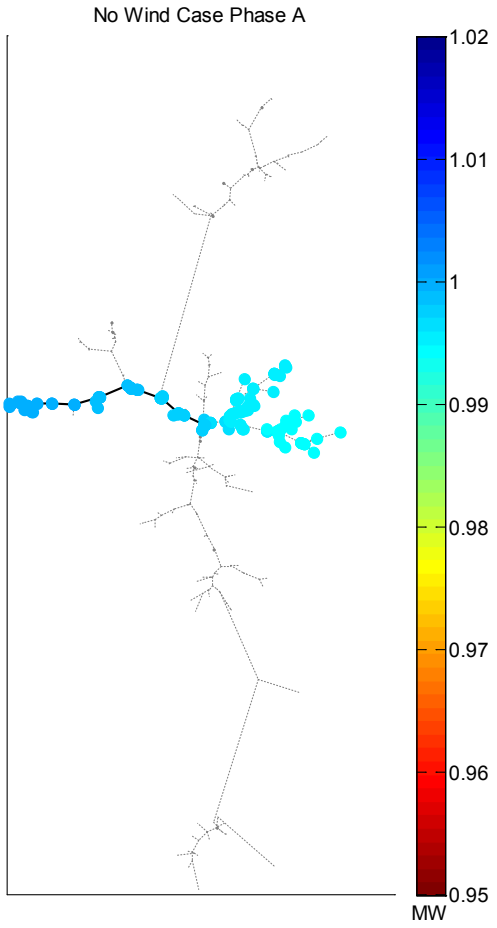

Figure 13.
Feeder R1-12.47-2. Heat map of Phase A per-unit bus voltages with 33% of full load and with 0 kW of wind power

Again, wind turbines are added to Bus 17, with the Phase A per-unit bus voltages shown in Figure 14, and to Bus 183, with the per-unit bus voltages shown in Figure 15. When the wind turbines are connected to Bus 183, the bus voltages at the end of the single-phase laterals rise above voltages of 1.02 per unit. The voltage profiles in Figure 16 and Figure 17 also show that the bus voltages are much larger when the wind turbines are connected to Bus 183.

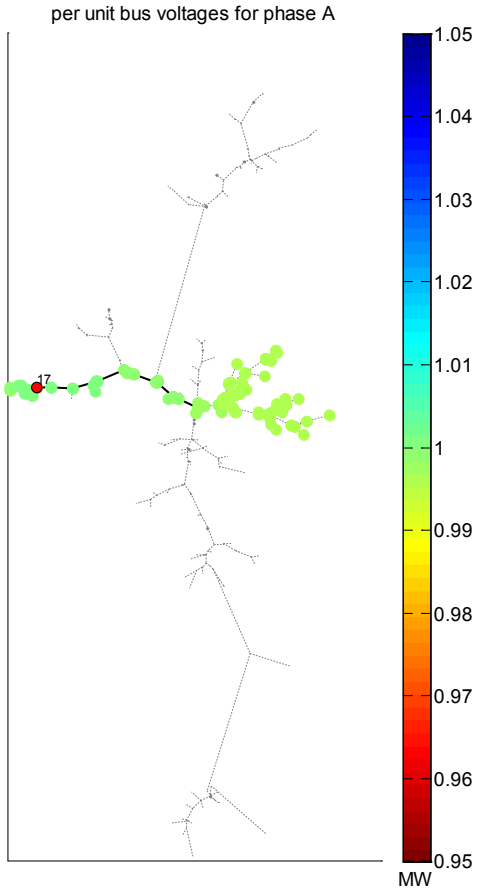

Figure 14.
Feeder R1-12.47-2. Heat map of Phase A per-unit bus voltages with 33% of full-load and with 3,000 kW of wind power

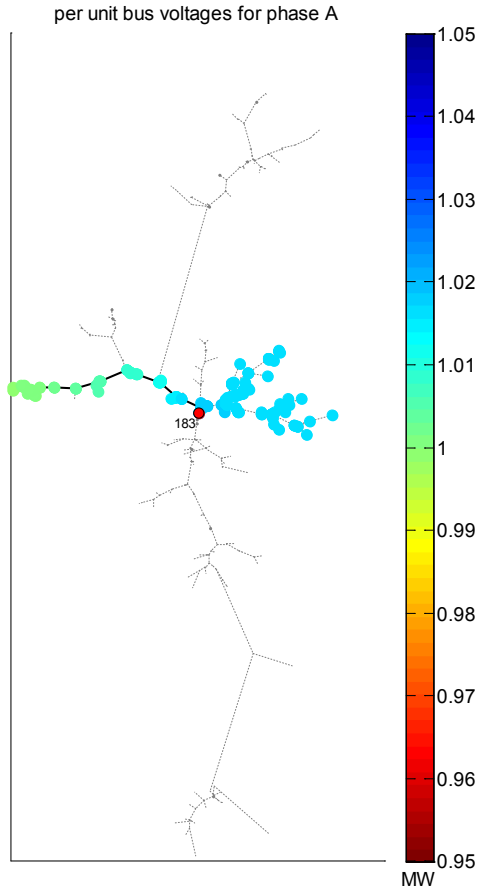

Figure 15.
Feeder R1-12.47-2. Heat map of Phase A per-unit bus voltages with 33% of full load and with 3,000 kW of wind power

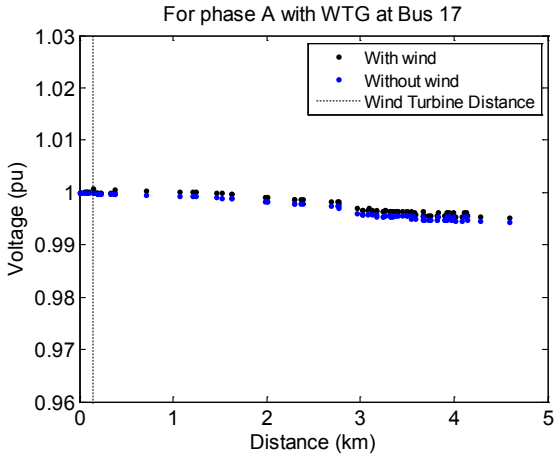

Figure 16.
Feeder R1-12.47-2. Phase A voltage profiles with 33% of full load without wind and with 3,000 kW of wind power connected to Bus 17

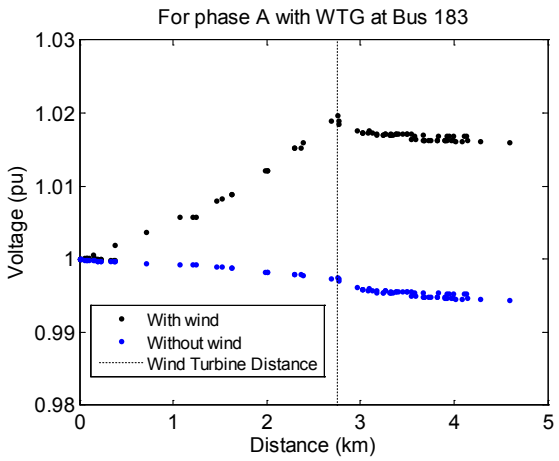

Figure 17.
Feeder R1-12.47-2. Phase A voltage profiles with 33% of full load without wind and with 3,000 kW of wind power connected to Bus 183

The change in voltage for Phase A buses when wind turbines are connected to Bus 17 is shown in Figure 18 and when wind turbines are connected to Bus 183 in Figure 19. The percent change in voltage for wind turbines at Bus 183 is about the same for both the case with a full load (Figure 12) and the case with 33% of full load (Figure 19). However, when the load is reduced, the per-unit voltages at the ends of the laterals are higher, and connecting wind power increases the voltage even more. The results from this analysis show that low-load conditions and including wind farther away from the substation increase voltages at the ends of the feeders and laterals. The same results are shown for Phase B and Phase C in Appendix A.

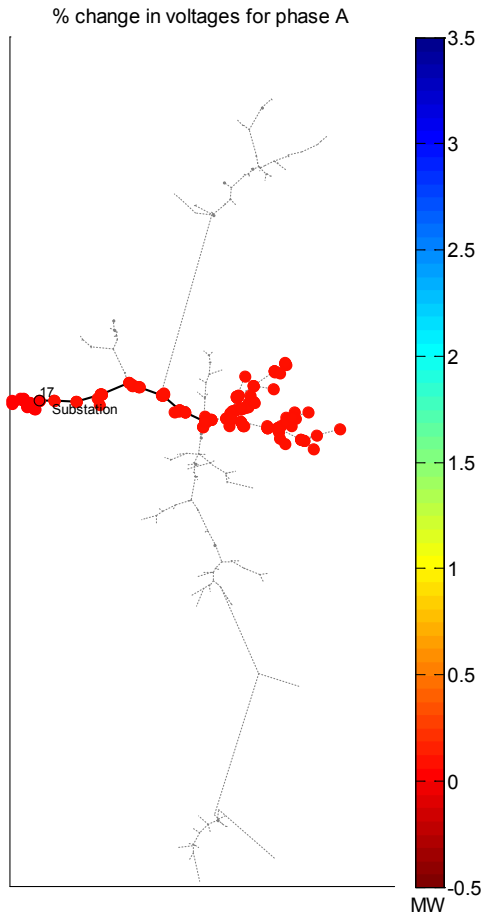

Figure 18.
Feeder R1-12.47-2. Heat map of Phase A change in bus voltage with 33% of full load and with 3,000 kW of wind power connected to Bus 17

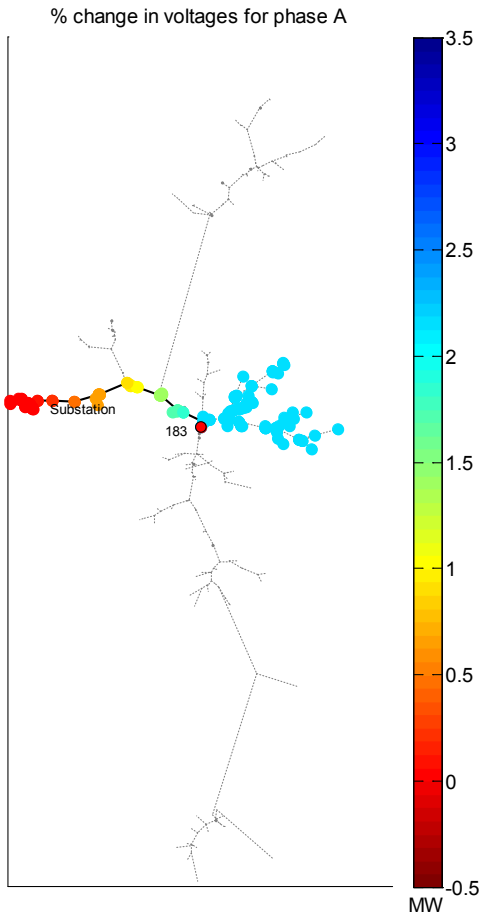

Figure 19.
Feeder R1-12.47-2. Heat map of Phase A change in bus voltage with 33% of full load and with 3,000 kW of wind power connected to Bus 183

3.2.3.1.1 Overvoltage Limits

ANSI C84.1-2011 [42] provides a description of maximum voltage tolerances but does not include voltage transients or temporary overvoltages caused by system conditions such as faults or load shedding. From the standard, 125 V is the lowest acceptable maximum voltage on a 120-V base. This is an approximate 0.042 per-unit increase from nominal voltage. In the simulations, the voltages do not reach above this limit—the voltages do not exceed 1.015 per unit with a full load and 1.023 per unit with a low load when the wind power output is 3,000 kW. The maximum per-unit voltage for each phase for all possible wind turbine locations is given in Table 3. The voltage rise is larger when the load is lower; therefore, the maximum voltages for the low-load cases are examined when the wind power output is 4,500 kW and 6,000 kW. The ANSI maximum voltage limits are exceeded when the wind power output is at 6,000 kW and phases A

and B experience maximum voltages of 1.043 per unit; therefore, 6,000 kW should not be added to the circuit when considering overvoltage limits.

Table 3. Maximum Per-Unit Voltages Anywhere on the Feeder with Different Amounts of Wind Power

	Wind (kW)	3,000		4,500	6,000
	Load (%)	100	33	33	33
Phase Voltage (pu)	A	1.015	1.023	1.033	1.043
	B	1.015	1.023	1.033	1.043
	C	1.001	1.016	1.027	1.036

3.2.3.1.2 Quantitative Relationship—Is Distance or Impedance Better Correlated to Voltage Rise?

The placement of WTGs within the circuit impacts the amount of voltage rise. The previous section showed that the farther away a WTG is located from a substation, the larger the maximum voltage rise in the circuit will be. Also, the largest rise in voltage occurs downstream (with feeder and lateral buses located opposite the substation side of the WTG bus) from the WTG location.

The comparison of voltage rise to the impedance between the wind turbine bus and the feeder substation has been studied in previous work, when another circuit was used to study the impact of wind power on distribution voltage rise [45]. In the cited study, the distance of the wind turbine from the substation did not always correctly predict the rise in voltage and instead resulted in a bifurcation (due to feeder branching) that provided two different possible voltage rises for a single wind turbine distance. When examining the impedance rather than the distance, the bifurcation disappears or is significantly reduced.

Therefore, the relationships examined in this section are among the physical parameters of the circuit (distance, impedance) and the voltage rise caused by the addition of wind power. In the first case, the maximum bus voltage rise for a selected wind turbine location is compared to the distance of the wind turbine bus from the circuit substation bus. An example for Phase A is shown in Figure 20.

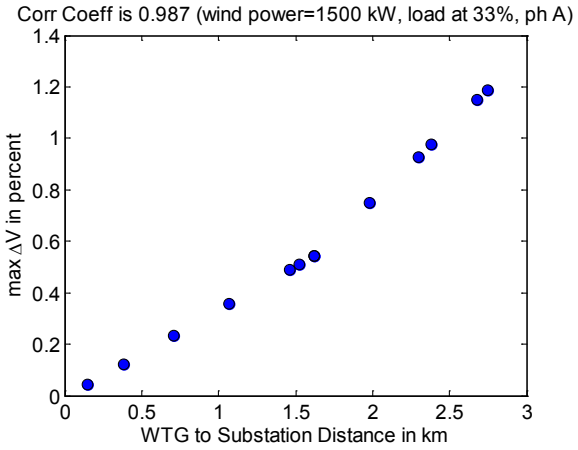

Figure 20.
Feeder R1-12.47-2. Relationship between maximum change in voltage and distance in km

Figure 20 shows the maximum voltage rise for Phase A buses extracted for each possible wind turbine location. The distance of the wind turbine to the substation along overhead and underground lines (not based on geographic information system data) is also extracted and compared to each maximum voltage rise for that WTG. Unlike the line resistance, for each phase the distance of each bus from the substation can be easily extracted in OpenDSS using the circuit class properties *AllNodeDistancesByPhase* and *AllNodeNamesByPhase*. The index of the circuit bus connected to the WTG can be found in the list of node names and used to determine the distance in the list of node distances. The linear fit correlation coefficient between the two variables is 0.987. Thus, the correlation between the WTG distance and the maximum voltage rise is close to linear.

Figure 21 shows the impedance from the WTG to the substation bus along the x-axis. The phase resistance from a specified bus to the substation is not extracted using the same interface as the node distance. Instead, the impedance from each line is extracted and saved in a tree format as described in Section 2.1. The sum of all the line impedances from the WTG bus to the substation is then calculated and saved. The results comparing the phase impedance to the maximum change in voltage is shown in the figure below. The linear fit correlation coefficient between these two variables is 0.99994—nearly perfectly linear.

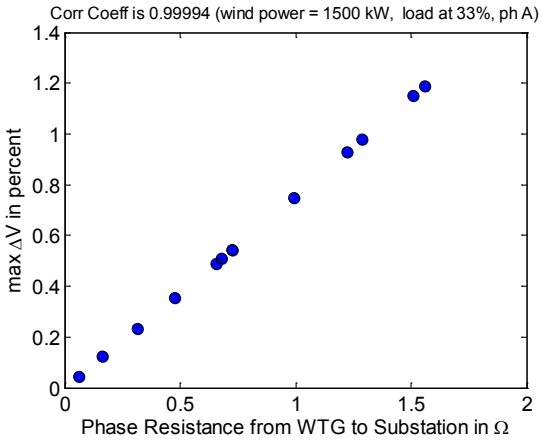

Figure 21.
Feeder R1-12.47-2. Relationship between maximum change in voltage and impedance

The correlation coefficient (r_1) between the maximum voltage rise and the distance in kilometers and the correlation coefficient (r_2) between the maximum voltage rise and the impedance for all three phases and different loading and wind power scenarios is provided in Table 4 below. The results show that r_1 and r_2 are similar for all wind power and load scenarios; however, the visual distinction shown in the figures above is more exaggerated for other more-complex feeders, as is the difference between r_1 and r_2. Also, r_2 indicates a closer linear relationship between impedance and maximum voltage rise. The quantitative relationship between impedance and maximum voltage rise will be further explored later in this section. Even though there is a close linear relationship between the WTG distance in kilometers and the max voltage rise in feeder R1-12.47-2, this is not always true for other taxonomy feeders. The same analysis will be repeated on another feeder to illustrate the better linear relationship between the impedance and voltage rise.

Table 4. Correlation Coefficients r_1 and r_2 for Different Wind and Load Scenarios

Wind Power (kw)	Fraction of Load Online	Phase	Correlation Coefficient r_1	Correlation Coefficient r_2
1,500	0.33	1	0.987	1.000
		2	0.987	1.000
		3	0.987	1.000
	0.66	1	0.987	1.000
		2	0.987	1.000
		3	0.987	1.000
	0.99	1	0.987	1.000
		2	0.987	1.000
		3	0.987	1.000
3,000	0.33	1	0.988	1.000
		2	0.988	1.000
		3	0.988	1.000
	0.66	1	0.987	1.000
		2	0.987	1.000
		3	0.987	1.000
	0.99	1	0.987	1.000
		2	0.987	1.000

		3	0.987	1.000
4,500	0.33	1	0.988	1.000
		2	0.988	1.000
		3	0.988	1.000
	0.66	1	0.988	1.000
		2	0.988	1.000
		3	0.988	1.000
	0.99	1	0.987	1.000
		2	0.987	1.000
		3	0.987	1.000

The relationship between wind turbine location and voltage rise is further explored below. As shown in Figure 22 and Figure 23, the circuit is at full load, and the wind power output is 3,000 kW. The red circle indicates the bus that experiences the maximum Phase A voltage change for all the wind turbine locations shown in blue. The figure on the left shows that Bus 163 experiences the largest change in voltage when wind turbines are placed at all possible WTG buses except Bus 183. The largest voltage change shown in the left figure occurs when a WTG is located at Bus 118. In this case, the pre-wind per-unit voltage at Bus 163 is 0.982, and the per-unit voltage when the WTG is connected to the circuit is 1.004—a 2.25% increase in voltage. When a WTG is placed at Bus 183, the same bus experiences the largest change in voltage. The pre-wind per-unit voltage at Bus 183 is 0.992, and the per-unit voltage when the WTG is connected to the circuit is 1.015—a 2.27% increase in voltage.

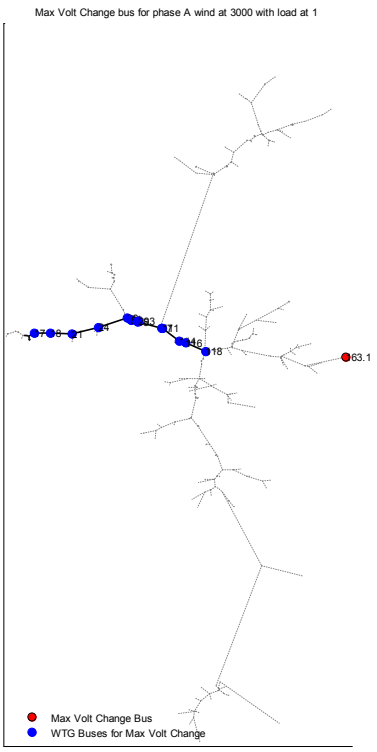

Figure 22.
Bus 163, which experiences the maximum voltage change, and the wind turbine locations that cause it—Phase A

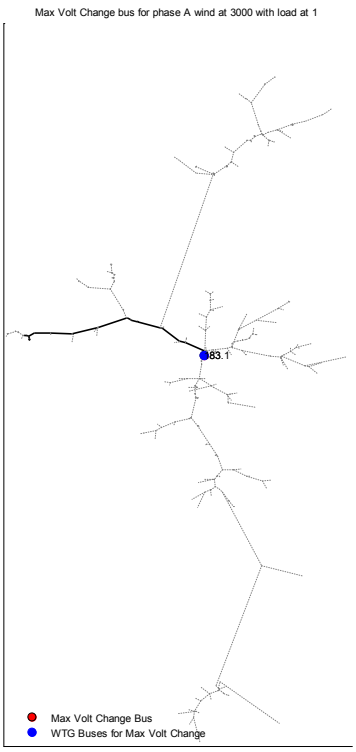

Figure 23.
Bus 183, which experiences the maximum voltage change, and the wind turbine locations that cause it—Phase A

Figure 24 and Figure 25 show the results for Phase B. The figure on the left shows that Bus 110 experiences the largest change in voltage when WTGs are placed at buses 17, 18, 21, 24, 28, 54, 55, 293, 56, 57, and 111. The largest voltage change in the left figure occurs when a WTG is located at Bus 111. The pre-wind per-unit voltage at Bus 110 is 0.956, and the per-unit voltage when the WTG is connected to the circuit is 0.971—a 1.57% increase in voltage. When WTGs are placed at buses 114, 116, 118, and 183, Bus 292 experiences the largest change in voltage, as shown in the figure on the right. The largest voltage change of these possible WTG locations occurs when a wind turbine is located at Bus 183; the pre-wind per-unit voltage is 0.959, and the per-unit voltage when the WTG is connected to the circuit is 0.982—a 2.47% increase in voltage.

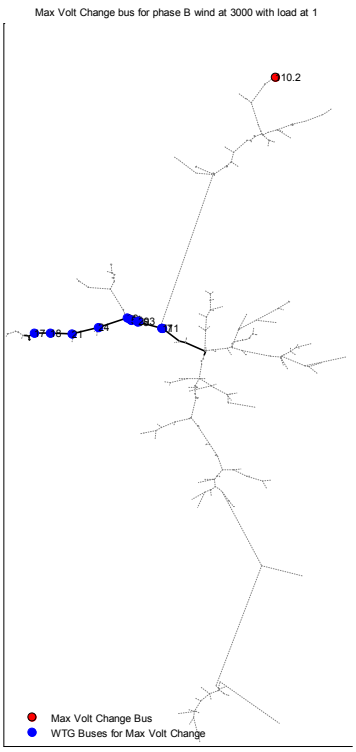

Figure 24.
Bus 110, which experiences the maximum voltage change, and the wind turbine locations that cause it—Phase B

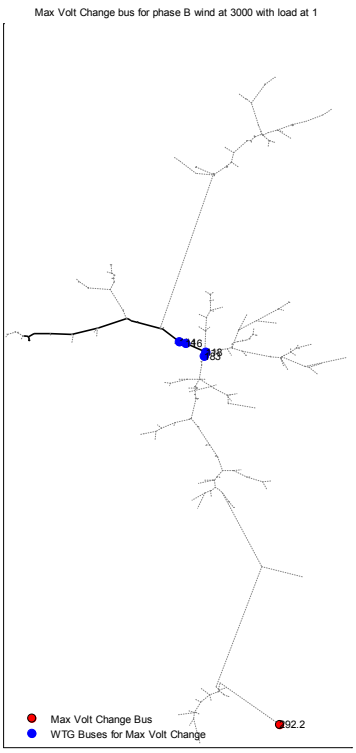

Figure 25.
Bus 292, which experiences the maximum voltage change, and the wind turbine locations that cause it—Phase B

Figure 26 shows the results for Phase C. Bus 248 experiences the largest change in voltage for any of the possible WTG locations. The largest voltage change in the figure occurs when a WTG is located at Bus 183. The pre-wind per-unit voltage at Bus 278 is 0.962, and the per-unit voltage when the WTG is connected to the circuit is 0.986—a 2.52% increase in voltage.

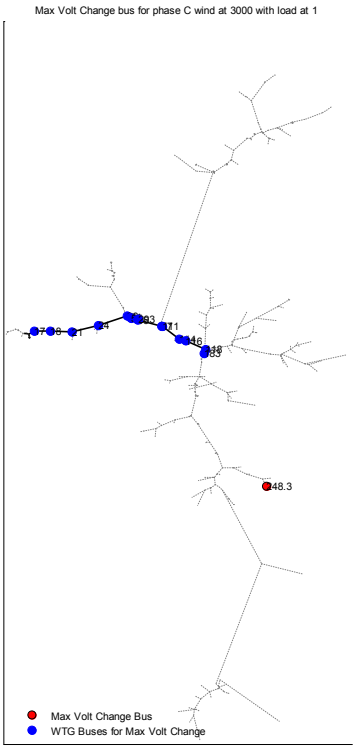

Figure 26.
Bus 248, which experiences the maximum voltage change, and the wind turbine locations that cause it—Phase C

The results show that for the same load conditions, each phase is impacted differently, such that the largest voltage rises are experienced by buses located in different parts of the circuit. Also, the largest rises in voltage tend to occur at the ends of very long, single-phase feeders, where the voltage drop is also very large. The rise in voltage may be large, but because the voltage at the ends of feeders tends to be low, the resulting voltage when WTGs are added is not very large and definitely not above the ANSI limits described in Section 3.2.3.1.1.

As previously mentioned, the maximum voltage rise is related to the phase resistance between the WTG bus and the substation. The relationship between voltage rise and phase resistance is very linear, as shown in Figure 27. The correlation coefficient between the two variables is nearly exactly 1—indicating a near perfect linear fit.

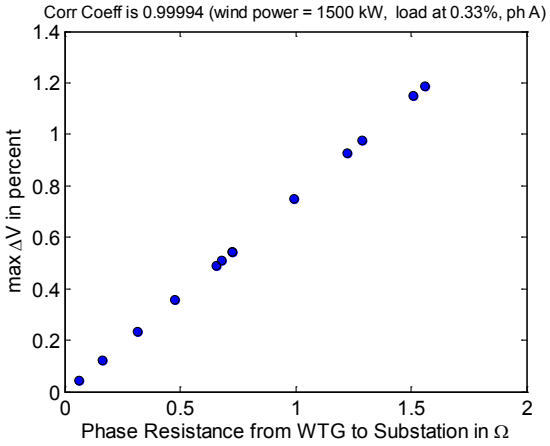

Figure 27.
Feeder R1-12.47-2. Relationship between max change in voltage and impedance to WTG

Using linear regression (polyfit function in MATLAB with degree n set to one), the regression coefficients ($p_1 = 0.764$, $p_2 = -0.007$) for the example in the figure above are given in the equation below.

$$\Delta V_{max} = 0.764 * R - 0.007$$

In the equation, ΔV_{max} is the maximum voltage change within the circuit for the WTG location, and R is the impedance from the WTG location to the substation. The equation reveals that (for circuit R1-12.47-2 with 1,500 kW of wind connected and during full load) for each 1 Ω increase between the WTG location and the substation, the maximum voltage rise will be 0.764%. The residual sum of squares (RSS) between the data in the figure and the model from the equation is 4.5641e-08, indicating a very good fit. It is important to note that this relationship would be more complex if a non-unity power factor were to be utilized.

The same analysis is applied to all three phases for 1,500 kW, 3,000 kW, and 4,500 kW of wind power and 33%, 67%, and 100% of full load. The total power measured at the substation is 2.86 MW (the total load is 2.83 MW [44]. The wind penetration, correlation coefficient between resistance and voltage change, regression coefficients, and RSS for each case is shown in Table 5.

Table 5. Relationship Between Max Change in Voltage and Impedance to WTG for Varying Amounts of Load and Wind Power

Wind Power (kw)	Fraction of Load Online	Instantaneous Wind Penetration (%)	Phase	Correlation Coefficient	P_1	P_2	RSS
1,500	0.33	162.0	1	0.9999	0.764	-0.007	0.0002
		162.0	2	0.9999	0.764	-0.007	0.0002
		162.0	3	0.9999	0.760	-0.007	0.0002
	0.66	80.3	1	0.9999	0.804	-0.010	0.0003
		80.3	2	0.9999	0.804	-0.010	0.0003
		80.3	3	0.9999	0.794	-0.010	0.0003
	0.99	53.1	1	0.9999	0.850	-0.014	0.0004

		53.1	2	0.9999	0.850	-0.014	0.0004
		53.1	3	0.9999	0.833	-0.013	0.0004
3,000	0.33	324.0	1	1.0000	1.485	-0.010	0.0005
		324.0	2	1.0000	1.485	-0.010	0.0005
		324.0	3	1.0000	1.477	-0.010	0.0005
	0.66	160.7	1	1.0000	1.562	-0.015	0.0007
		160.7	2	1.0000	1.562	-0.015	0.0007
		160.7	3	0.9999	1.543	-0.015	0.0007
	0.99	106.2	1	0.9999	1.649	-0.020	0.0011
		106.2	2	0.9999	1.649	-0.020	0.0011
		106.2	3	0.9999	1.618	-0.020	0.0010
4,500	0.33	485.9	1	1.0000	2.168	-0.008	0.0007
		485.9	2	1.0000	2.168	-0.008	0.0007
		485.9	3	1.0000	2.155	-0.008	0.0007
	0.66	241.0	1	1.0000	2.279	-0.015	0.0010
		241.0	2	1.0000	2.279	-0.015	0.0010
		241.0	3	1.0000	2.251	-0.015	0.0010
	0.99	159.2	1	1.0000	2.403	-0.022	0.0014
		159.2	2	1.0000	2.403	-0.022	0.0014
		159.2	3	1.0000	2.358	-0.022	0.0014

The results show that the steepness of the slope (indicated by the regression coefficient p_1) increases as both load increases and wind power increases, and it is not related to the penetration of wind power in the circuit. This means that for full load and 4,500 kW of wind power, the maximum voltage rise will be 2.4% per 1 Ω increase between the WTG and the substation.

As shown in the results presented in Figure 27 and Table 5, the largest rise in voltage occurs for the wind turbine located farthest from the substation. When a wind turbine is placed at this bus, Bus 183, the maximum amount of wind power that the circuit can tolerate without exceeding ANSI overvoltage limits is 4,500 MW of wind power, or three 1.5-MW wind turbines.

The next step is to determine the maximum amount of wind power that can be connected to the circuit at each of the other possible wind turbine locations without exceeding ANSI overvoltage limits. Each possible wind turbine location will be connected to an increasing amount of wind power, starting with 4,500 MW, until overvoltage limits are reached. The entire circuit load is reduced to 33% of full load. Figure 28 gives the results of this analysis for each phase. The x-axis is the resistance from the wind turbine bus to the substation, and the y-axis is the maximum wind power that is connected to that bus location that does not exceed overvoltage limits. Figure 28 shows that the farther the wind turbines are from the substation, the lower the amount of wind power the circuit can tolerate when voltage rise is the only factor taken into consideration.

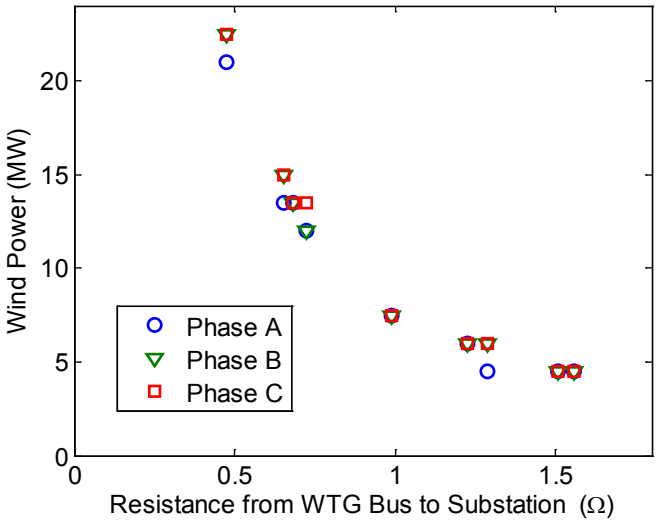

Figure 28.
Maximum wind power that can be tolerated for wind turbine resistance to the substation when only overvoltage limits are considered

The results are also given in Table 6. The overvoltage limits are tested for up to 30,000 kW, or 20 1.5-MW turbines. Even with this large amount of wind power possible, wind turbine buses located closest to the substation never exceeded the overvoltage limits. However, other factors such as current limits and transient voltage limits could potentially be prohibitive at these high levels of wind power installation.

Table 6. Maximum Wind Power That Can Be Tolerated for Wind Turbine Resistance to the Substation When Only Overvoltage Limits Are Considered

		Wind Power (kW)			
Bus Name	Bus Resistance	Phase A	Phase B	Phase C	Max Allowable (kW)
24	0.476	22,500	24,000	24,000	22,500
28	0.655	15,000	16,500	16,500	15,000
54	0.682	15,000	15,000	15,000	15,000
55	0.682	15,000	15,000	15,000	15,000
56	0.725	13,500	13,500	15,000	13,500
293	0.725	13,500	13,500	15,000	13,500
57	0.991	9,000	9,000	9,000	9,000
111	0.991	9,000	9,000	9,000	9,000
114	1.225	7,500	7,500	7,500	7,500
116	1.288	6,000	7,500	7,500	6,000
118	1.508	6,000	6,000	6,000	6,000
183	1.559	6,000	6,000	6,000	6,000

3.2.3.2 Steady-State Analysis II—Line and Transformer Ratings

This section considers the ratings of equipment within the distribution system, particularly line and transformer ratings. Care must be taken to ensure that these ratings are not exceeded by too

much when installing wind turbines. The line ratings are provided with the taxonomy feeder data. For this circuit, the ratings for the substation voltage regulator are not provided by the taxonomy feeder and thus needed to be approximated. The MVA rating will be calculated based on the total real and reactive power through the transformer during full load. Three different cases when the transformer is rated at 10%, 20%, and 30% above full load apparent power are examined.

First, the proximity of the current through the lines to the line ratings defined in the taxonomy feeder conductor data is examined for different wind power scenarios. Previously, the ANSI overvoltage limits were exceeded for cases when the wind turbine output was 6,000 kW. When the line ratings are examined for these same conditions, they are also exceeded, as shown in the figures below. In Figure 29 to Figure 31, the green indicates buses in which current flow through the connected lines is equal to or less than 75% of the rating.

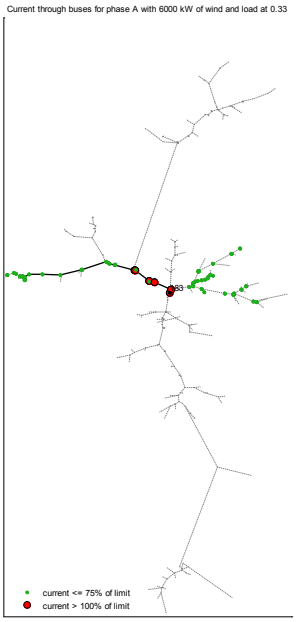

Figure 29.
Line rating exceeded for Phase A

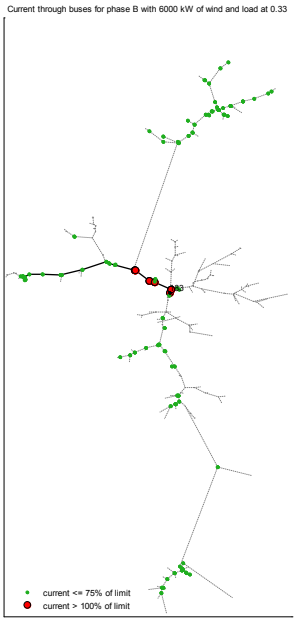

Figure 30.
Line rating exceeded for Phase B

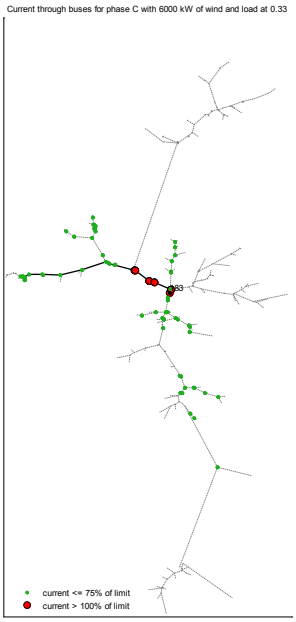

Figure 31.
Line rating exceeded for Phase C

The portions of the three-phase lines in which the current limits are exceeded (shown in red) have a continuous current rating of 230 A when the three-phase portions of the line have a continuous current rating of 334 A. The line ratings were selected based on power flows of load distribution and without considering the placement of DG in the circuit. If the largest amount of wind power is added to the circuit without replacing any equipment in the circuit, 6,000 kW of wind power is not possible.

Next, the nearness of the current to the line rating when 4,500 kW of wind power is added to the circuit is shown in the figures below. The figures show that the worst-case scenario—the wind turbine location at Bus 183 causes the highest number of lines near its line rating—results for all three phases.

In Figure 32 to Figure 34, yellow indicates buses in which the current flow through the connected line is between 75% and 100% of the rating, and red indicates buses in which the current flow through the connected line exceeds 100% of the rating.

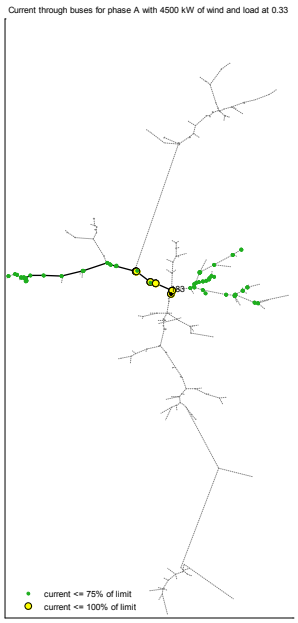

Figure 32.
Line rating not exceeded for Phase A

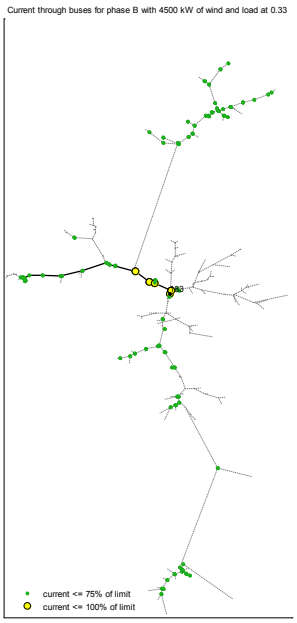

Figure 33.
Line rating not exceeded for Phase B

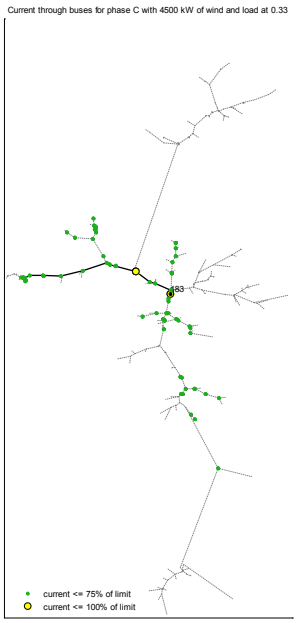

Figure 34.
Line rating not exceeded for Phase C

For the case with 4,500 kW, the line ratings are not exceeded. A few lines along the three-phase feeder have a rating of 230 A, and the current through the lines is above 75% of the rating. For the Phase C current, some points along the feeder do not exceed 75% of the rating because of the distribution of Phase C loads along that portion of the feeder. Based on these observations, the maximum amount of wind power that can be added without exceeding the line ratings is 4,500 kW, or three 1.5-MW wind turbines.

Next, the power rating for the regulator located at the substation of the circuit is examined. The taxonomy feeder data does not include ratings for the transformer; instead, three different ratings will be created to determine if the power through the transformer is near these possible ratings. The ratings are calculated using the total apparent power through the transformer during full load rounded up to the nearest MVA. The three ratings are set to 10%, 20%, and 30% above the full-load MVA.

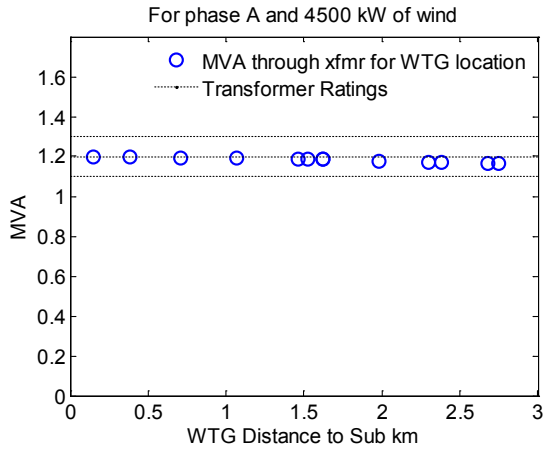

Figure 35.
Transformer MVA ratings for Phase A

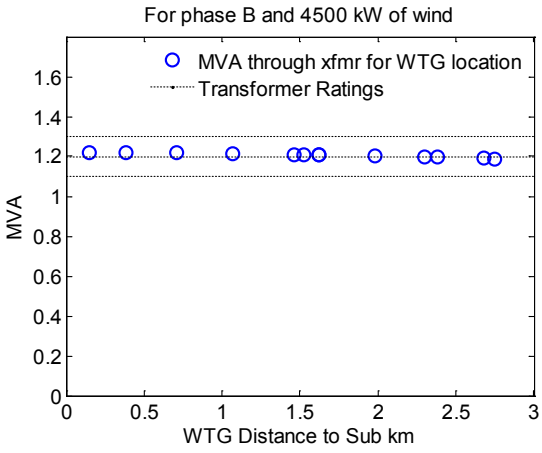

Figure 36.
Transformer MVA ratings for Phase B

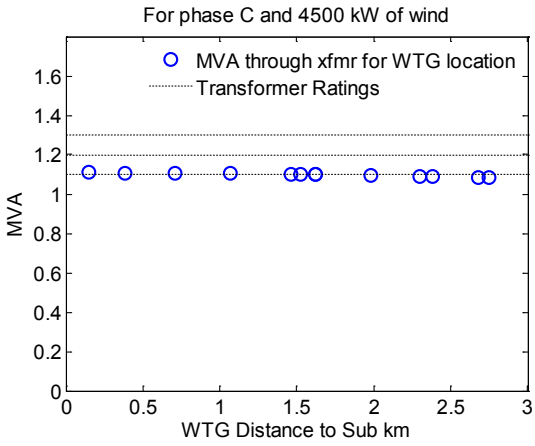

Figure 37.
Transformer MVA ratings for Phase C

For the cases shown here, the load is 33% full and the wind power output is 4,500 kW. The substation transformer rating set to 20% above 3 MVA (for each phase, it is 1.2 MVA) is exceeded when the wind power output is 4,500 kW. Also, the closer the wind turbine is located to the substation, the larger the power flow is through the substation transformer. This report assumes that the transformer rating is 30% above full load. Only if the total power through the transformer exceeds this rating will the number of wind turbines in the circuit be reduced.

The maximum amount of wind power and the location of the wind turbine that exceeded voltage rise limits, line ratings, and substation transformer rating are identified for this circuit. If a wind turbine or wind turbines are placed farther from the substation, voltage rise and line ratings should be checked. If a wind turbine is located closer to the substation, the substation transformer rating should be checked.

3.2.3.3 Steady-State Analysis III—Regulation Devices Examined

As stated previously, the original circuit did not contain a line-drop compensator in its regulator controls and therefore was not influenced by changes in load and wind power output. Line-drop compensation was included, and the R setting on the line-drop compensator was set to 2 V and the X setting to 0 V. With these changes, the tap positions for different levels of wind power output are shown in Figure 38 and Figure 39. Cases with full load and low load are also included. The wind turbine is located at Bus 17 for both cases. It is important to note that the high levels of back feeding seen the in analysis would likely exceed transformer rating limitations.

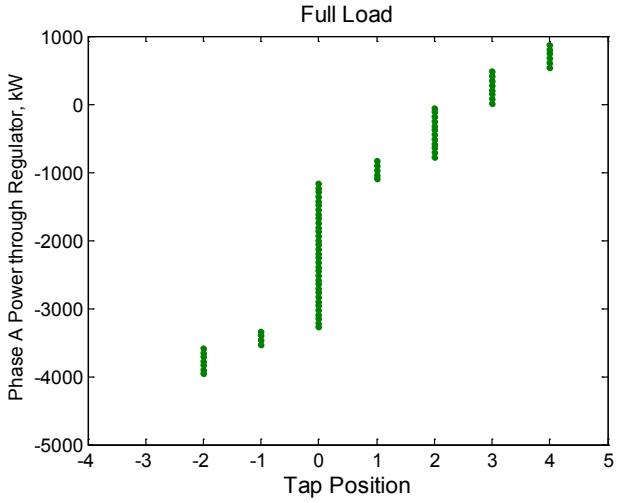

Figure 38.
Tap position for different wind power levels during full load

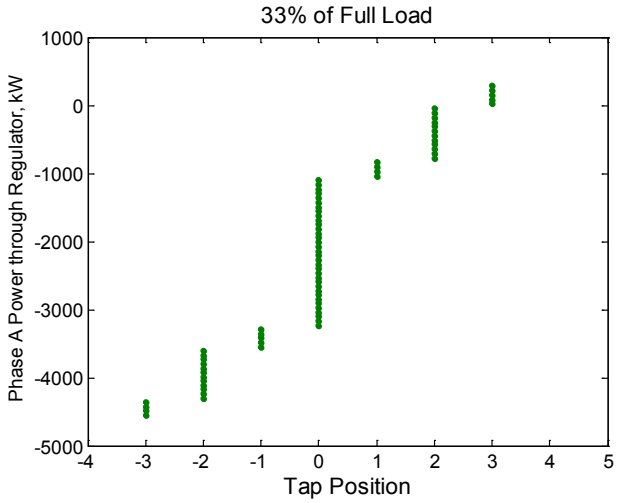

Figure 39.
Tap position for different wind power levels during 33% of full load

The figures indicate that the tap position starts closer to zero when the load is low. Future work will examine the impacts that adding varying amounts of wind power have on the number of tap changes that occur. A base case with varying load will be set up. The number of tap changes that occur for the base case will be compared to the number of tap changes that occur when a WTG is connected.

3.2.4 Conclusions for Feeder R1-12.47-2

Wind turbine locations and maximum wind power output for each of these locations were tested against consumer voltage tolerances and equipment ratings for feeder R1-12.47-2. The first step was to determine the maximum amount of wind power that each wind turbine location could tolerate without exceeding the ANSI overvoltage limits. When wind turbines are located farther from the substation, or when there is larger resistance between the wind turbine bus and the substation, the circuit could tolerate lower amounts of wind power than when wind turbines are located closer to the substation. The lines are the first equipment type that was examined. The overhead and underground lines have different line ratings for different sections of the circuit. The results show that the line ratings limit the amount of power that can be added without damaging or replacing the feeder equipment. The next equipment rating that was examined was the voltage-regulating transformer. Similar limits were reached, except that the transformer ratings place tighter constraints on the amount of power from wind turbines located closer to the substation. The relationship between the resistance from the wind turbine bus to the substation and the maximum voltage rise was also quantified and will be compared to the other taxonomy feeder resistance and voltage rise relationships to determine a generalized guideline for circuit-based wind turbine siting. The voltage-regulating transformer controls were also tested when line-drop compensation was included. The voltage-regulation device controls will be tested in future work. Load profiles and wind power profiles will be applied to the circuit, and the number of tap changes that occur will be compared to the number of tap changes that happen when varying amounts of wind power are added to the circuit.

The same analysis that was used for this taxonomy feeder is applied to the feeders in the following sections. The conclusion of this report provides general observations and guidelines for wind turbine placement and power output within a distribution circuit.

3.3 Results for Feeder R1-12.47-1

Feeder R1-12.47-1 is located in a moderately populated suburban and rural area that consists of approximately 60% overhead lines and 40% underground lines [21]. Some inconsistencies that were present in the original taxonomy feeder data were corrected before the analysis began. The taxonomy feeder report states that the total load of the feeder is 7,150 kW [21], but the sum of the loads in the data was short of the reported amount. Also, load on the distribution system is typically balanced at the substation, but load data showed that the Phase A load was only a fraction of the Phase B load and Phase C load. All loads connected to Phase A were uniformly adjusted so that all three phases were more closely balanced and the total kilowatt load was closer to the reported 7,150 kW.

Errors also appeared when Capacitor Bank 3 was switched open and power flow results were incorrect. Because the capacitor banks will be switched open for feeder R1-12.47-1 analysis, Capacitor Bank 3 was removed from the circuit and the analysis. The following sections provide circuit details and steady-state analysis results for feeder R1-12.47-1.

3.3.1 Circuit Load Description

This section describes the load for feeder R1-12.47-1. Table 7 shows the real, reactive, and apparent power through the substation bus for each phase. Figure 40, Figure 41, and Figure 42 show the distributions of load throughout the feeder for phases A, B, and C, respectively.

Table 7. Total Real and Reactive Power for Each Phase

Phase	kW	kVar	kVA
Phase A	2,258.45	948.133	2,449.398
Phase B	2,415.68	1,018.82	2,621.737
Phase C	2,628.19	1,170.84	2,877.195
Total	7,302.32	3,137.793	7,948.33

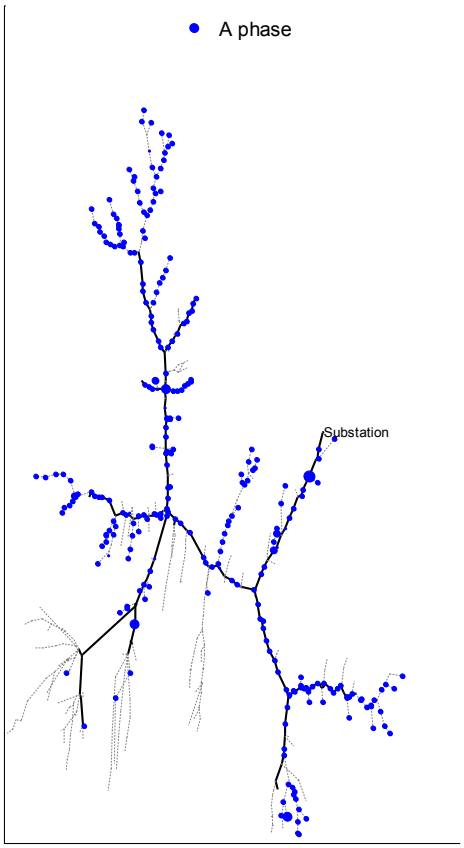

Figure 40.
Feeder R1-12.47-1. Phase A load distribution

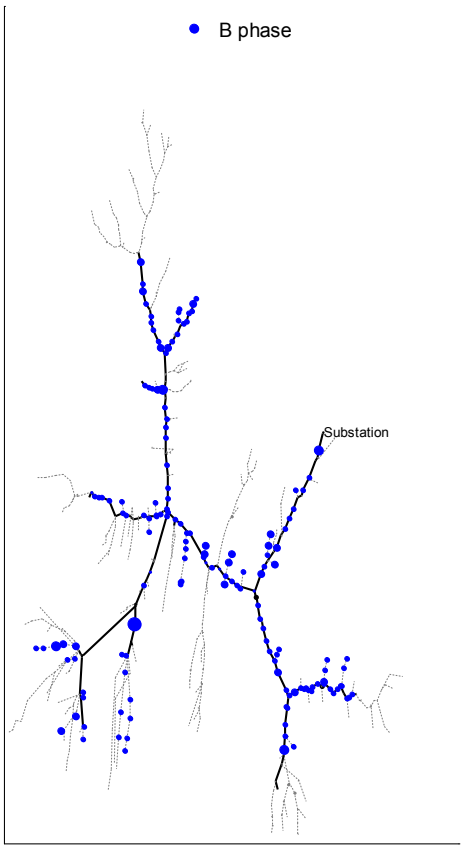

Figure 41.
Feeder R1-12.47-1. Phase B load distribution

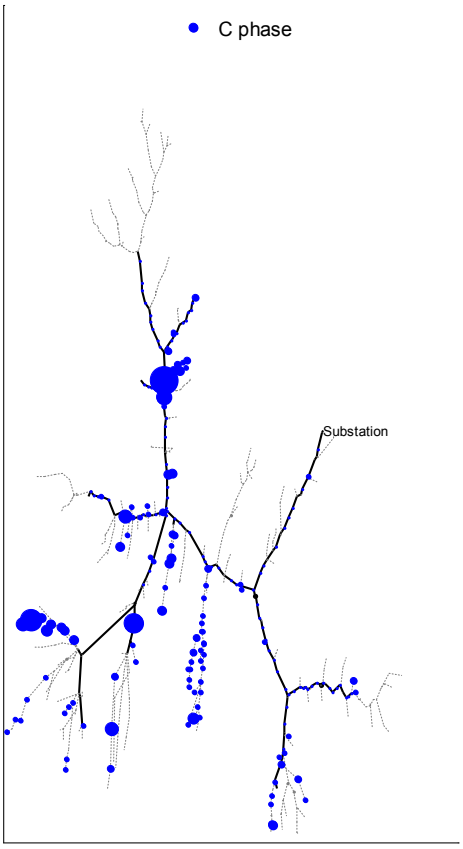

Figure 42.
Feeder R1-12.47-1. Phase C load distribution

To create low-load conditions, all loads attached to the circuit are uniformly scaled to a fraction of the total load.

3.3.2 Circuit Voltage-Regulation Devices

The circuit has two three-phase capacitor banks and one single-phase capacitor bank that have been removed from the circuit. Also, one step-voltage regulator is located at the substation. The locations of these devices are shown in Figure 43. The regulator controls are not altered for this circuit. For the analysis of this feeder, the control mode is turned off for the power flow solution so that the regulator tap position will not change.

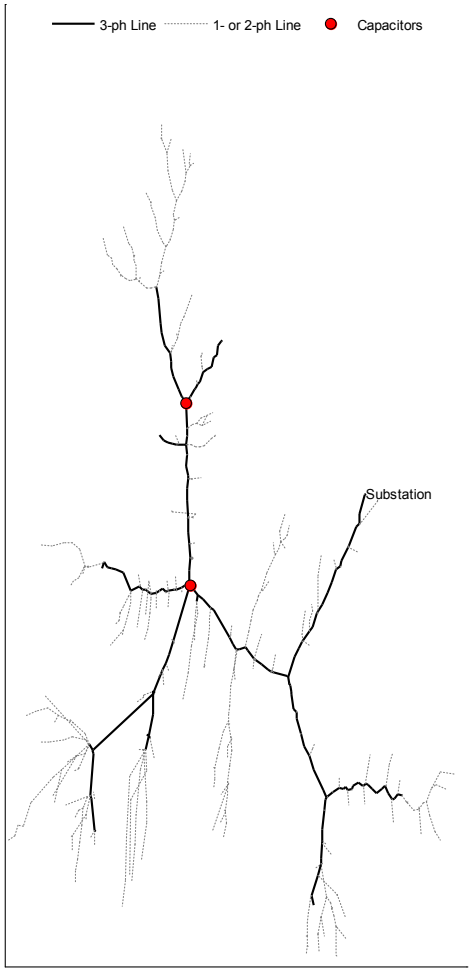

Figure 43.
Feeder R1-12.47-1. Substation and capacitor bank locations

3.3.3 Wind Turbine Location Impact—Steady-State Analysis

Similar analysis that was used to determine the maximum wind power for possible feeder wind turbine locations is applied to feeder R1-12.47-1. First, the overvoltage limits are used to determine the maximum amount of wind power that can be added to the feeder. Also, the relationship between the maximum rise in voltage and the resistance from the wind turbine bus is identified. Next, the line and transformer ratings are used to determine if the maximum wind power connected to the circuit is further limited.

For feeder R1-12.47-1, all 175 possible wind turbine connections are shown in Figure 44. A wind turbine connection to a feeder bus is considered in the analysis if the feeder bus is connected to a three-phase line.

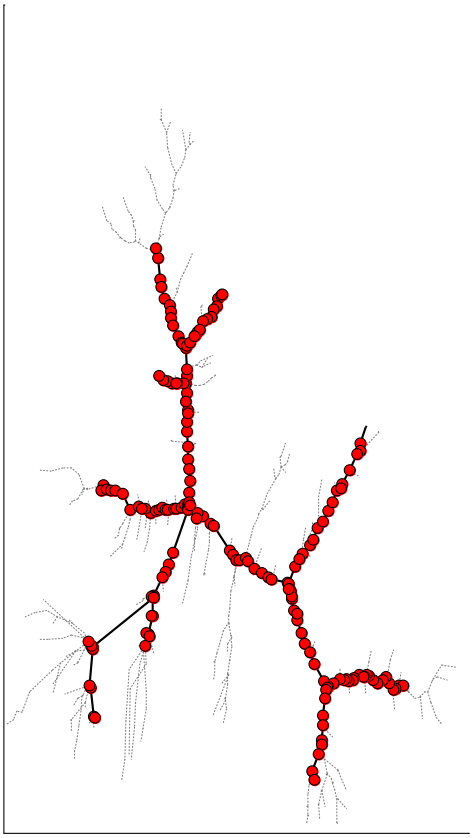

Figure 44.
Possible wind turbine connections for feeder R1-12.47-1

3.3.3.1 Steady-State Analysis I—Overvoltage Limits

The steady-state voltage analysis compares the voltages at every bus in the circuit to two scenarios: before wind turbines are added to the circuit and after wind turbines are added to the circuit. The changes that occur to bus voltages in Phase A are shown below.

Examples in the figures below show the best and worst wind turbine locations in terms of change in voltage. For the power flow solution, the capacitor banks are switched open, the voltage-regulation device controls are turned off, and the circuit is at full load. The wind power output for the cases shown below is set to 4,500 kW.

First, the voltage profiles are shown in Figure 45 for the feeder when wind turbines are located near the substation at Bus 3 and in Figure 46 when wind turbines are located near the end of the feeder away from the substation at Bus 594. The distances of the wind turbines from the substation are indicated in the figures. In both figures, the voltage profiles when wind turbines are connected (black) to the feeder are compared to the voltage profile of the feeder without wind turbines (blue).

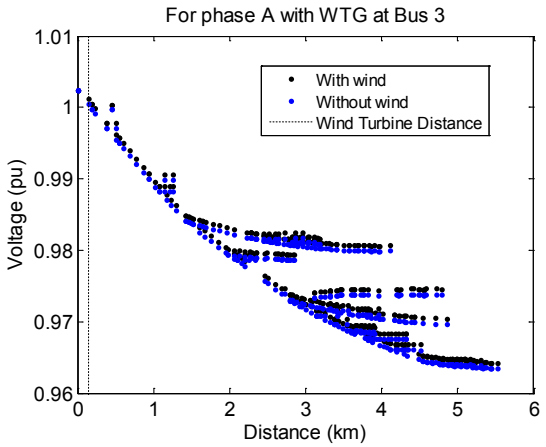

Figure 45.
Feeder R1-12.47-1. Phase A voltage profiles without wind and with 4,500 kW of wind power connected to Bus 3

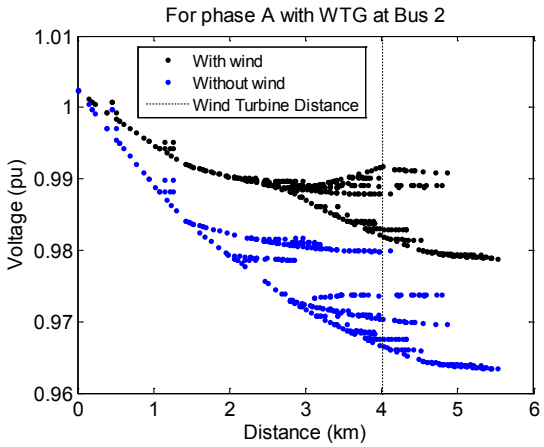

Figure 46.
Feeder R1-12.47-1. Phase A voltage profiles without wind and with 4,500 kW of wind power connected to Bus 594

Figure 45 and Figure 46 show that the ends of the laterals experience low per-unit voltage before wind turbines are added to Bus 594 and Bus 3. Figure 47 shows that when wind turbines are connected to Bus 3, the bus voltages experience a low increase in voltage, Figure 48 shows that when wind turbines are added to Bus 594, the bus voltages near the wind turbine connection experience a larger increase.

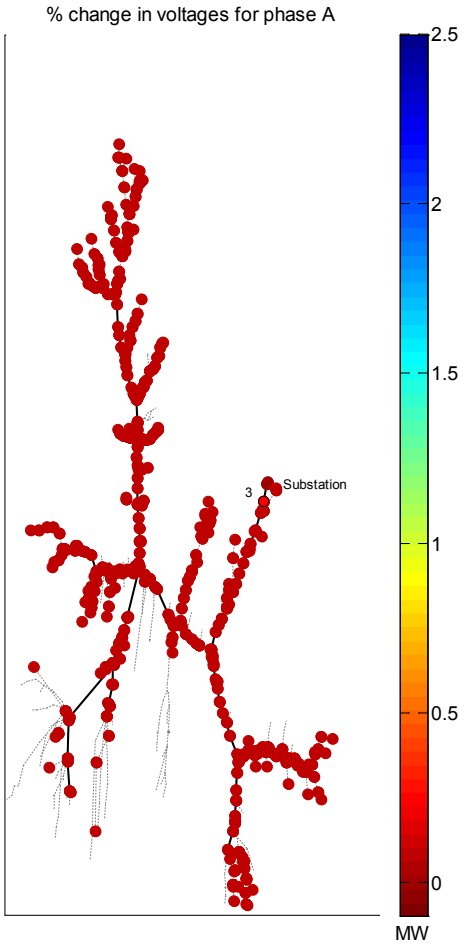

Figure 47.
Feeder R1-12.47-1. Heat map of Phase A change in bus voltage with 4,500 kW of wind power connected to Bus 3

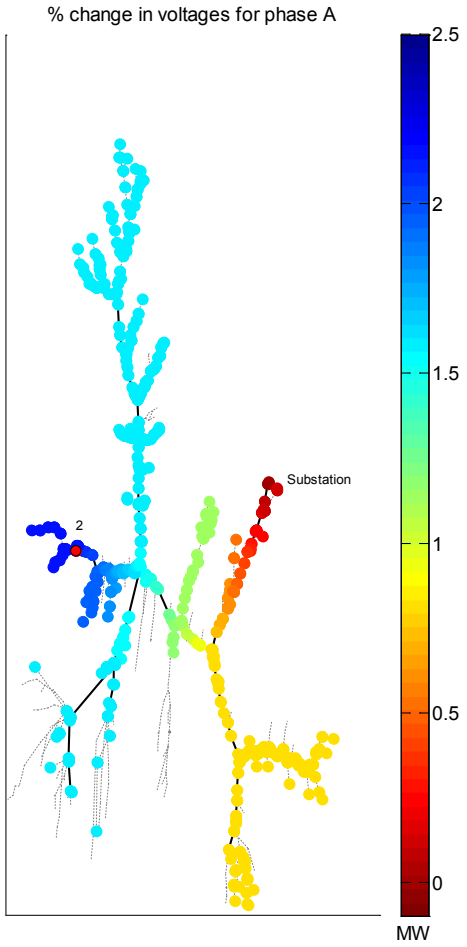

Figure 48.
Feeder R1-12.47-1 Heat map of Phase A change in bus voltage with 4,500 kW of wind power connected to Bus 594

A worst-case scenario is explored when the capacitor banks are closed so that low-voltage conditions are improved. Initially, the wind turbine output is 0 kW. Next, the wind turbine output reaches the maximum before the delay for the capacitor bank controls is reached. The maximum voltage is reached when the wind turbine is placed at Bus 3 and Bus 594, as shown in Figure 49 and Figure 50, respectively. When the wind turbine is at Bus 594, the maximum per-unit voltage is 1.021, which is still below overvoltage conditions.

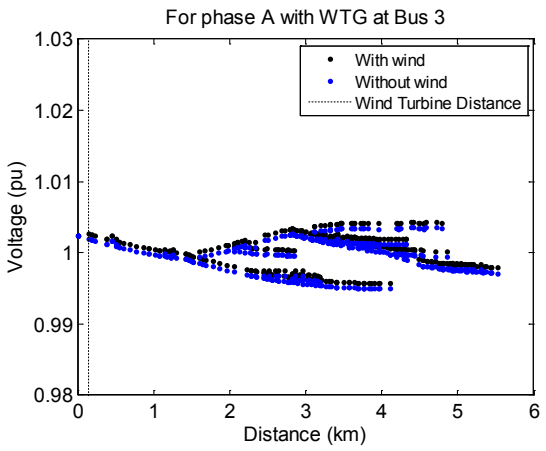

Figure 49.
Feeder R1-12.47-1 with capacitor bank switches closed. Phase A voltage profiles without wind and with 4,500 kW of wind power connected to Bus 3

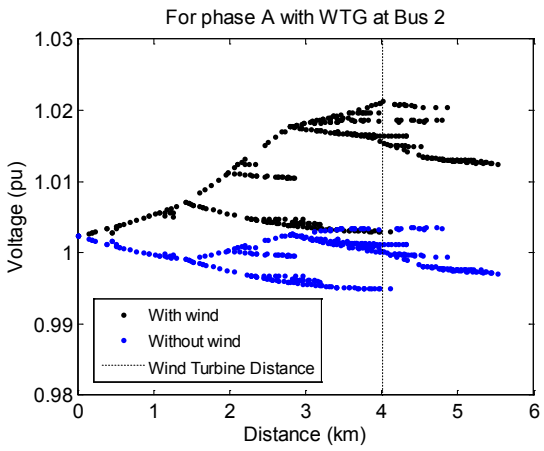

Figure 50.
Feeder R1-12.47-1 with capacitor bank switches closed. Phase A voltage profiles without wind and with 4,500 kW of wind power connected to Bus 594

The capacitor controls for feeder R1-12.47-1 have a delay of 30 s, with an on setting of 7,100 V line-to-neutral and an off setting of 7,300 V line-to-neutral. If the voltages at the lines to the capacitor banks stay above 7,300 for 30 s, the capacitor banks will switch off. Another case is run in which the capacitor controls are turned on for a power flow solution (for the analysis, all voltage-regulation controls are typically turned off), and the voltage profiles for the case without wind are compared to the voltage profiles for the cases with wind connected to Bus 3 and Bus 594. For the case without wind, both Capacitor Bank 1 and Capacitor Bank 2 are closed. When a wind turbine is added to Bus 3, the capacitor banks remain closed; a comparison of the voltage profiles is shown in Figure 51. When a wind turbine is added to Bus 594, Capacitor Bank 1 remains closed, but Capacitor Bank 2 opens, and the voltage profile for the case with wind is *lower* than it is for the case without wind. The voltage profile is shown in Figure 52. The changing status of the capacitor bank produces this result. This is the only circuit in which this control mode has been tested and the results observed. It should be noted that capacitor banks can only raise the voltage in a distribution system; hence, the effect shown here cannot be thought of as a mitigation strategy for voltage rise.

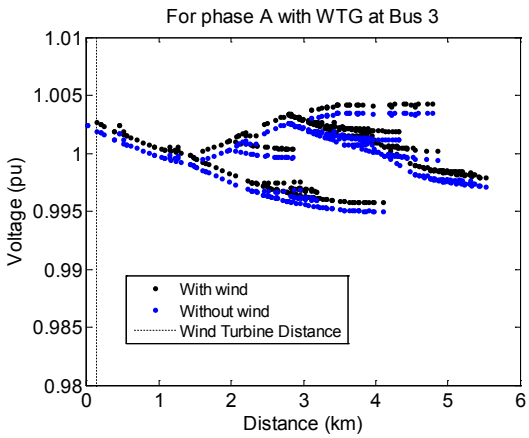

Figure 51.
Feeder R1-12.47-1 with control mode set to "static." Phase A voltage profiles without wind and with 4,500 kW of wind power connected to Bus 3

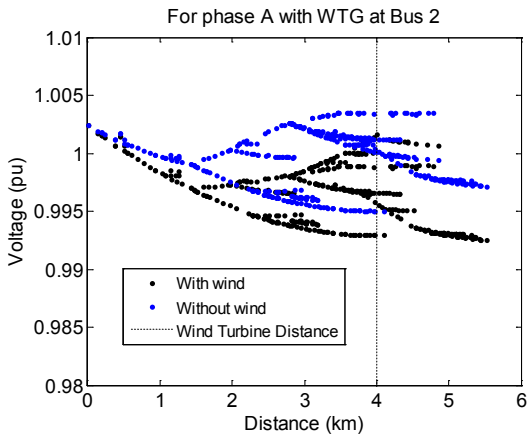

Figure 52.
Feeder R1-12.47-1 with control mode set to "static." Phase A voltage profiles without wind and with 4,500 kW of wind power connected to Bus 594

Results are similar for Phase B and Phase C, as shown by the voltage profiles given in Figure 53 to Figure 56.

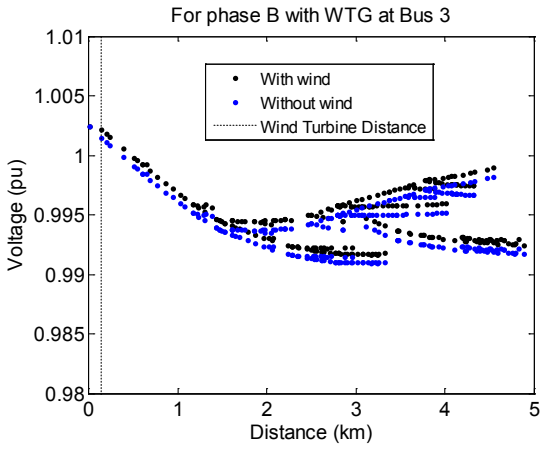

Figure 53.
Feeder R1-12.47-1 with control mode set to "static." Phase B voltage profiles without wind and with 4,500 kW of wind power connected to Bus 3

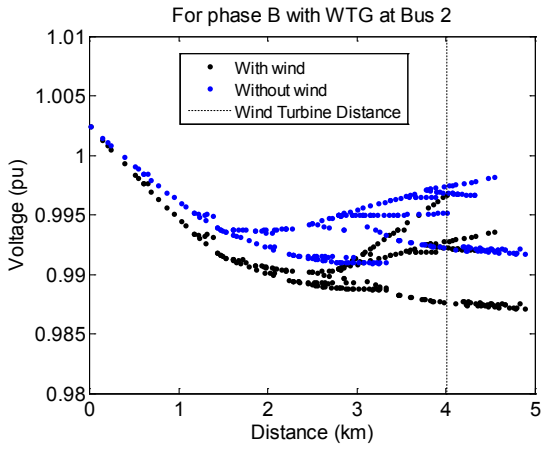

Figure 54.
Feeder R1-12.47-1 with control mode set to "static." Phase B voltage profiles without wind and with 4,500 kW of wind power connected to Bus 594

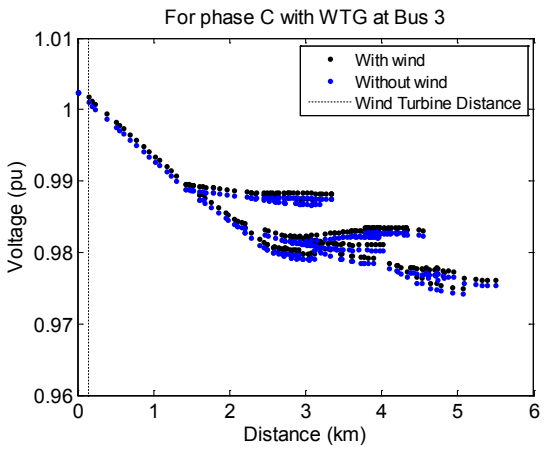

Figure 55.
Feeder R1-12.47-1 with control mode set to "static." Phase C voltage profiles without wind and with 4,500 kW of wind power connected to Bus 3

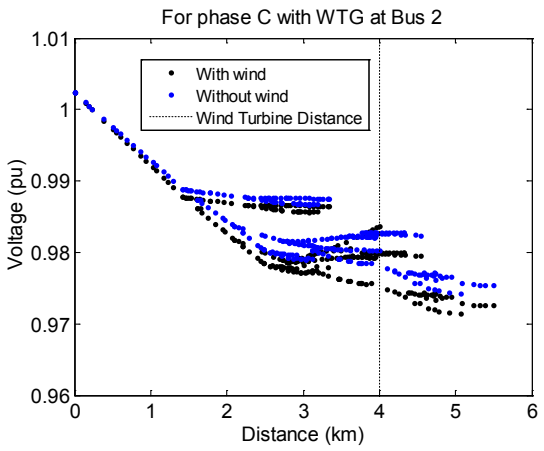

Figure 56.
Feeder R1-12.47-1 with control mode set to "static." Phase C voltage profiles without wind and with 4,500 kW of wind power connected to Bus 594

When the load is reduced to 33% of full load, both capacitor banks 1 and 2 are switched open. Figure 57 shows the voltage rise in the voltage profiles for Phase A when the wind turbine is connected to Bus 3. Figure 58 shows the voltage rise in the voltage profiles for Phase A when the wind turbine is connected to Bus 594.

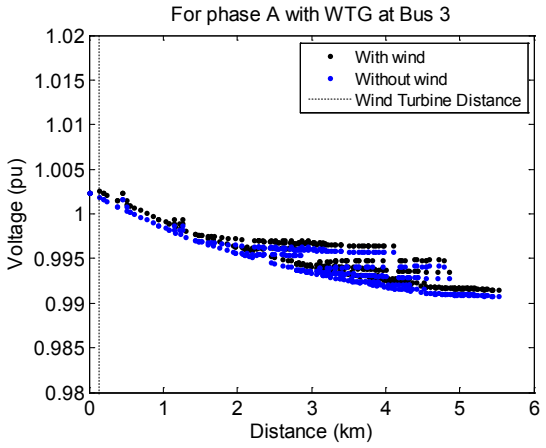

Figure 57.
Feeder R1-12.47-1 with control mode set to "static" and low load. Phase A voltage profiles without wind and with 4,500 kW of wind power connected to Bus 3

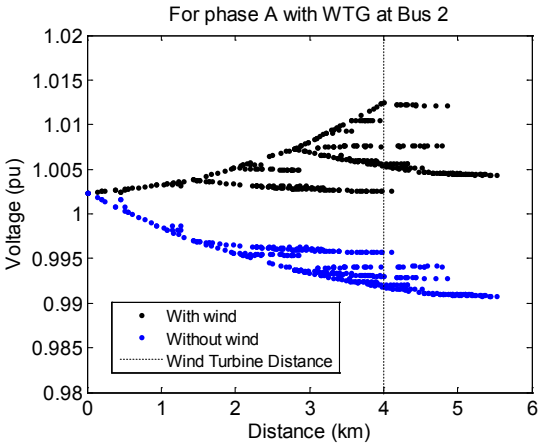

Figure 58.
Feeder R1-12.47-1 with control mode set to "static" and low load. Phase A voltage profiles without wind and with 4,500 kW of wind power connected to Bus 594

The results indicate that when wind power increases dramatically, the voltages could temporarily increase above overvoltage limits, but the duration of the overvoltage is limited to the delay settings of the voltage-regulation devices. For this circuit, the capacitor controls are left on when

wind turbines are added and bus voltages are compared to overvoltage limits. The delay of the capacitor bank should not be adjusted to less than 30 s or the utility's preferred setting, because switching the banks more often will create unwanted transients that will increase the wear and tear on the equipment and may cause the equipment to be operated incorrectly.

3.3.3.1.1 Voltage Rise Quantified and Feeder Overvoltage Limits

As previously mentioned, the maximum voltage rise is related to the phase resistance between the WTG bus and the substation. The relationship between the maximum change in voltage for each possible wind turbine location in the feeder and the resistance between the wind turbine bus and the substation is shown in Figure 59 and Figure 60. The correlation coefficient between the two variables shown in Figure 59 is 0.996 and is the best fit for wind power output and load levels. The correlation coefficient shown in Figure 60 is 0.992 and represents the worst fit for wind power output and load levels. Even though this is the worst fit in the analysis, the correlation coefficient is still nearly 1.

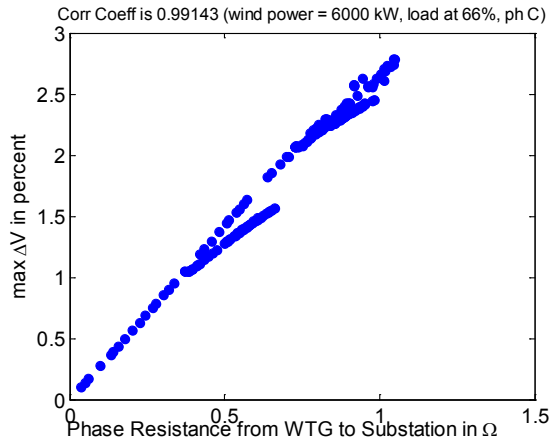

Figure 59.
Relationship between Phase C max change in voltage and phase resistance to WTG with 6,000 kW of wind power and 66% load

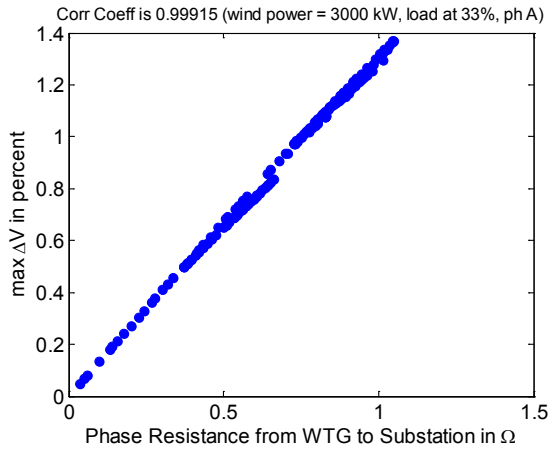

Figure 60.
Relationship between Phase A max change in voltage and phase resistance to WTG with 3,000 kW of wind power and 33% load

Using linear regression (polyfit function in MATLAB with degree n set to one), the regression coefficients (p_1 and p_2) are given in Table 8. The same analysis is applied to all three phases for 3,000 kW, 4,500 kW, and 6,000 kW of wind power and 33%, 67%, and 100% of full load. The RSS between the power flow data and the model from the equation is given in the table for each wind power and load scenario. These results will be used in the final analysis to determine a generalized relationship between the placement of wind turbines and voltage rise.

Table 8. Relationship Between Max Change in Voltage and Phase Resistance to WTG for Varying Amounts of Load and Wind Power

Wind Power (kw)	Fraction of Load Online	Instantaneous Wind Penetration (%)	Phase	Correlation Coefficient	P_1	P_2	RSS
3,000	0.33	125.9	1	0.9992	1.300	0.008	0.0293
		125.9	2	0.9980	1.288	0.022	0.0671
		125.9	3	0.9976	1.338	0.003	0.0896
	0.66	62.3	1	0.9983	1.373	-0.001	0.0671
		62.3	2	0.9945	1.360	0.026	0.2068
		62.3	3	0.9945	1.469	-0.016	0.2445
	0.99	41.5	1	0.9952	1.513	-0.019	0.2283
		41.5	2	0.9987	1.413	0.001	0.0529
		41.5	3	0.9972	1.456	-0.026	0.1199
4,500	0.33	188.9	1	0.9986	1.852	0.024	0.1016
		188.9	2	0.9971	1.834	0.045	0.1974
		188.9	3	0.9966	1.905	0.019	0.2539
	0.66	93.4	1	0.9977	1.956	0.012	0.1779
		93.4	2	0.9934	1.935	0.052	0.5104
		93.4	3	0.9932	2.089	-0.006	0.6149
	0.99	62.2	1	0.9945	2.150	-0.010	0.5210
		62.2	2	0.9973	2.023	0.017	0.2239
		62.2	3	0.9958	2.087	-0.028	0.3713
6,000	0.33	251.9	1	0.9976	2.345	0.048	0.2689
		251.9	2	0.9959	2.320	0.076	0.4555
		251.9	3	0.9952	2.409	0.043	0.5681
	0.66	124.5	1	0.9969	2.477	0.033	0.3935
		124.5	2	0.9918	2.446	0.086	1.0113
		124.5	3	0.9914	2.639	0.013	1.2337
	0.99	83.0	1	0.9936	2.712	0.011	0.9667
		83.0	2	0.9957	2.564	0.045	0.5844
		83.0	3	0.9938	2.667	-0.024	0.9119

The next step is to determine the maximum amount of wind power that can be connected to the circuit at each possible wind turbine location without exceeding ANSI overvoltage limits. Each possible wind turbine location will be connected to an increasing amount of wind power, starting with 1,500 kW, until overvoltage limits are reached. Wind power output is tested up to 27,500 kW. The entire circuit load is reduced to 33% of full load. The results of this analysis are given for each phase in Figure 61. The x-axis is the resistance from the wind turbine bus to the substation, and the y-axis is the maximum wind power that is connected to that bus location that does not exceed overvoltage limits. *Figure 61 shows that the larger the resistance between the wind turbine location and the substation, the lower the amount of wind power the circuit can tolerate when voltage rise is the only factor taken into consideration.*

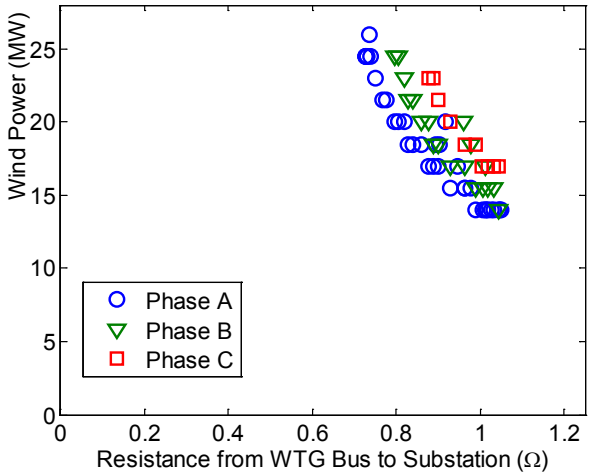

Figure 61.
Maximum wind power that can be tolerated for wind turbine resistance to substation when only overvoltage limits are considered

The bus locations and the maximum amount of wind power that can be placed at the bus without exceeding overvoltage limits are given in Table 9. A large amount of wind power can be connected to this circuit without exceeding overvoltage limits. The minimum amount of wind power that the circuit can tolerate when only overvoltage limits are considered is 14 MW, and the maximum is 26 MW.

Table 9. Maximum Wind Power at a Bus That Does Not Exceed Overvoltage Limits

		Wind Power (kW)			
Bus Name	Bus Resistance	Phase A	Phase B	Phase C	Max Allowable (kW)
594	1.034	14,000	15,500	17,000	14,000
2	1.044	14,000	14,000	17,000	14,000
593	1.019	14,000	15,500	17,000	14,000
592	1.005	14,000	15,500	17,000	14,000
591	0.991	14,000	15,500	18,500	14,000
249	1.013	14,000	17,000	-	14,000
290	1.047	14,000	-	-	14,000
293	1.049	14,000	-	-	14,000
289	1.027	14,000	-	-	14,000
273	1.015	14,000	-	-	14,000
590	0.962	15,500	17,000	18,500	15,500
576	0.929	15,500	17,000	20,000	15,500
244	0.963	15,500	20,000	-	15,500
246	0.978	15,500	18,500	-	15,500
245	0.979	15,500	18,500	-	15,500
560	0.877	17,000	20,000	23,000	17,000
562	0.900	17,000	18,500	21,500	17,000
561	0.888	17,000	18,500	23,000	17,000
272	0.945	17,000		-	17,000
559	0.859	18,500	20,000	-	18,500

552	0.841	18,500	21,500	-	18,500
551	0.829	18,500	21,500	-	18,500
242	0.893	18,500	-	-	18,500
243	0.903	18,500	-	-	18,500
550	0.818	20,000	23,000	-	20,000
547	0.805	20,000	24,500	-	20,000
546	0.797	20,000	24,500	-	20,000
269	0.916	20,000	-	-	20,000
1	0.917	20,000	-	-	20,000
270	0.918	20,000	-	-	20,000
271	0.918	20,000	-	-	20,000
540	0.776	21,500	-	-	21,500
539	0.767	21,500	-	-	21,500
538	0.750	23,000	-	-	23,000
536	0.737	24,500	-	-	24,500
535	0.727	24,500	-	-	24,500
217	0.727	24,500	-	-	24,500
227	0.731	24,500	-	-	24,500
334	0.727	24,500	-	-	24,500
228	0.731	24,500	-	-	24,500
216	0.727	24,500	-	-	24,500
329	0.736	26,000	-	-	26,000

The results are also given in Figure 62. The color bar on the right of the figure shows the amount of wind power, and the location of the wind turbine bus connection is shown on the circuit. Feeder R1-12.47-1 is able to tolerate large amounts of wind power when only overvoltage limits are considered. Many of the possible wind turbine buses did not exceed overvoltage limits when 26 MW of wind power were connected to these locations.

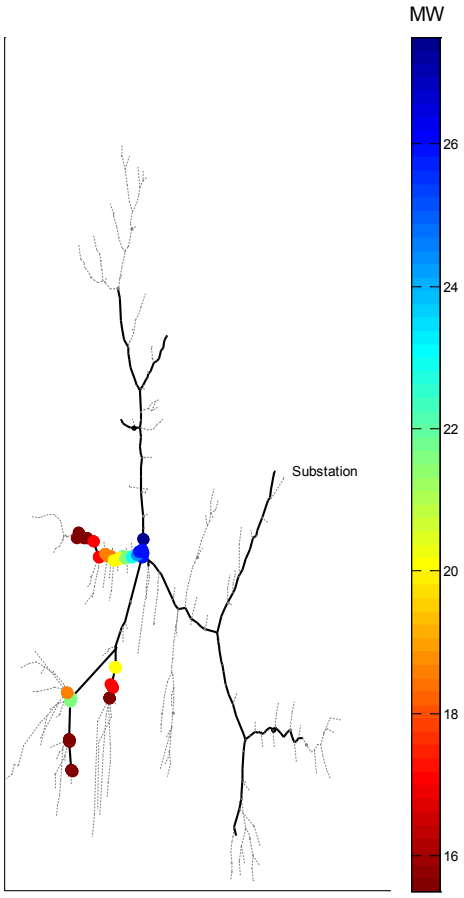

Figure 62.
Maximum wind power at a bus that does not exceed overvoltage limits

3.3.3.2 Steady-State Analysis II—Line and Transformer Ratings

Total wind power outputs of up to 18 MW are used to test the amount of wind power at each possible wind turbine location that would not exceed any line ratings within the circuit. Figure 63 to Figure 65 show the results for each phase. The color bar indicates the maximum wind power that can be connected to that bus without exceeding line ratings. The lowest amount of wind power that can be tolerated is 4,500 kW for connections located farther from the substation. Because of the different line ratings, a relationship between the maximum wind power and resistance between the wind turbine location and the substation cannot be established in the same way as that shown in the previous section for voltage change. However, the results shown in the figures indicate that the line ratings are exceeded for lower levels of wind power compared to when only overvoltage limits were considered. Some buses located close to the substation never exceed line ratings when the wind power output is up to 18 MW. These results are expected, because power flow from wind turbines located near the substation to loads located downstream would be similar to power flow from the substation to loads located downstream.

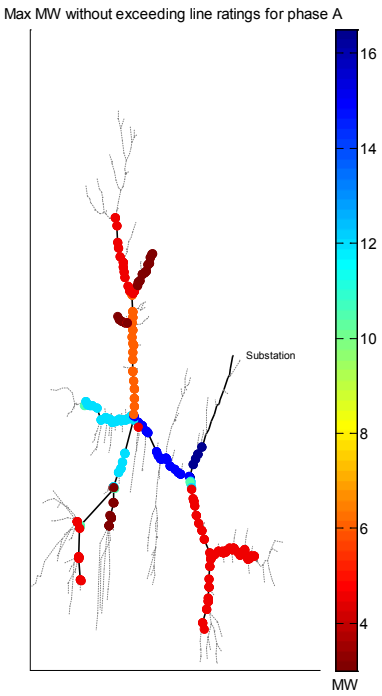

Figure 63.
Maximum wind power at a bus that does not exceed line ratings for Phase A

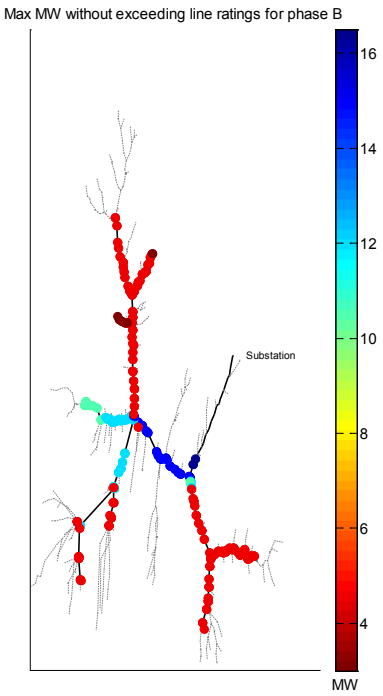

Figure 64.
Maximum wind power at a bus that does not exceed line ratings for Phase B

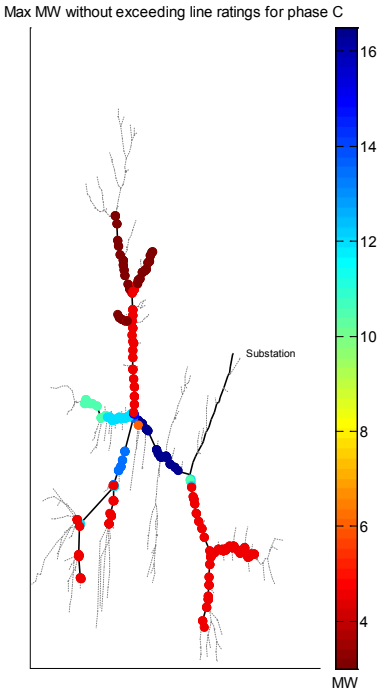

Figure 65.
Maximum wind power at a bus that does not exceed line ratings for Phase C

Next, the amounts of wind power that can be tolerated based on the regulator transformer ratings are tested. Feeder R1-12.47-1 has only one voltage regulator located at the substation. The total wind power output is set to 1,500 kW for each possible wind turbine location, and the apparent power through the regulator is extracted. The wind power output for each wind turbine location is increased by 1,500 kW, until the regulator transformer ratings (set to 30% above full load for the base case without wind power) are exceeded. Figure 66 to Figure 68 show the phase power through the substation regulator and the ratings of the regulator when the wind power is at 12 MW.

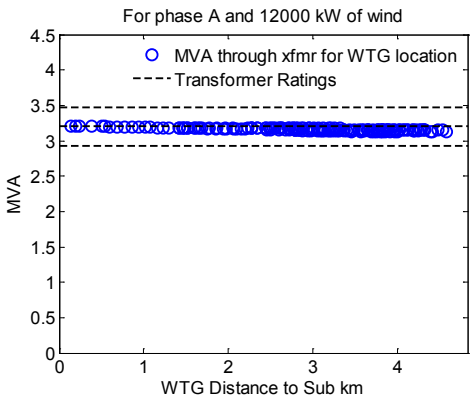

Figure 66.
Transformer MVA ratings and apparent power for Phase A

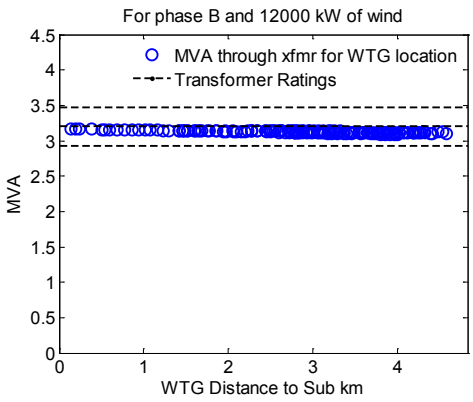

Figure 67.
Transformer MVA ratings and apparent power for Phase B

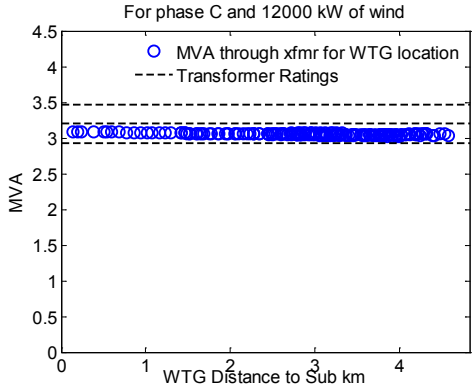

Figure 68.
Transformer MVA ratings and apparent power for Phase C

Feeder R1-12.47-1 is able to tolerate 12 MW of wind power at all possible wind turbine locations without exceeding the regulator transformer ratings.

The maximum amounts of wind power that can be placed within feeder R1-12.47-1 are given in Figure 69. The maximum wind power that this particular circuit can tolerate for each possible location is limited by the line ratings or the substation regulator transformer rating. The amount of wind power that can be connected to the circuit without exceeding overvoltage limits is very high compared to limits set by equipment ratings. Note that this is not necessarily true for all feeders and cannot be considered a general conclusion.

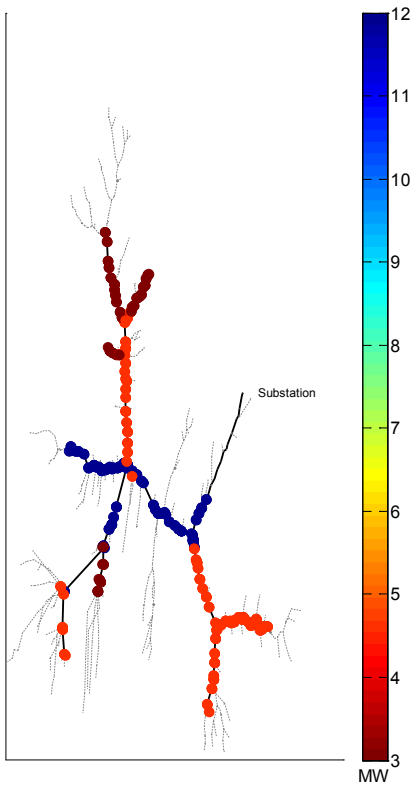

Figure 69.
Maximum wind power for each wind turbine location that does not exceed line ratings, substation regulator transformer ratings, and overvoltage limits

3.3.4 Conclusions for Feeder R1-12.47-1

Wind turbine locations and maximum wind power output for each of these locations were tested against consumer voltage tolerances and equipment ratings for feeder R1-12.47-1. The first step was to determine the maximum amount of wind power that each wind turbine location could tolerate without exceeding the ANSI overvoltage limits. When wind turbines are located farther from the substation, or when there is larger resistance between the wind turbine bus and the substation, the circuit could tolerate lower amounts of wind power than when wind turbines are located closer to the substation. Also, feeder R1-12.47-1 is able to tolerate large amounts of wind power in most locations throughout the circuit without exceeding any overvoltage limits. Line ratings were the first type of equipment that was examined. The overhead and underground lines have different line ratings for different sections of the circuit. Different wind turbine locations and wind power outputs were tested. The results show that the line ratings further limit the amount of power that can be added. Next, the regulator transformer rating was examined. The line and transformer ratings combined limit the amount of wind power that can be added to the feeder. The relationship between the resistance from the wind turbine bus to the substation and the maximum voltage rise was also quantified and will be compared to the other taxonomy feeder resistance and voltage rise relationships to determine a generalized guideline for circuit-based wind turbine siting.

3.4 Results for Feeder R4-12.47-1

Taxonomy feeder R4-12.47-1 is analyzed in this section. The taxonomy feeder serves a heavily populated urban area and a lightly populated rural area connected through the primary feeder. The urban load is located near the substation, and the rural load is located farther from it. The feeder consists of approximately 92% overhead lines and 8% underground lines [21]. The following sections provide circuit details and steady-state analysis results for feeder R4-12.47-1.

3.4.1 Circuit Load Description

This section describes the load for feeder R4-12.47-1. Table 10 shows the real, reactive, and apparent power through the substation bus for each phase when the capacitor banks are switched open and the control mode is turned off for the power flow solution.

Table 10. Real and Reactive Power for Each Phase Through the Substation

Phase	kW	kVar	kVA
Phase A	1,870.4	1,019.1	2,130.1
Phase B	1,637.9	9,01.8	1,869.7
Phase C	1,846.3	998.6	2,099.0
Total	5,354.6	2,919.5	6,098.8

The distributions of load throughout the feeder for phases A, B, and C are shown in Figure 70, Figure 71, and Figure 72, respectively. The diameter of the circles representing the loads is proportional to the size of each kilowatt load for each phase. As stated earlier, the majority of the load is in a heavily populated urban area. The more heavily loaded urban area is near the substation in all three phases.

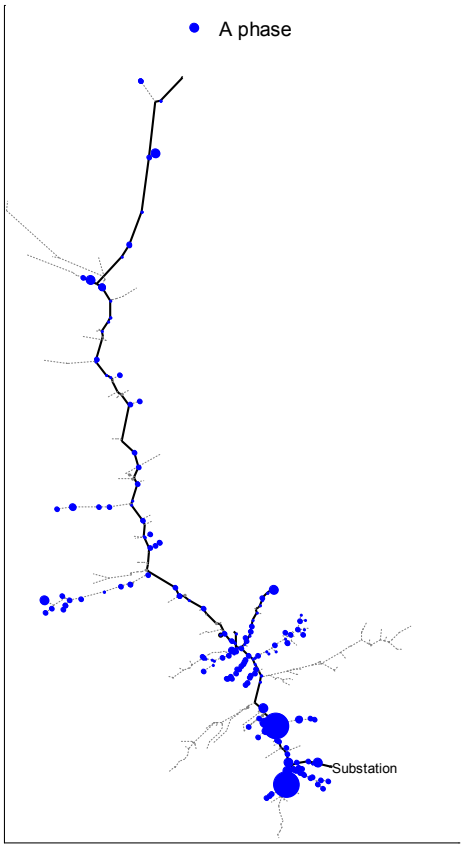

Figure 70.
Feeder R4-12.47-1. Phase A load distribution

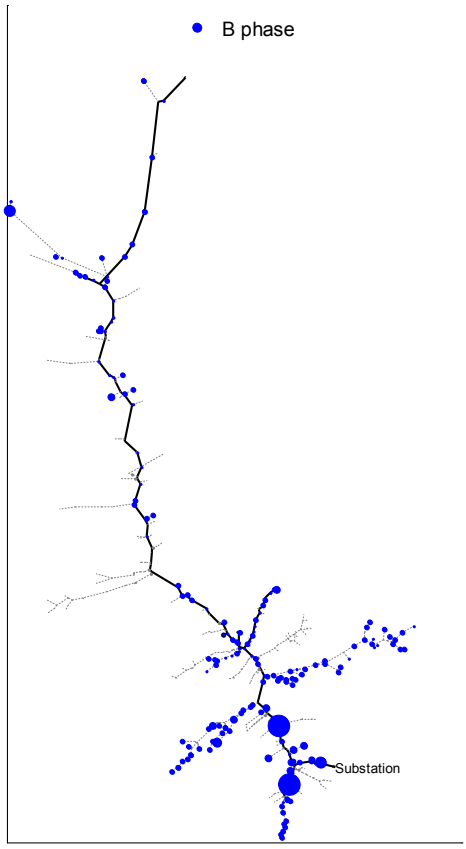

Figure 71.
Feeder R4-12.47-1. Phase B load distribution

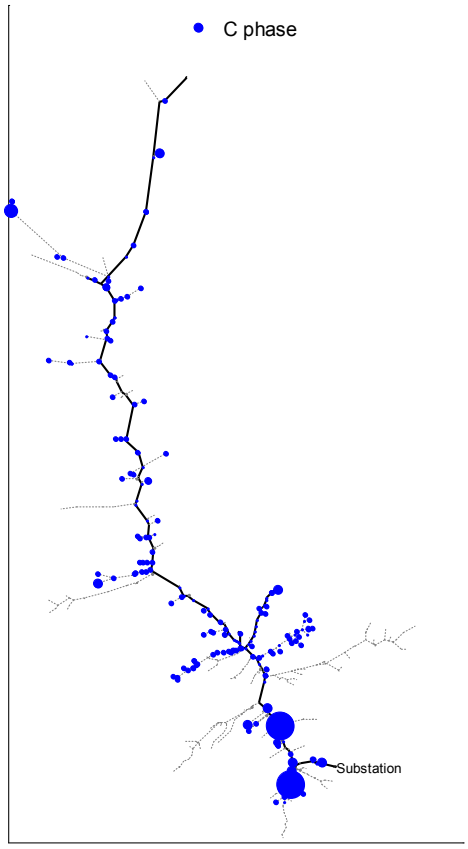

Figure 72.
Feeder R4-12.47-1. Phase C load distribution

To create low-load conditions, all loads attached to the circuit are uniformly scaled to a fraction of the total load.

3.4.2 Circuit Voltage-Regulation Devices

The circuit has four three-phase capacitor banks and two single-phase capacitor banks. One step-voltage regulator is located at the substation. The locations of these devices are shown in Figure 73.

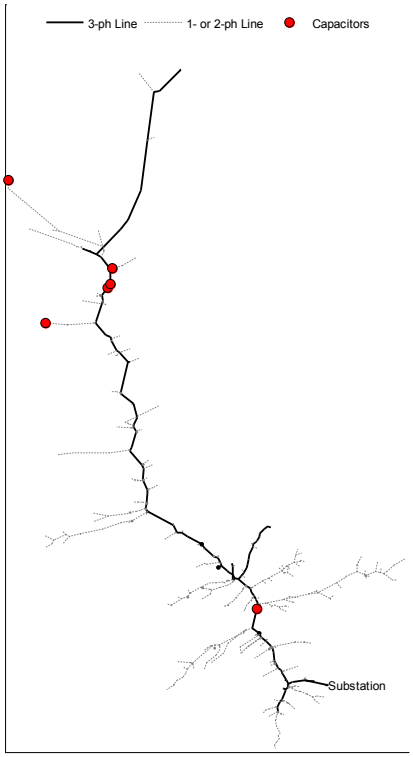

Figure 73.
Feeder R4-12.47-1. Substation and capacitor bank locations

3.4.3 Wind Turbine Location Impact—Steady-State Analysis

A similar analysis to what was used to determine the maximum wind power for possible feeder wind turbine locations is applied to feeder R4-12.47-1. First, the overvoltage limits are used to determine the maximum amount of wind power that can be added to the feeder. Also, the relationship between the maximum rise in voltage and the resistance from the wind turbine bus is identified. Next, the line and transformer ratings are used to determine if the maximum wind power connected to the circuit is further limited.

For feeder R4-12.47-1, all 130 possible wind turbine connections are shown in Figure 44. A wind turbine connection to a feeder bus is considered in the analysis if the feeder bus is connected to a three-phase line.

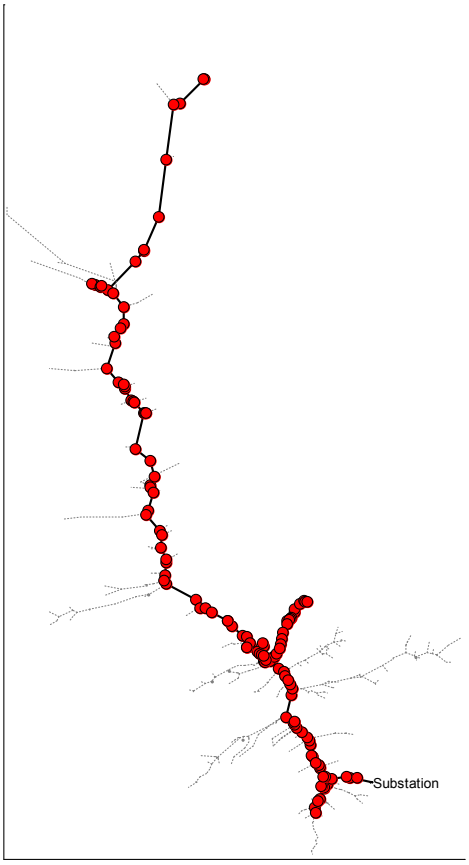

Figure 74.
Possible wind turbine connections for feeder R4-12.47-1

3.4.3.1 Steady-State Analysis I—Overvoltage Limits

The steady-state voltage analysis compares the voltages at every bus in the circuit to two scenarios: before wind turbines are added to the circuit and after wind turbines are added to the circuit. The changes that occur to bus voltages in Phase A are shown below.

Examples in the figures below show the best and worst wind turbine locations in terms of changes in voltage. For the power flow solution, the capacitor banks are switched open, the voltage-regulation device controls are turned off, and the circuit is at full load. The wind power output for the cases shown below is set to 4,500 kW.

Figure 75 shows the voltage profiles for the feeder when wind turbines are located near the substation at Bus 381. Figure 76 shows the voltage profiles for the feeder when wind turbines are located near the end of the feeder away from the substation at Bus 46. The distances of the wind turbines from the substation are indicated in the figures. In both figures, the voltage profiles when wind turbines are connected (black) to the feeder are compared to the voltage profile of the feeder without wind turbines (blue).

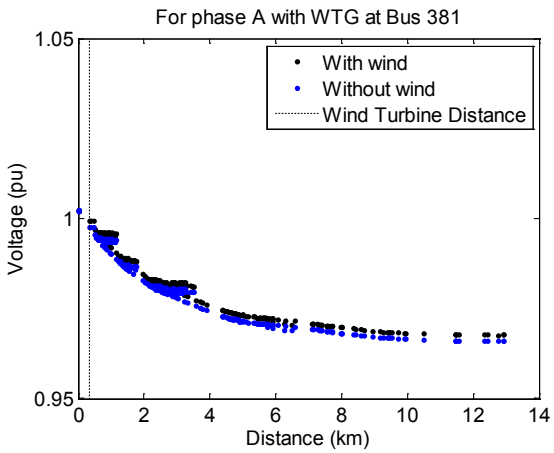

Figure 75.
Feeder R4-12.47-1. Phase A voltage profiles without wind and with 4,500 kW of wind power connected to Bus 381

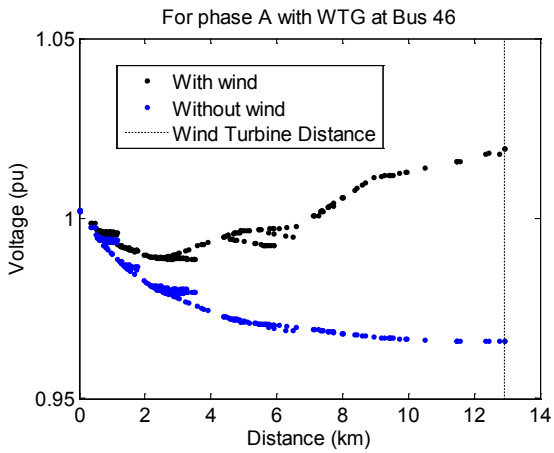

Figure 76.
Feeder R4-12.47-1. Phase A voltage profiles without wind and with 4,500 kW of wind power connected to Bus 46

Figure 75 and Figure 76 show that the ends of the laterals experience low per-unit voltage before wind turbines are added to Bus 381 and Bus 46. When wind turbines are connected to Bus 381, the bus voltages experience a low increase in voltage, as shown in Figure 77. When wind turbines are added to Bus 46, the bus voltages near the wind turbine connection experience a larger increase, as shown in Figure 78.

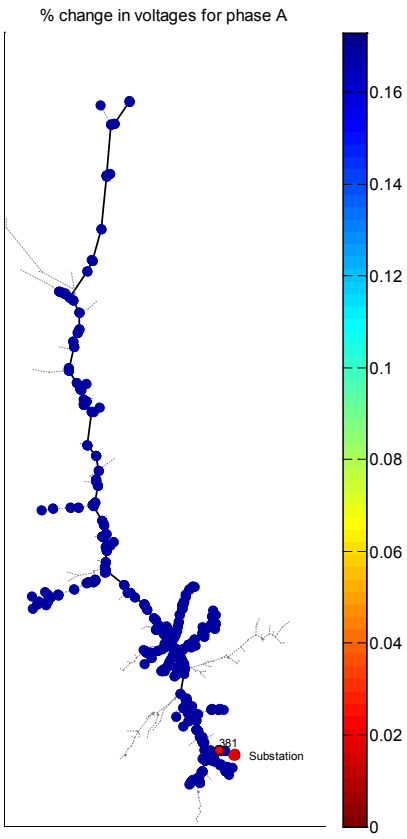

Figure 77.
Feeder R4-12.47-1. Heat map of Phase A change in bus voltage with 4,500 kW of wind power connected to Bus 381

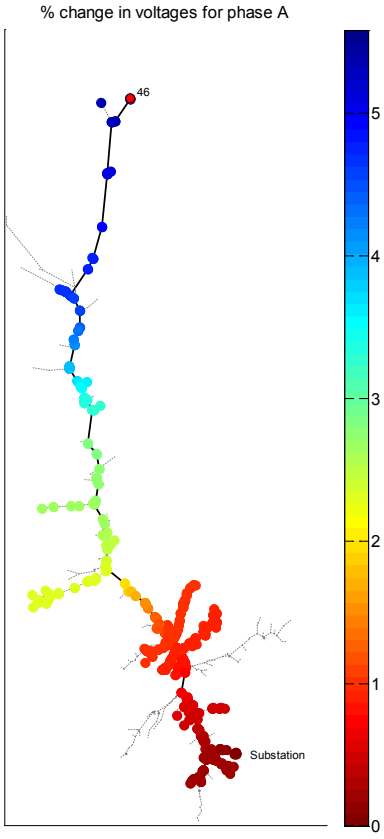

Figure 78.
Feeder R4-12.47-1. Heat map of Phase A change in bus voltage with 4,500 kW of wind power connected to Bus 46

Figure 79 shows the same voltage profiles but for 33% of full load when wind turbines are connected to Bus 381, and Figure 80 shows the same voltage profiles for 33% of full load when wind turbines are connected to Bus 46. When load is lower, the bus voltages at the end of the feeder do not experience as high of a voltage drop compared to that of the case with full load. The changes in voltage when wind turbines are added to Bus 381 and Bus 46 are shown in Figure 81 and Figure 82, respectively.

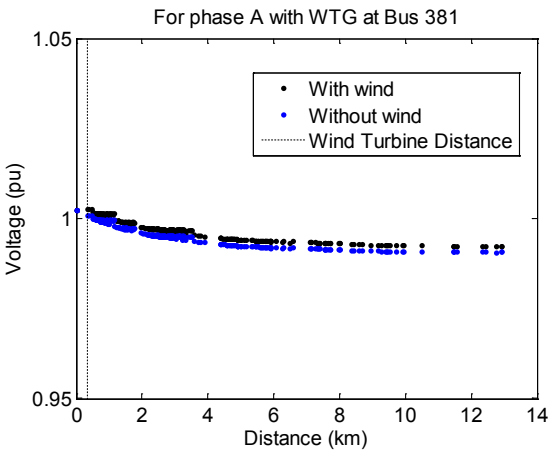

Figure 79.
Feeder R4-12.47-1. Phase A voltage profiles with 33% of full load without wind and with 4,500 kW of wind power connected to Bus 381

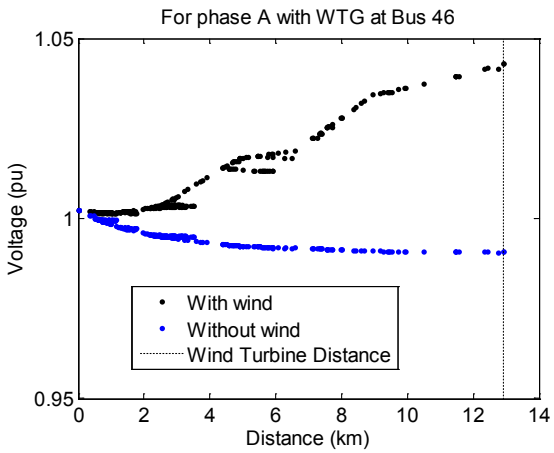

Figure 80.
Feeder R4-12.47-1. Phase A voltage profiles with 33% of full load without wind and with 4,500 kW of wind power connected to Bus 46

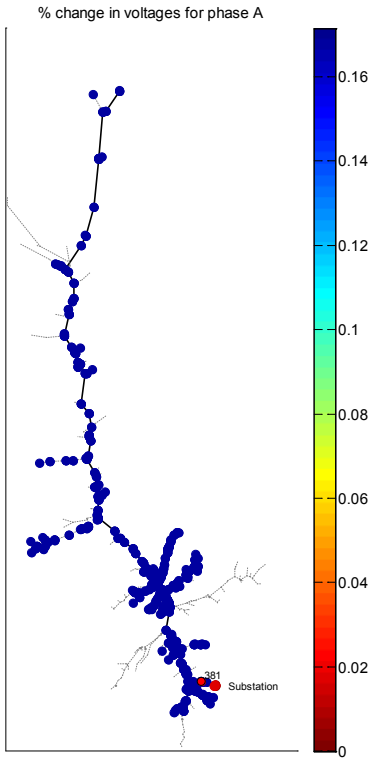

Figure 81.
Feeder R4-12.47-1. Heat map of Phase A change in bus voltage with 33% of full load with 4,500 kW of wind power connected to Bus 381

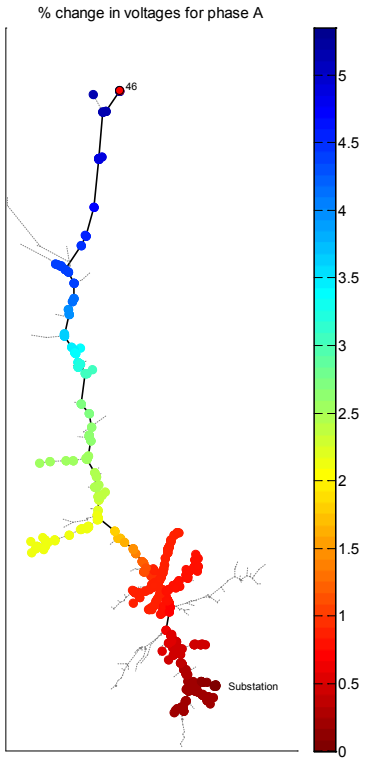

Figure 82.
Feeder R4-12.47-1. Heat map of Phase A change in bus voltage with 33% of full load with 4,500 kW of wind power connected to Bus 46

3.4.3.1.1 Voltage Rise Quantified and Feeder Overvoltage Limits

As previously mentioned, the maximum voltage rise is related to the phase resistance between the WTG bus and the substation. The relationship between the maximum change in voltage for each possible wind turbine location in the feeder and the resistance between the wind turbine bus and the substation is shown in Figure 83 and Figure 84 for different wind power outputs and during full load. The correlation coefficient between the two variables in Figure 83 is 0.994, and it is the worst fit for wind power output and load levels. Even though this is the worst fit in the analysis for this feeder, the correlation coefficient is still nearly 1. The correlation coefficient in Figure 84 is 0.999, and it represents the best fit for wind power output and load levels. The flattening at the end is caused by very small loads near the ends of the single-phase laterals.

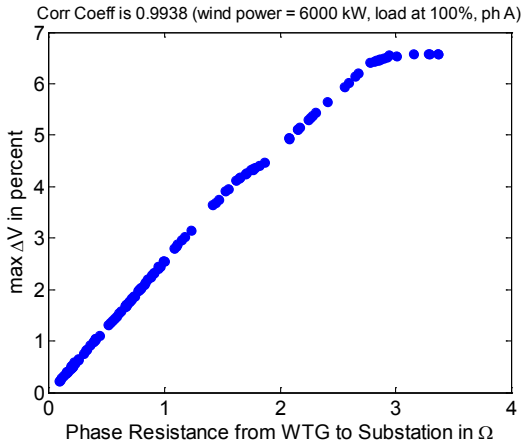

Figure 83.
Relationship between Phase A max change in voltage and phase resistance to WTG with 6,000 kW of wind power and 100% load

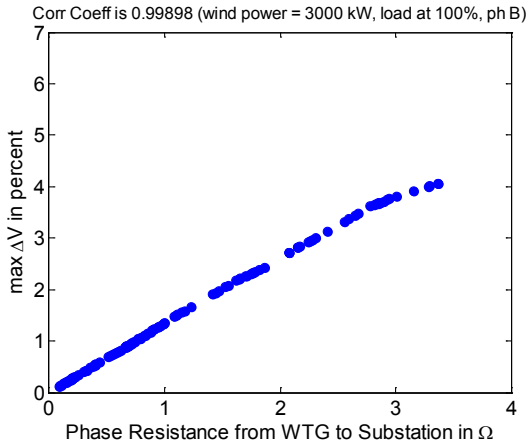

Figure 84.
Relationship between Phase B max change in voltage and phase resistance to WTG with 3,000 kW of wind power and 100% load

Using linear regression (polyfit function in MATLAB with degree n set to one), the regression coefficients (p_1 and p_2) are given in Table 11. The same analysis is applied to all three phases for 3,000 kW, 4,500 kW, and 6,000 kW of wind power and 33%, 67%, and 100% of full load. The RSS between the power flow data and the model from the equation is given in the table for each wind power and load scenario. These results will be used in the final analysis to determine a generalized relationship between the placement of wind turbines and voltage rise.

Table 11. Relationship Between Max Change in Voltage and Phase Resistance to WTG for Varying Amounts of Load and Wind Power

Wind Power (kw)	Fraction of Load Online	Instantaneous Wind Penetration (%)	Phase	Correlation Coefficient	P_1	P_2	RSS
3,000	0.33	164.4	1	0.9986	1.225	0.061	0.4849
		164.4	2	0.9988	1.217	0.060	0.4279
		164.4	3	0.9988	1.258	0.049	0.4573
	0.66	83.5	1	0.9986	1.257	0.058	0.5208
		83.5	2	0.9989	1.241	0.054	0.4044

		83.5	3	0.9988	1.322	0.032	0.4728
	0.99	56.6	1	0.9985	1.289	0.054	0.5609
		56.6	2	0.9990	1.266	0.049	0.3812
		56.6	3	0.9989	1.386	0.015	0.4988
4,500	0.33	246.6	1	0.9969	1.691	0.144	2.0959
		246.6	2	0.9971	1.680	0.141	1.9137
		246.6	3	0.9970	1.734	0.128	2.0671
	0.66	125.3	1	0.9968	1.734	0.141	2.2553
		125.3	2	0.9973	1.712	0.135	1.8665
		125.3	3	0.9971	1.819	0.108	2.1997
	0.99	84.8	1	0.9967	1.777	0.137	2.4243
		84.8	2	0.9974	1.745	0.128	1.8254
		84.8	3	0.9972	1.904	0.088	2.3572
6,000	0.33	328.9	1	0.9941	2.071	0.255	5.9315
		328.9	2	0.9944	2.057	0.251	5.5205
		328.9	3	0.9943	2.122	0.238	5.9919
	0.66	167.1	1	0.9939	2.123	0.253	6.3806
		167.1	2	0.9947	2.096	0.244	5.4791
		167.1	3	0.9944	2.222	0.218	6.5118
	0.99	113.1	1	0.9938	2.174	0.251	6.8641
		113.1	2	0.9949	2.135	0.237	5.4452
		113.1	3	0.9944	2.322	0.197	7.0975

The next step is to determine the maximum amount of wind power that can be connected to the circuit at each possible wind turbine location without exceeding ANSI overvoltage limits. Each possible wind turbine location will be connected to an increasing amount of wind power, starting with 1,500 kW, until overvoltage limits are reached. Wind power output is tested up to 16,500 kW. The entire circuit load is reduced to 33% of full load. The results of this analysis are given for each phase in Figure 85. The x-axis is the resistance from the wind turbine bus to the substation, and the y-axis is the maximum wind power that is connected to that bus location that does not exceed overvoltage limits. *Figure 85 shows that the larger the resistance between the wind turbine location and the substation, the lower the amount of wind power the circuit can tolerate when voltage rise is the only factor taken into consideration.*

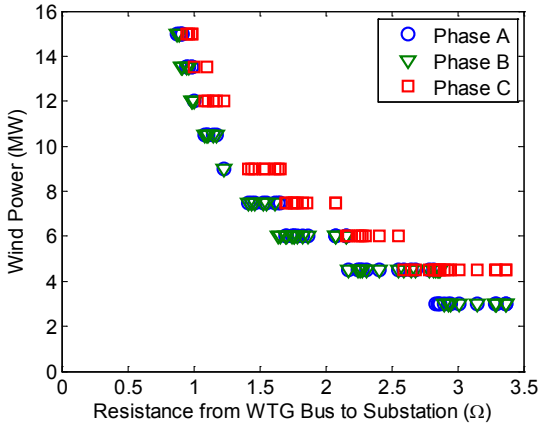

Figure 85.
Maximum wind power that can be tolerated for wind turbine resistance to substation when only overvoltage limits are considered

Figure 86 shows the bus locations and the maximum amount of wind power that can be placed at the bus without exceeding overvoltage limits. Wind turbines located near the substation are able to tolerate high amounts of wind power exceeding the 16,500 kW that were tested in this analysis.

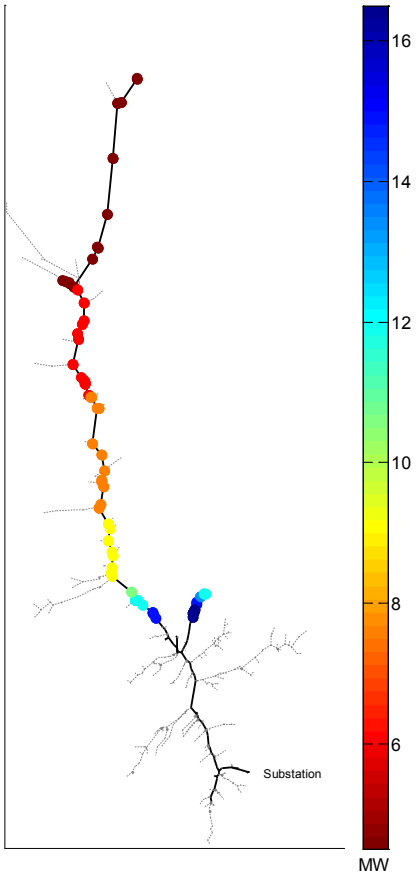

Figure 86.
Maximum wind power at a bus that does not exceed overvoltage limits

3.4.3.2 Steady-State Analysis II—Line and Transformer Ratings

Total wind power outputs of up to 16.5 MW are used to test the amount of wind power at each possible wind turbine location that would exceed any line ratings within the circuit. Figure 87 to Figure 89 show the results for each phase. The color bar indicates the maximum wind power that can be connected to that bus without exceeding line ratings. The lowest amount of wind power that can be tolerated is 3,000 kW for connections located farther from the substation. Because of the different line ratings, a relationship between the maximum wind power and resistance between the wind turbine location and the substation cannot be established in the same way as that shown in the previous section for voltage change. However, the results shown in the figures indicate that the line ratings are exceeded for lower levels of wind power compared to when only overvoltage limits are considered.

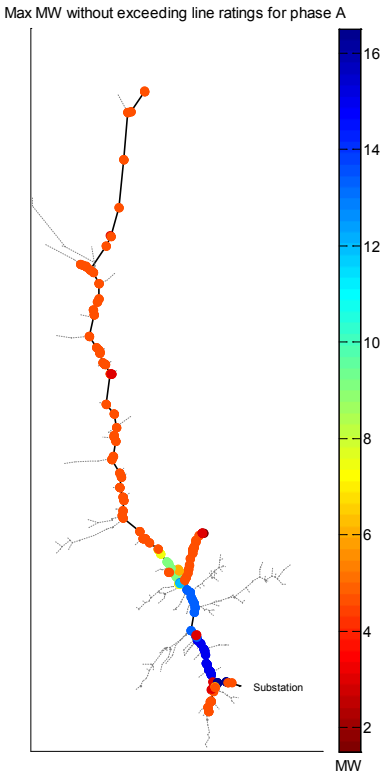

Figure 87.
Maximum wind power at each bus that does not exceed line ratings for Phase A

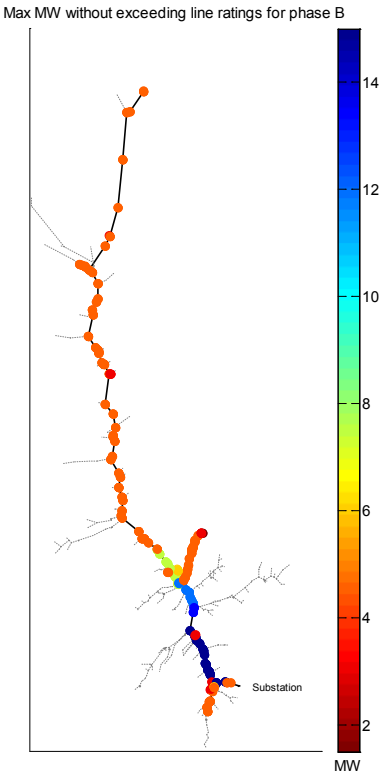

Figure 88.
Maximum wind power at each bus that does not exceed line ratings for Phase B

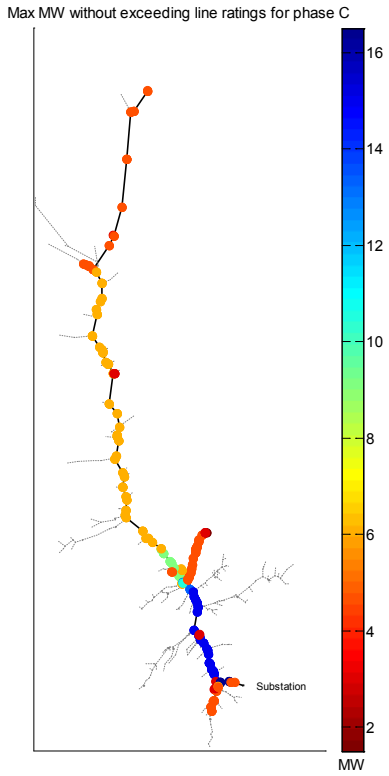

Figure 89.
Maximum wind power at each bus that does not exceed line ratings for Phase C

Next, the amounts of wind power that can be tolerated based on the regulator transformer ratings are tested. Feeder R4-12.47-1 has only one voltage regulator located at the substation. The total wind power output is set to 1,500 kW for each possible wind turbine location, and the apparent power through each regulator is extracted. The ratings (set to 30% above full load for the base case without wind power) are also included to indicate conditions when the ratings are exceeded. The wind power output for each wind turbine location is increased by 1,500 kW, until the regulator transformer ratings are exceeded. Figure 90 to Figure 92 show the phase power through the substation regulator and the ratings of the regulator when the wind power is at 10.5 MW.

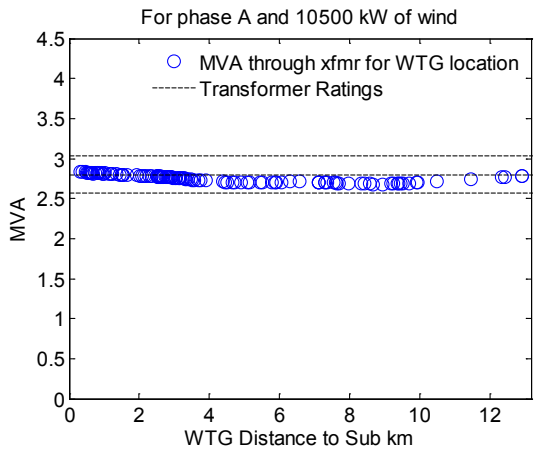

Figure 90.
Transformer MVA ratings and apparent powerr flows for Phase A

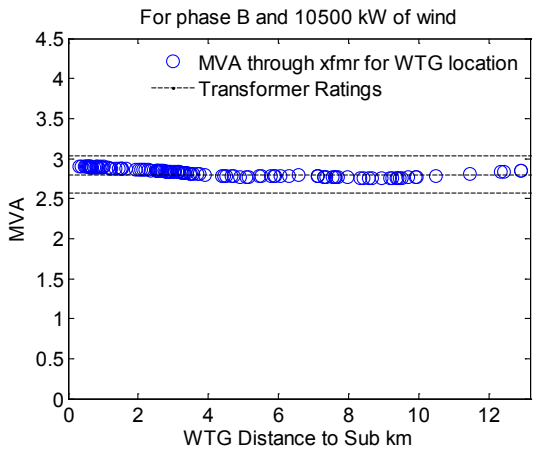

Figure 91.
Transformer MVA ratings and apparent powerr flows for Phase B

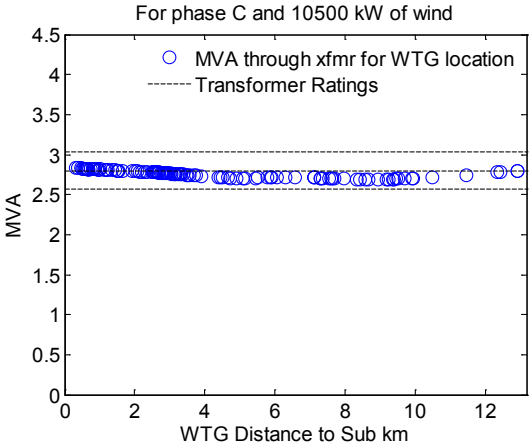

Figure 92.
Transformer MVA ratings and apparent powerr flows for Phase C

The maximum amounts of wind power that can be placed within feeder R4-12.47-1 are given in Figure 93. The maximum wind power that the circuit can tolerate for each possible location is limited by the line ratings or the substation regulator transformer rating. The amount of wind power that can be connected to the circuit without exceeding overvoltage limits is higher than the limits set by the equipment ratings.

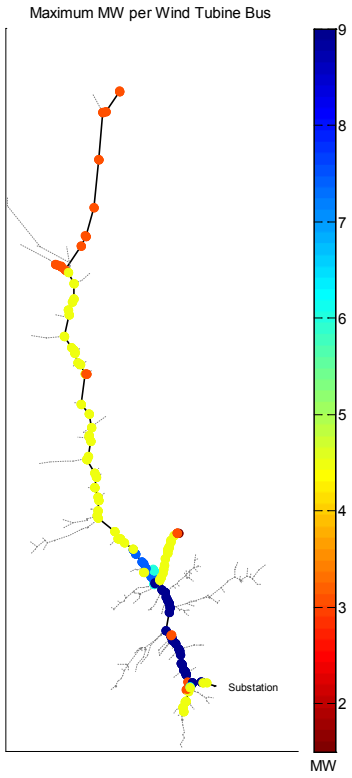

Figure 93.
Maximum wind power for each wind turbine location that does not exceed line ratings, substation regulator transformer ratings, and overvoltage limits

In Figure 93, it appears that wind turbines connected to buses located near the substation are limited to 4,500 kW of wind power output. A magnified view given in Figure 94 of the buses located near the substation shows that they are actually feeders that branch off the primary feeder. The line ratings for these branches are lower than the line ratings of the primary feeder—placing a lower limit on the amount of wind power that can be added to these locations.

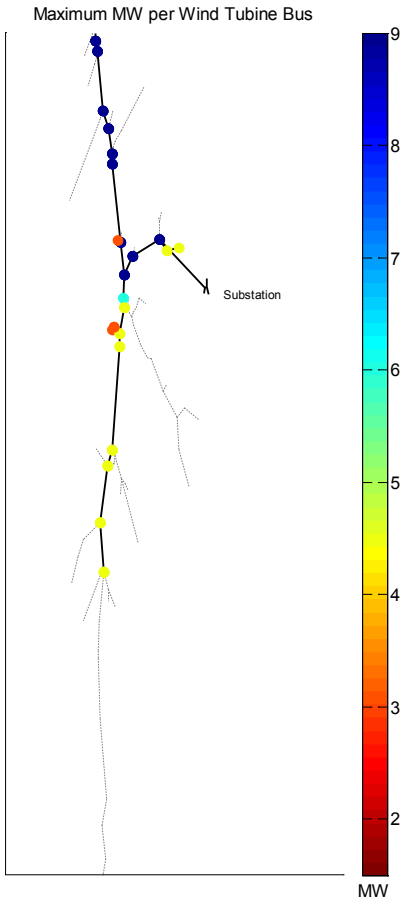

Figure 94.
Magnified view of the maximum wind power for each wind turbine location that does not exceed line ratings, substation regulator transformer ratings, and overvoltage limits

Table 12. Penetration for Each Level of Wind Power When Feeder R4-12.47-1 Is at Full Load

Wind Power (kW)	Penetration (% of Full Load)
1,500	24.59
3,000	49.19
4,500	73.78
6,000	98.38
7,500	122.97
9,000	147.57

3.4.4 Conclusions for Feeder R4-12.47-1

Wind turbine locations and maximum wind power output for each of these locations were tested against consumer voltage tolerances and equipment ratings for feeder R4-12.47-1. The first step was to determine the maximum amount of wind power that each wind turbine location could tolerate without exceeding the ANSI overvoltage limits. When wind turbines are located farther from the substation, or when there is larger resistance between the wind turbine bus and the substation, the circuit could tolerate lower amounts of wind power than when wind turbines are

located closer to the substation. Also, feeder R4-12.47-1 is able to tolerate large amounts of wind power in most locations throughout the circuit without exceeding any overvoltage limits. Line ratings were the first type of equipment that was examined. The overhead and underground lines have different line ratings for different sections of the circuit. Different wind turbine locations and wind power outputs were tested. The results show that the line ratings further limit the amount of power that can be added. Next, the regulator transformer rating was examined. The line and transformer ratings combined limit the amount of wind power that can be added to the feeder. The relationship between the resistance from the wind turbine bus to the substation and the maximum voltage rise was also quantified and will be compared to the other taxonomy feeder resistance and voltage rise relationships to determine a generalized guideline for circuit-based wind turbine siting.

3.5 Results for Feeder R5-12.47-3

Taxonomy feeder R5-12.47-3 is analyzed in this section. The taxonomy feeder serves a moderately populated rural area and consists of approximately 92% overhead lines and 8% underground lines [44].

The following sections provide circuit details and steady-state analysis results for feeder R5-12.47-3.

3.5.1 Circuit Load Description

This section describes the load distribution for feeder R5-12.47-3. From [42], the feeder has a low-load density spread throughout a large rural area, with most of the load located far from the substation. Load distributions for each phase are shown in Figure 95 to 97. The figures also indicate the substation locations.

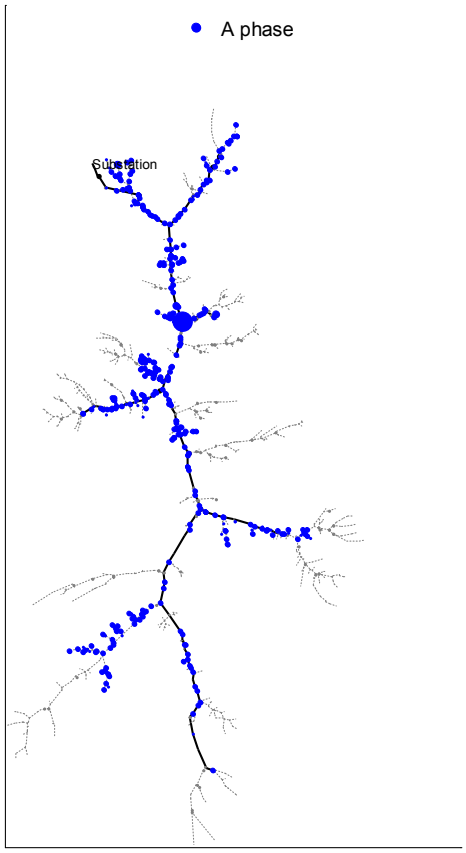

Figure 95.
Feeder R5-12.47-3. Phase A load distribution

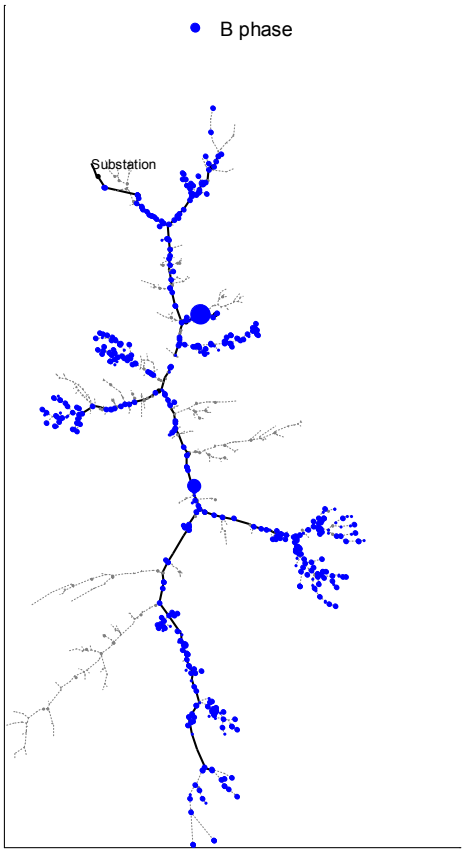

Figure 96.
Feeder R5-12.47-3. Phase B load distribution

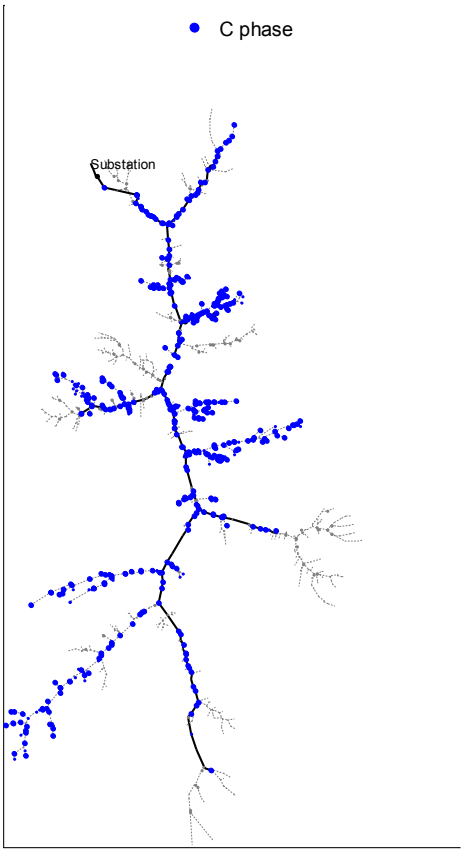

Figure 97.
Feeder R5-12.47-3. Phase C load distribution

Table 13 shows the real, reactive, and apparent power through the substation bus for each phase. The power flow solution for the circuit is solved when the regulator control mode is turned off and all capacitor banks are switched open. With the control mode turned off, the regulator tap changes do not occur for any regulators in the circuit. The circuit voltage-regulation devices are described in the next subsection.

Table 13. Real and Reactive Power for the Feeder When Capacitor Banks Are Switched Open and When Regulator Controls Are Turned Off

Phase	kW	kVar	kVA
Phase A	1,498.5	1,129.7	1,876.6
Phase B	1,798.8	1,475.8	2,326.7
Phase C	1,637.6	1,458.2	2,192.7
Total	4,934.8	4,063.7	6,392.7

The total kilowatt load in the feeder, equal to 6,392 kW, does not match the taxonomy feeder report kilowatt load of 9,200 kW. The total load in the feeder is calculated by summing all load objects from the original GLM file. However, for this particular feeder, the load is not altered to match the report. To create low-load conditions, all loads attached to the circuit are uniformly scaled to a fraction of the total load.

3.5.2 Circuit Voltage-Regulation Devices

The circuit has 13 capacitor banks and 4 step-voltage regulators located throughout. Capacitor banks 1, 2, and 5 are three-phase, and the remaining 8 capacitor banks are single-phase. Regulator 1 is located at the substation, and regulators 2, 3, and 4 are located along the primary feeder of the circuit. The locations of these devices are shown in Figure 98. The state of all voltage-regulation devices, such as the switch position of all capacitor banks and the control mode setting for regulators, is indicated for all analysis completed for this feeder.

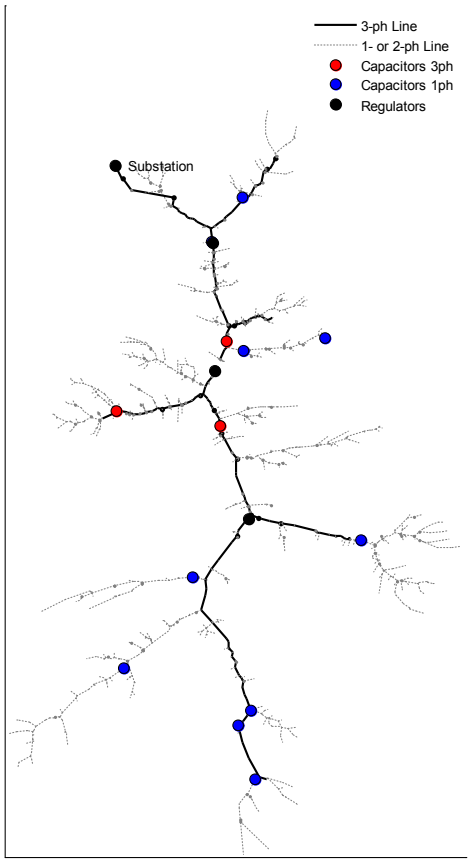

Figure 98.
Location of regulators and capacitor banks for feeder R5-12.47-3

3.5.3 Wind Turbine Location Impact—Steady-State Analysis

Steady-state analysis or snapshot mode is used for the analysis in this section. The impacts that wind power from each possible wind turbine location have on the bus voltages, current flows, and power flows are examined. If these values exceed ANSI C84.1-2011 Range A, then either the number of wind turbines must be reduced or the location of the wind turbines must be altered.

Figure 99 shows each of the possible wind turbine locations for the circuit for feeder R5-12.47-3. A total of 216 possible wind turbine locations are analyzed for this feeder. The method used to describe the selection of possible wind turbine locations is described in Section 2.3.

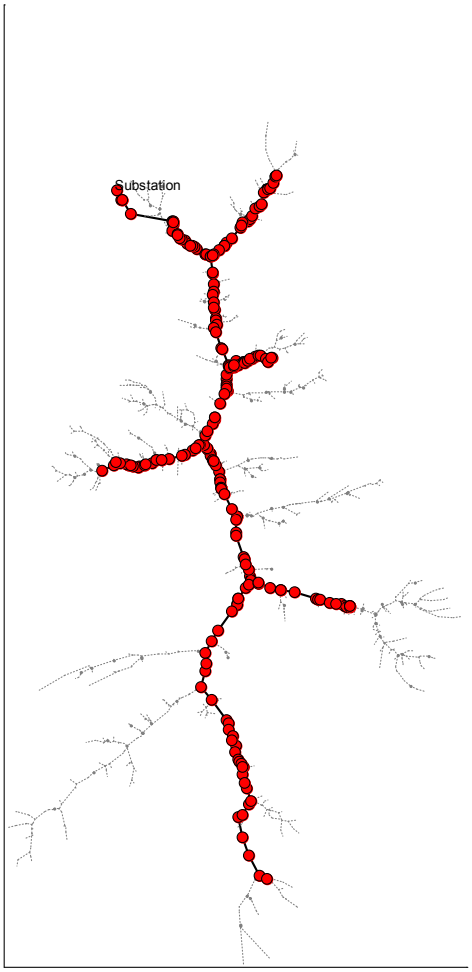

Figure 99.
Possible wind turbine connections for feeder R5-12.47-3

The following sections will determine the maximum amount of wind power that can be added to each of the possible locations shown above without exceeding the ANSI overvoltage limits, the feeder line ratings, and transformer ratings. Also, the quantitative relationship between the phase resistance between the wind turbine bus and the substation to the maximum change in voltage caused by wind power at each location is provided.

3.5.3.1 Steady-State Analysis I—Overvoltage limits

The steady-state voltage analysis compares the voltages at every bus in the circuit to two scenarios: before wind turbines are added to the circuit and after wind turbines are added to the circuit. The changes in bus voltages are shown below. Because the distribution feeder consists of three phases with some single-phase laterals, the bus voltages are separated by phase. The changes in Phase B voltages are shown. Results are similar for Phase A and Phase C. For the

power flow solution, capacitor banks 1, 2, and 5 are switched closed, and the control mode is turned off so that the regulator controls do not adjust the regulator tap positions. The wind power output for each wind turbine location is set to 4,500 kW during full-load conditions.

Figure 100 shows the voltage profiles for the feeder when wind turbines are located near the substation at Bus 907. Figure 101 shows the voltage profiles for the feeder when wind turbines are located near the end of the feeder away from the substation at Bus 1,054. The distances of the wind turbines from the substation are indicated. In both figures, the voltage profiles when wind turbines are connected (black) to the feeder are compared to the voltage profile of the feeder without wind turbines (blue). Obviously, feeder voltage levels would not be allowed to reach the levels shown in Figure 100 and Figure 101, which is why the regulators and capacitors are installed. Nonetheless, this analysis provides some indication of the feeder limits and possible benefits of WTGs when no voltage support equipment is available.

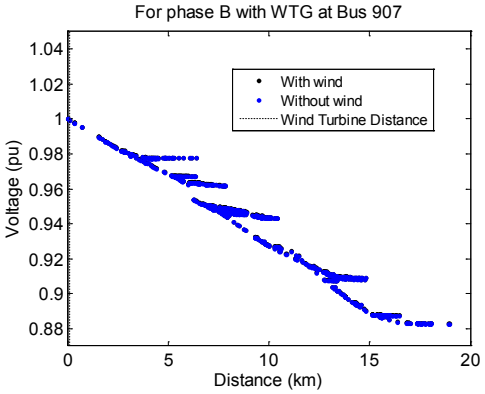

Figure 100.
Feeder R5-12.47-3. Phase B voltage profiles without wind and with 4,500 kW of wind power connected to Bus 907

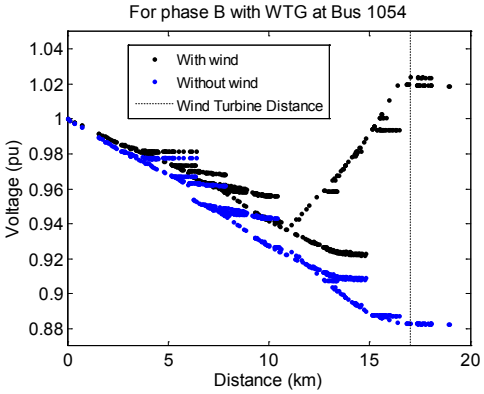

Figure 101.
Feeder R5-12.47-3. Phase B voltage profiles without wind and with 4,500 kW of wind power connected to Bus 1,054

Figure 100 shows that the wind turbine is located near the end of the feeder at Bus 1,054. When the wind turbine is located near the substation, the difference between the bus voltages before and after wind turbines are connected is very small. The percent change in each bus voltage is shown in the circuit in Figure 102. A heat map of the feeder is used to show the small percent change in voltage (approximately 0.03%) and to show that the change in voltage is uniform across the entire feeder for Phase B.

Figure 103 shows the percent change in each bus voltage when wind turbines are added to Bus 1,054. Both Figure 101 and Figure 103 show that the change in voltage is greatest near the wind turbine connection. When 4,500 kW of wind power is connected to this bus, the maximum voltage increase for Phase B is approximately 15%.

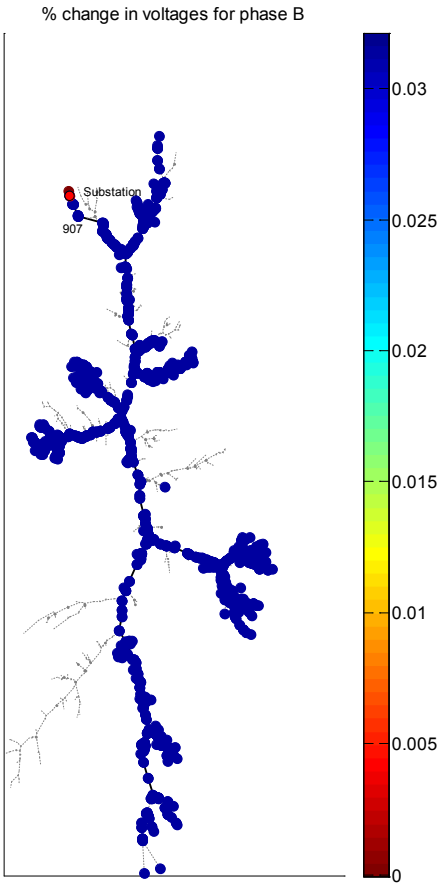

Figure 102.
Feeder R5-12.47-3. Heat map of Phase B change in bus voltage with 4,500 kW of wind power connected to Bus 907

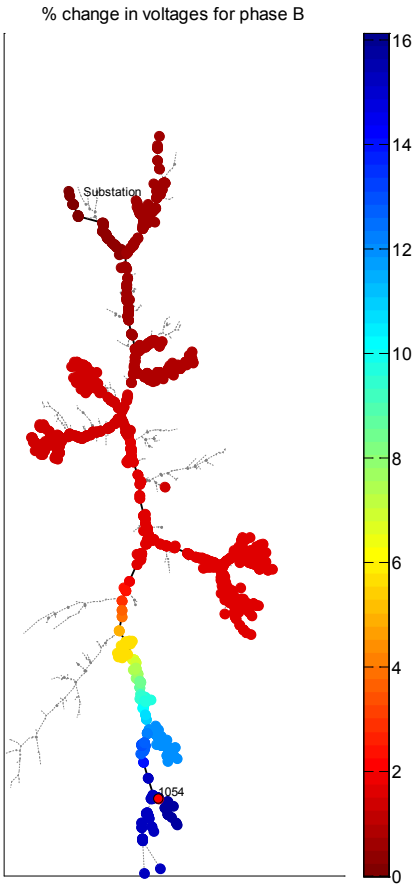

Figure 103.
Feeder R5-12.47-3. Heat map of Phase B change in bus voltage with 4,500 kW of wind power connected to Bus 1,054

The same analysis is done when the load is set to 33% of full load and the voltage-regulation device settings are not altered. The change in voltage for both wind turbine locations, shown in Figure 106 for Bus 907 and Figure 107 for Bus 1,054, is approximately the same when the load is 33% full. However, as shown in Figure 105, when the wind turbine is located at Bus 1,054, the bus voltages are near 1.15 per unit—much higher than the ANSI overvoltage limits. The voltage limits will be further explored in the next section.

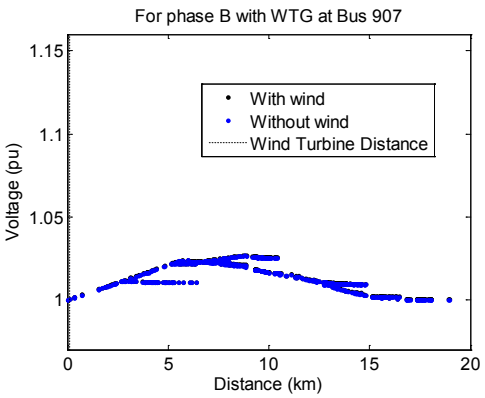

Figure 104.
Feeder R5-12.47-3. Phase B voltage profiles with 33% of full load without wind and with 4,500 kW of wind power connected to Bus 907

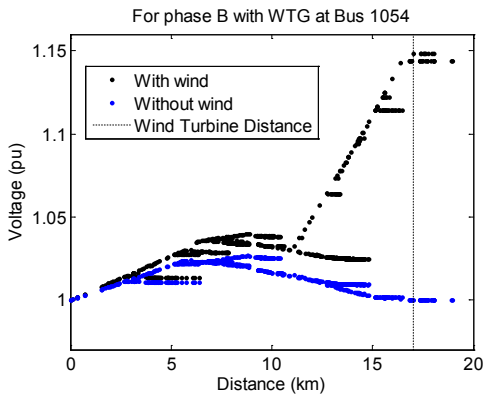

Figure 105.
Feeder R5-12.47-3. Phase B voltage profiles with 33% of full load without wind and with 4,500 kW of wind power connected to Bus 1,054

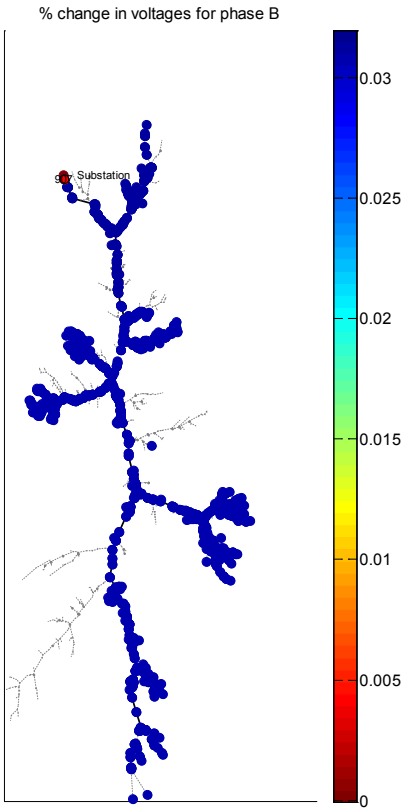

Figure 106.
Feeder R5-12.47-3. Heat map of Phase B change in bus voltage with 33% of full load and with 4,500 kW of wind power connected to Bus 907

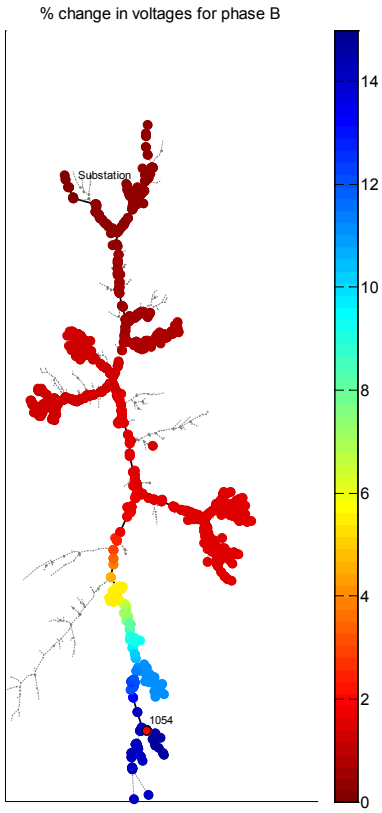

Figure 107.
Feeder R5-12.47-3. Heat map of Phase B change in bus voltage with 33% of full load and with 4,500 kW of wind power connected to Bus 1,054

3.5.3.1.1 Overvoltage Limits/Quantitative Relationship

As previously mentioned, the maximum voltage rise is related to the phase resistance between the WTG bus and the substation. The relationship between the maximum change in voltage for each possible wind turbine location in the feeder and the resistance between the wind turbine bus and the substation is shown in Figure 108 and Figure 109. The correlation coefficient between the two variables in Figure 108 is 0.996, and it is the best fit for wind power output and load levels. The correlation coefficient in Figure 109 is 0.992, and it represents the worst fit for wind power output and load levels. Even though this is the worst fit in the analysis, the correlation coefficient is still nearly 1.

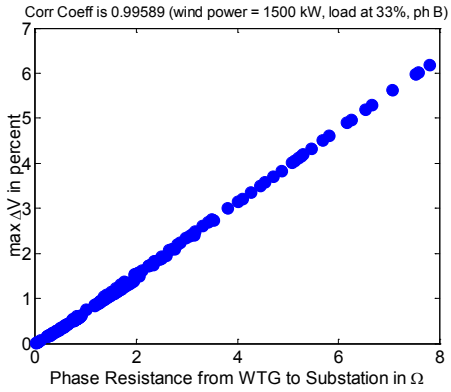

Figure 108.
Relationship between Phase B max change in voltage and phase resistance to WTG with 33% load and 1,500 kW of wind power

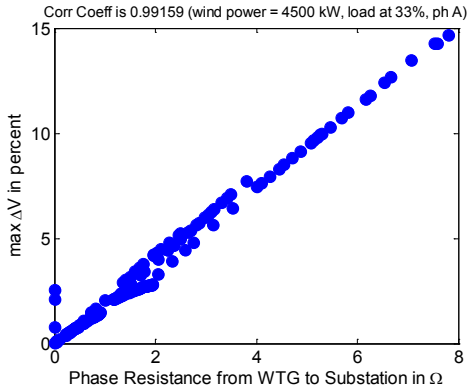

Figure 109.
Relationship between Phase B max change in voltage and phase resistance to WTG with 33% load and 4,500 kW of wind power

Using linear regression (polyfit function in MATLAB with degree n set to one), the regression coefficients (p_1 and p_2) are given in Table 14. The same analysis is applied to all three phases for 1,500 kW, 3,000 kW, and 4,500 kW of wind power and 33%, 67%, and 100% of full load. The RSS between the power flow data and the model from the equation is given in the table for each wind power and load scenario.

Table 14. Relationship Between Max Change in Voltage and Phase Resistance to WTG for Varying Amounts of Load and Wind Power

Wind Power (kw)	Fraction of Load Online	Instantaneous Wind Penetration (%)	Phase	Correlation Coefficient	P_1	P_2	RSS
1,500	0.33	83.4	1	0.9950	0.737	-0.051	2.9348
		83.4	2	0.9959	0.796	-0.065	2.8233
		83.4	3	0.9956	0.763	-0.046	2.7834
	0.66	43.8	1	0.9952	0.767	-0.055	3.0452
		43.8	2	0.9958	0.886	-0.091	3.5764
		43.8	3	0.9958	0.821	-0.050	3.0560
	0.99	30.7	1	0.9951	0.794	-0.058	3.3663
		30.7	2	0.9953	0.965	-0.117	4.7623
		30.7	3	0.9956	0.888	-0.057	3.7302
3,000	0.33	166.8	1	0.9936	1.360	-0.079	12.7779
		166.8	2	0.9953	1.461	-0.097	10.9440
		166.8	3	0.9946	1.406	-0.068	11.5964
	0.66	87.7	1	0.9940	1.413	-0.082	12.9695
		87.7	2	0.9959	1.616	-0.132	11.6936
		87.7	3	0.9952	1.508	-0.068	11.7563
	0.99	61.3	1	0.9944	1.471	-0.087	13.2422
		61.3	2	0.9957	1.771	-0.176	14.4849
		61.3	3	0.9954	1.613	-0.074	12.9189
4,500	0.33	250.2	1	0.9916	1.905	-0.119	33.2892
		250.2	2	0.9940	2.029	-0.124	27.0292
		250.2	3	0.9929	1.989	-0.132	30.3750

	0.66	131.5	1	0.9921	1.970	-0.111	33.4007
		131.5	2	0.9952	2.229	-0.157	25.6812
		131.5	3	0.9940	2.094	-0.085	28.6591
	0.99	92.0	1	0.9926	2.048	-0.111	33.6537
		92.0	2	0.9957	2.431	-0.206	27.5901
		92.0	3	0.9945	2.233	-0.086	29.5759

The results show that the steepness of the slope (indicated by the regression coefficient p_1) increases as both load increases and wind power increases and is not related to the penetration of wind power in the circuit. This means that for full load and 4,500 kW of wind power, the maximum voltage rise will be 2.23% per 1 Ω increase between the WTG and the substation.

The results shown in Table 14 indicate that the largest rise in voltage will occur for the wind turbine location with the greatest resistance between the wind turbine bus and the substation. The next step is to determine the maximum amount of wind power that can be connected to the circuit at each possible wind turbine location without exceeding ANSI overvoltage limits. Each possible wind turbine location will be connected to an increasing amount of wind power, starting with 1,500 kW, until overvoltage limits are reached. Wind power output is tested up to 15,000 kW. The entire circuit load is reduced to 33% of full load, and all three phase capacitor banks are switched open with voltage-regulator controls turned off. The results of this analysis are given for each phase in Figure 110. The x-axis is the resistance from the wind turbine bus to the substation, and the y-axis is the maximum wind power that is connected to that bus location that does not exceed overvoltage limits. *Figure 110 shows that the larger the resistance between the wind turbine location and the substation, the lower the amount of wind power the circuit can tolerate when voltage rise is the only factor taken into consideration.*

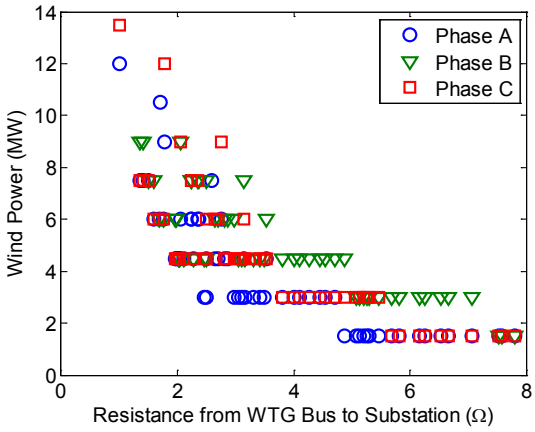

Figure 110.
Maximum wind power that can be tolerated for wind turbine resistance to substation when only overvoltage limits are considered

The bus locations and the maximum amount of wind power that can be placed at the bus without exceeding overvoltage limits are given in Figure 111. The color bar on the right of the figure show the amount of wind power, and the location of the wind turbine bus connection is shown on the circuit. For feeder R5-12.47-3, the wind turbines connected to buses located farthest from the substation tolerate the least amount of wind power (shown in dark red).

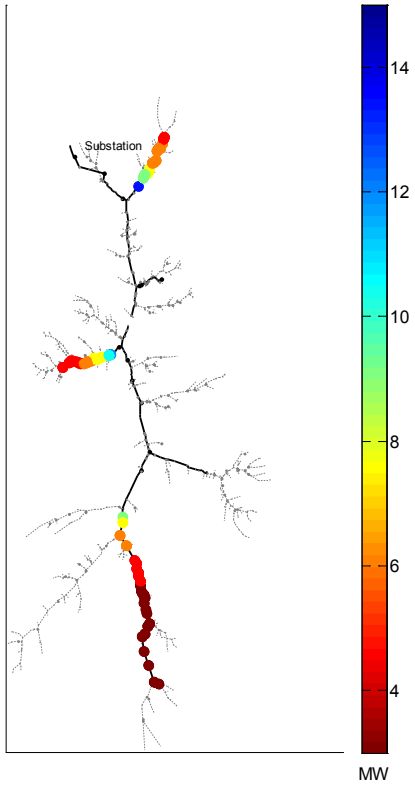

Figure 111.
Maximum wind power at a bus that does not exceed overvoltage limits

Only 66 buses exceeded the overvoltage limits when 15,000 kW or less of wind power was connected. Wind power above 15,000 kW can be added to the 150 remaining three-phase buses located along the primary feeder without exceeding overvoltage limits, but the exact amount of wind power that can be tolerated by these wind turbine locations is not tested here. The next subsection shows that other circuit elements further limit the amount of wind power that can be connected.

3.5.3.2 Steady-State Analysis II—Line and Transformer Ratings

The ratings of equipment within the distribution system are considered in this section, particularly line and transformer ratings. For feeder R5-12.47-3, the ratings for the substation voltage regulator are not given and are approximated. The MVA rating is calculated based on the total real and reactive power through the transformer during full load and without wind power. Three cases in which the transformer is rated at 10%, 20%, and 30% above full load apparent power are examined.

First, the maximum amount of wind power that can be connected to the feeder without exceeding line ratings is examined. Previously, the ANSI overvoltage limits were exceeded for cases when the wind turbine output was 1,500 kW to 15,000 kW—depending on the location of the wind turbine within the circuit. The maximum amount of wind power that can be added to each

possible location without exceeding line ratings for each phase is shown in Figure 112 to Figure 114.

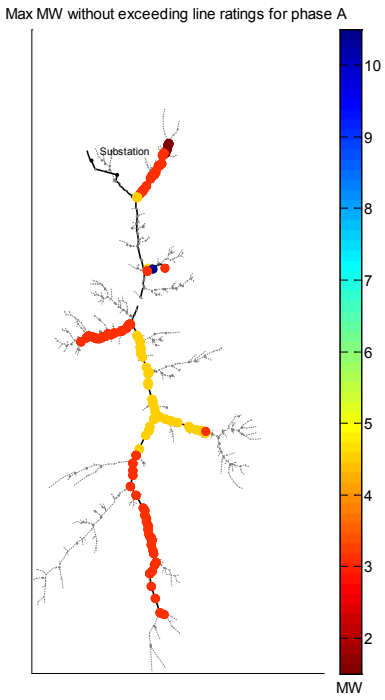

Figure 112.
Maximum wind power at a bus that does not exceed line ratings for Phase A

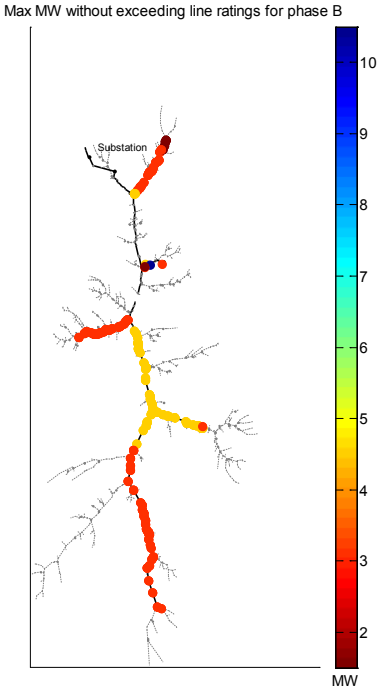

Figure 113.
Maximum wind power at a bus that does not exceed line ratings for Phase B

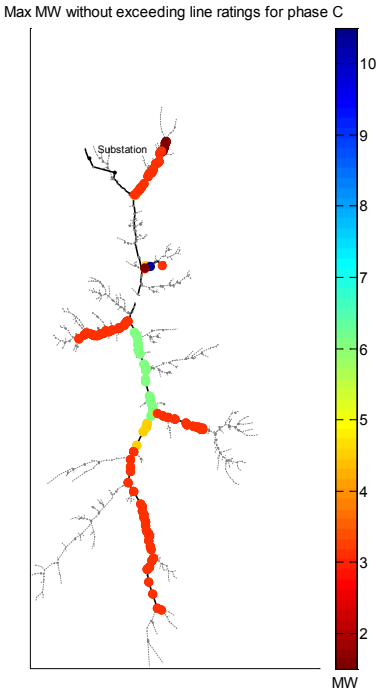

Figure 114.
Maximum wind power at a bus that does not exceed line ratings for Phase C

Some of the wind turbine locations along the primary feeder near the substation do not exceed any of the line ratings when up to 15,000 kW of wind power are added. Other wind turbines located off the primary feeder are only able to tolerate lower amounts of wind power without exceeding line ratings. The portions of the circuit that are able to tolerate the largest amount of wind power based on line ratings are along the main primary feeder; these are able to have 6,000 kW or 4,500 kW of wind power connected. Figure 114 shows the limits for Phase C, in which this portion of the circuit is indicated by light green. Figure 113 and Figure 112 show the limits for Phase A and Phase B, respectively, in which this portion of the circuit is indicated by yellow.

Next, the amounts of wind power that can be tolerated based on the regulator transformer ratings are tested. Feeder R5-12.47-3 is different from the previous circuits analyzed, because a total of four voltage regulators are connected to the circuit. The ratings of all four regulators are considered in this analysis. The locations of these regulators are shown in Figure 115.

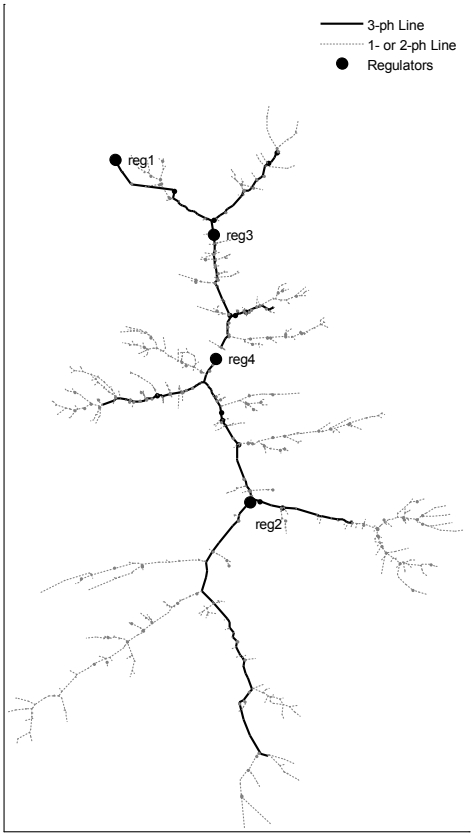

Figure 115.
Locations of voltage regulators in feeder R5-12.47-3

The total wind power output is set to 1,500 kW for each possible wind turbine location, and the apparent power through each regulator is extracted. The ratings (set to 30% above full load for the base case without wind power) are also included to indicate conditions when the ratings are exceeded. The wind power output for each wind turbine location is increased by 1,500 kW until the regulator transformer ratings are exceeded. Figure 116 to Figure 119 show Phase A power through all four regulators and the ratings of each regulator when the wind power is 3,000 kW. The discontinuity shown in Figure 117 is caused by wind turbine locations downstream and upstream from a regulator that is not at the substation but rather in the middle of the circuit.

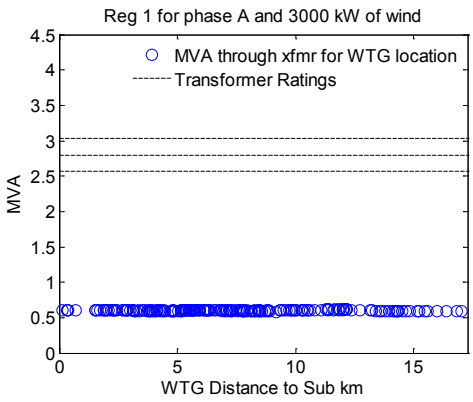

Figure 116.
Transformer 1 MVA ratings for Phase A

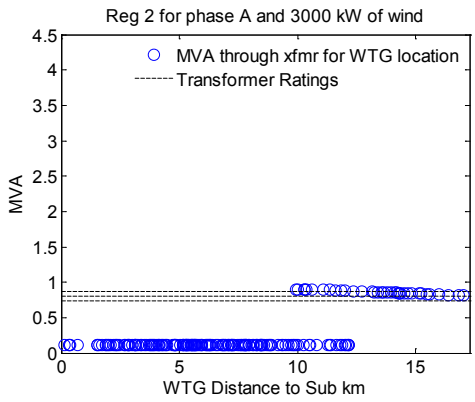

Figure 117.
Transformer 2 MVA ratings for Phase A

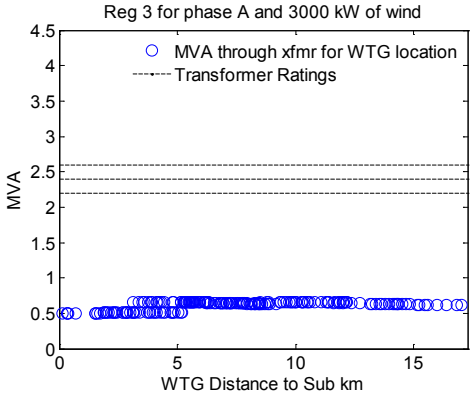

Figure 118.
Transformer 3 MVA ratings for Phase A

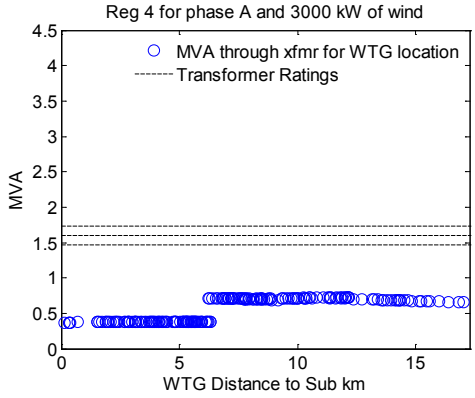

Figure 119.
Transformer 4 MVA ratings for Phase A

Figure 116, Figure 118, and Figure 119 show that the regulator transformer ratings are not exceeded for regulators 1, 3, and 4, respectively. Figure 117 shows that the ratings are exceeded for Regulator 2, but that not all wind turbine locations exceed the transformer ratings. When wind turbines are connected to a certain branch downstream from Regulator 2, the ratings are exceeded for Phase A, because the power flow to loads located downstream is relatively low (376.8 kW at 33% load for all three phases). The same analysis is repeated until the maximum amount of wind power that can be connected to each possible wind turbine bus without exceeding any of the transformer ratings for all three phases is found.

When results from the overvoltage analysis and equipment ratings are combined, the maximum amount of wind power that can be tolerated at each possible location is calculated. The results are shown in Figure 121 below. Buses that are located directly downstream from the substation do not exceed any of the limits tested for wind power output of up to 15,000 kW—these buses are able to tolerate the highest amount of wind power for feeder R5-12.47-3.

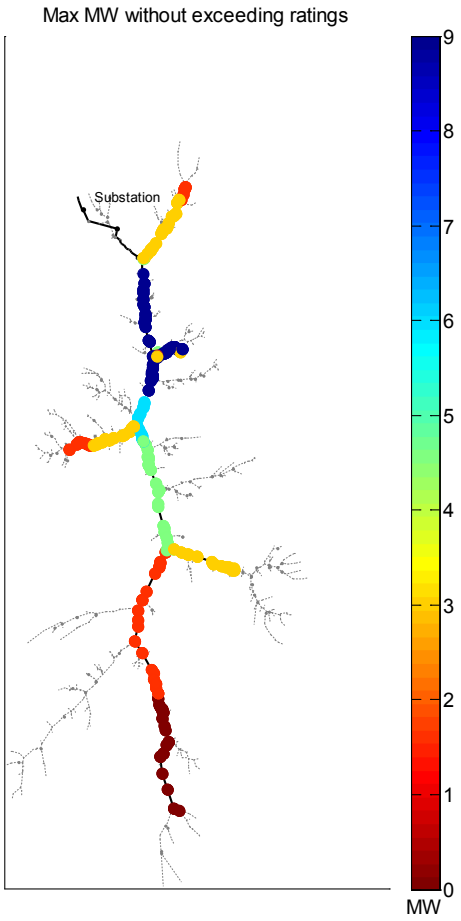

Figure 120.
Feeder R5-12.47-3. Maximum amount of wind power that can be tolerated at each bus without exceeding overvoltage limits, line ratings, and regulator transformer ratings

3.5.4 Conclusions for Feeder R5-12.47-3

Wind turbine locations and maximum wind power output for each of these locations were tested against consumer voltage tolerances and equipment ratings for feeder R5-12.47-3. The first step was to determine the maximum amount of wind power that each wind turbine location could tolerate without exceeding the ANSI overvoltage limits. When wind turbines are located farther from the substation, or when there is larger resistance between the wind turbine bus and the substation, the circuit could tolerate lower amounts of wind power than when wind turbines are located closer to the substation. Next, the feeder line ratings were used to determine the largest amount of wind power that the circuit could tolerate at different locations. The overhead and underground lines have different line ratings for different sections of the circuit. Different wind turbine locations and wind power outputs were tested. The results show that the line ratings further limit the amount of power that can be connected. The next equipment rating that was examined was the voltage-regulating transformer. Feeder R5-12.47-3 has four regulating transformers, which put stricter constraints on the amount of wind power that can be added without exceeding any transformer ratings. Wind turbines connected directly downstream from Regulator 2 tolerate the lowest amount of wind power because of the low transformer rating for

Regulator 2 (as calculated according to the load through the transformer during no-wind conditions). The relationship between the resistance from the wind turbine bus to the substation and the maximum voltage rise was also quantified and will be compared to the other taxonomy feeder resistance and voltage rise relationships to determine a generalized guideline for circuit-based wind turbine siting. The final concluding section provides general observations and guidelines for wind turbine placement and power output within a distribution circuit.

4 Overall Observations: Combining Results From All Feeders

This section combines the results from the four taxonomy feeders analyzed (R1-12.47-2, R1-12.47-1, R4-12.47-1, and R5-12.47-3) to provide a generalized relationship between the placement of wind turbines in a distribution feeder and the corresponding amount of wind power that can be tolerated without exceeding overvoltage limits. Even though other factors were considered in determining the amount of power and the location of wind turbines in a distribution feeder (feeder line and transformer ratings), these limits tend to be specific to each feeder and are more difficult to generalize; therefore, the results for the analysis on overvoltage alone are provided and analyzed further.

4.1 Overvoltage Limits

The data analyzed here is taken from the analysis of the maximum wind power that can be connected to each possible wind turbine bus without exceeding ANSI Range A overvoltage limits. The voltage limit that was used in this analysis was set to 1.04 per unit, and the power factor for the wind turbines was set to unity. When any bus voltage within the circuit exceeds this limit for the amount of wind power being analyzed, that amount of wind power is marked as exceeding the limits for that particular wind turbine location.

The results from all four taxonomy feeders are shown in Figure 122. The x-axis is the location of the wind turbine measured as the phase resistance from the feeder substation to the bus to which the wind turbine is connected. The y-axis is the maximum wind power that does not cause any bus voltages within the feeder to exceed overvoltage limits. For all of these circuits, the load was set to 33% of full load.

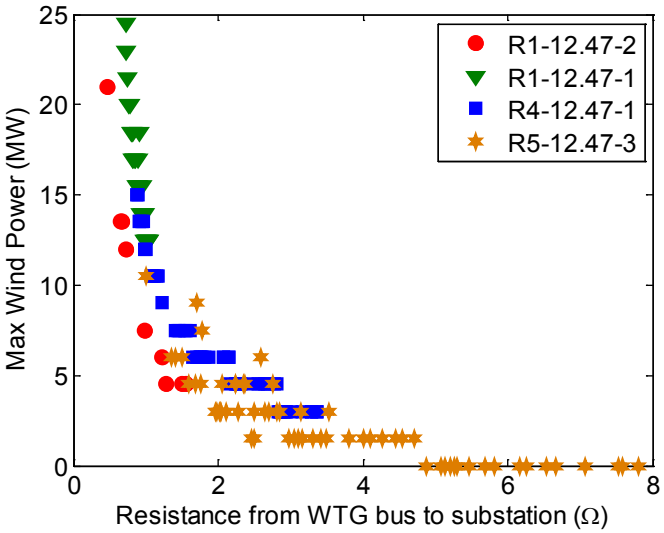

Figure 121.
Summary of the relationship between resistance and max wind power when only overvoltage is considered

The final results show that after approximately 4.8 Ω between the wind turbine bus and the substation, the connection of a 1.5-MW turbine could cause overvoltage conditions during low-load conditions. Buses that have a "distance" of less than 0.5 Ω from the substation could tolerate more than approximately 24.5 MW of wind power. (Again, note that transformer limits, line limits, and other factors are not considered here. At locations near the substation, it is likely that transformer ratings will be the limiting factor for wind power, at least when only steady-state voltage and current constraints are considered. This is explained in greater detail in Subsection 4.2.)

When all the data from the taxonomy feeders are combined, as shown in Figure 122, the relationship between the resistance and the maximum wind power has an exponential shape. The next step is to fit an exponential curve to the data using a curve-fitting MATLAB toolbox [46]. The data from all the feeders analyzed and the curve that best fits the data is shown in Figure 123.

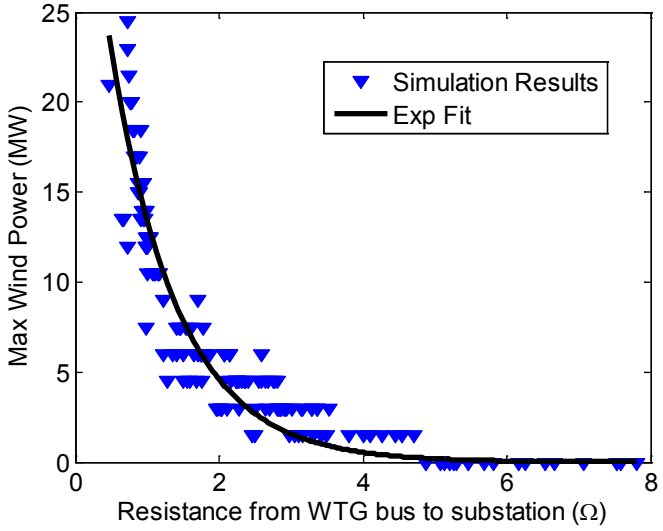

Figure 122.
Exponential curve fit to the relationship between resistance and max wind power when only overvoltage is considered

The equation for the fitted curve is given below. In the equation, P_{wind} is the maximum wind power that can be added without exceeding overvoltage limits, and Ω is the resistance between the bus to which the wind turbine is connected and the feeder substation.

$$P_{wind} = 39.6\, e^{-1.08\Omega}$$

The exponential curve from the equation above has been extrapolated for a wider range of resistance values and is shown in Figure 124. The minimum number of wind turbines with a rated power output of 1.5 MW is also marked in the figure below. The intersection of these two curves indicates the maximum resistance between the WTG bus and the feeder substation that can be tolerated without exceeding overvoltage limits as identified in the analysis from previous sections. Figure 124 shows that for one 1.5-MW turbine, a single wind turbine can be connected

up to 3.03 Ω away from the feeder substation, and that during the worst-case scenario with low-load conditions, the bus voltages will not exceed ANSI overvoltage limits.

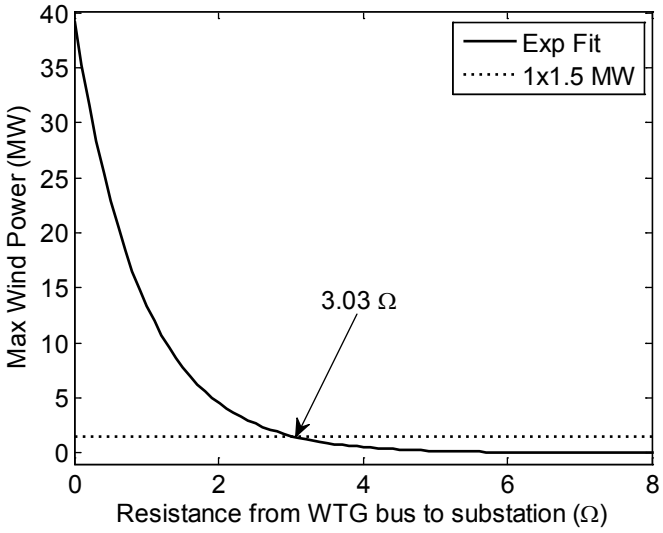

Figure 123.
Intersection of different megawatt wind power output levels and the exponential equation describing the relationship between the resistance between the WTG and the substation and the maximum wind power that can be interconnected to the feeder when only overvoltage limits are considered

The same process is repeated to identify the maximum resistance from the feeder substation at which wind turbines can be connected without exceeding overvoltage limits identified in the analysis in previous sections. The different wind turbine power outputs for an integer number of wind turbines alongside the exponential curve is shown in Figure 125. Up to six 1.5-MW turbines are considered in the figure. As wind turbines are located closer to the feeder substation, the feeder is able to tolerate higher amounts of wind power without exceeding the overvoltage limits. The maximum resistance for each of these wind power output levels is identified in Table 15.

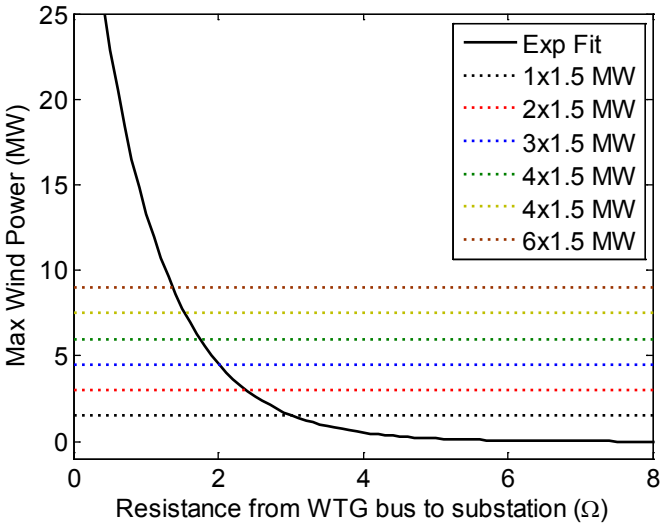

Figure 124.
Intersection of different megawatt wind power output levels and the exponential equation describing the relationship between the resistance between the WTG and the substation and the maximum wind power that can be interconnected to the feeder when only overvoltage limits are considered

Table 15. Maximum Resistance Between the WTG and the Substation That a Radial Distribution Feeder Can Tolerate Without Exceeding Overvoltage Limits for Each Megawatt Wind Power Output Level

Wind Power (MW)	No. of 1.5-MW Turbines	Maximum Resistance (Ω)
1.5	1	3.03
3.0	2	2.39
4.5	3	2.01
6.0	4	1.73
7.5	5	1.55
9.0	6	1.39

The results in Table 15 indicate that larger amounts of wind power or a larger number of wind turbines can be connected closer to the substation or with conductors that are larger and have a lower resistance. Also, the amount of wind power that can be connected increases exponentially with inverse impedance. The table also shows that if a 1.5-MW wind turbine is connected more than 3.03 Ω from the substation, full wind power output and low-load conditions could cause the voltage to rise above ANSI overvoltage limits. These guidelines can be used to determine the best placement of a wind turbine within a distribution feeder as well as the size and number of wind turbines that can be added to a feeder without exceeding ANSI overvoltage limits.

4.2 Line and Transformer Ratings

The maximum amount of wind power that can be added to a feeder bus without exceeding the feeder's line ratings for all four studied feeders is provided in this section. The results for Phase

C of these four feeders are shown in Figure 126. The figure shows the resistance from the WTG bus to the substation and the maximum amount of wind power that can be placed at that bus without exceeding the line ratings for the feeder. There is no clear relationship between the placement of wind turbines when considering line ratings alone. This can be expected, because the ratings of the feeder lines are not proportional to the distance of the line from the substation and are decided based on loading on that feeder.

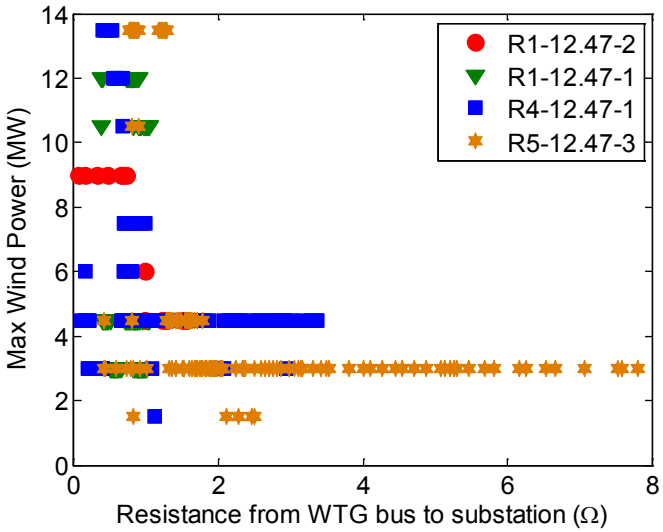

Figure 125.
Relationship between the resistance from the WTG bus to the feeder substation and the maximum wind power that can be placed at that bus; no generalization possible

From the feeders analyzed, a generalized rule cannot be extracted with respect to transformer ratings either. Each transformer rating will depend on the load and does not depend on the circuit parameters, such as resistance. The rating will also depend on how the utility decides to size the transformer for future load growth. Additionally, some feeders contain multiple transformers, which makes finding general rules for relating transformer ratings to circuit parameters even more challenging. Ultimately, transformer and line ratings arise from utility decisions based on optimality and not from any innate characteristics of the circuit [47].

5 Conclusions

This report studied the power system impact that megawatt-scale (1.5-MW Type 3 and Type 4) wind turbines have when connected to rural distribution feeders, with emphasis on the voltage impacts. Megawatt-scale wind turbines connected to the distribution circuit are generally located away from heavily-populated areas; therefore, the impact that megawatt-scale wind turbines will have on rural distribution feeders in particular has been studied.

Rural distribution feeders differ from those in more-heavily-populated and -loaded urban and suburban areas. Rural distribution feeders tend to be radial, have longer feeder lengths, and are relatively lightly loaded. In this report, we have examined a few select distribution feeders to establish the limits on inclusion of wind generation. The limiting factors observed in this study can be used to establish general guidelines for the inclusion of wind turbines in other rural distribution circuits, particularly regarding the placement and ratings of wind turbines that can be connected to a distribution circuit. The rural distribution feeders studied come from the 24 Pacific Northwest National Laboratory distribution taxonomy feeders available in GridLAB-D. The analysis is applied to taxonomy feeders R1-12.47-2, R1-12.47-1, R4-12.47-1, and R5-12.47-3, all of which contain rural areas.

To perform this analysis, first, a single power flow solution at the selected load level was calculated, and the voltages from all buses in the circuit were extracted. An initial base case was run before a wind turbine was placed on the distribution circuit. For this initial power flow solution, the circuit characteristic data were extracted, and the bus voltages were saved. The circuit characteristics did not change between each case, except when a wind turbine or wind turbines were added.

The next step was to place a wind turbine at each of the selected wind turbine locations and to find the power flow solutions for each location. After a wind turbine was placed at a three-phase bus within the circuit, the power flow solution was found, and the bus voltage, power, and current were saved. This analysis was done for every possible wind turbine location within the feeder. The bus voltages for the base case without any wind turbines could then be compared to the bus voltages for cases with different wind turbine locations. The amount of wind power that could be added without exceeding ANSI Range A overvoltage limits was found and saved. The amount of wind power that could be added without exceeding line ratings and regulator transformer ratings was also found. Based on the overvoltage and equipment ratings analysis, the overall wind power and location of the wind turbines in the circuit was given.

A generalized rule was created for relating the maximum allowable wind power generation at any three-phase bus on the feeder to the resistance to the substation from that bus. The rule has been developed considering only the voltage rise criterion, not equipment ratings, though it was found that in some cases the equipment ratings will be the limiting factors rather than the voltage rise. However, because the equipment ratings are based solely on utility preferences, a generalized rule that includes these ratings could not be created and a case-by-case examination will have to be performed for a feeder in which wind is considered for inclusion.

The relationship between voltage rise and the resistance between the wind turbine bus and the substation was quantified for all feeders analyzed as well. The results show that there is a nearly

perfect linear relationship between the resistance from the substation to the wind turbine bus and the voltage rise, at least when WTGs are operated at unity power factor. If we were to use distance rather than resistance, the linear relationship would be less obvious because branches of the same feeder employ different conductor types with different resistances. Branching would lead to multiple voltage rise values for the same feeder distance, obfuscating the linear relationship.

Many other factors were not considered in this report that can be considered in future work. The coordination of overcurrent protection (from reclosers, fuses, breakers, and sectionalizers) can be included when determining the best placement for wind turbines and the amount of wind power that can be easily accommodated in these locations. Other power quality issues were not considered—specifically flicker, which is often a concern when connecting wind turbines to the distribution system; however, the wind turbines considered in the report are inverter-connected and thus not likely to cause flicker if operated properly. Harmonics were also not considered. Although harmonics could be introduced into the circuit by wind turbine inverters, modern pulse-width modulation inverters produce lower harmonic energy content and higher harmonic numbers than have traditionally been a concern in distribution circuits (i.e., very little 3rd and 5th harmonic).

A number of options are available to mitigate voltage rise caused by distributed-connected wind turbines. Techniques proposed to reduce voltage rise were described in the literature review and can be found in references [30-35]. These references approach the voltage rise problem by modifying controls for tap-changing transformers, or by controlling the DG source directly. Another mitigation technique would be to include only Type 3 or Type 4 wind turbines, for which the power factor can be controlled. During conditions that would cause excessive voltage rise, the power factor can be adjusted so that it is lagging. The reactive power consumed by the wind turbine would then cause a voltage drop, which would negate the voltage rise.

References

1. Brancucci Martinez-Anido, C.H.; Hodge, B.-M. *Impact of Utility-Scale Distributed Wind on Transmission-Level System Operations.* Golden, CO: National Renewable Energy Laboratory, forthcoming.

2. Smith, J.W.; Dugan, R.; Rylander, M.; Key, T. "Advanced Distribution Planning Tools for High Penetration PV Deployment." *IEEE Power and Energy Society General Meeting Proceedings*; 2012; pp. 1–7.

3. Mather, B. "Analysis of High-Penetration Levels of PV Into the Distribution Grid in California." *High Penetration Solar Forum*; 2011.

4. Katiraei, K.; Aguero, J.R. "Solar PV Integration Challenges." *IEEE Power and Energy Magazine* (9), 2011; pp. 62–71.

5. Smith, J.W.; Dugan, R.; Sunderman, W. "Distribution Modeling and Analysis of High Penetration PV." *IEEE Power and Energy Society General Meeting Proceedings*; 2011; pp. 1–7.

6. Kauhaniemi, K.; Kumpulainen, L. "Impact of Distributed Generation on the Protection of Distribution Networks." *Eighth IEE International Conference on Developments in Power System Protection Proceedings.* Vol. I; 2004; pp. 315–318.

7. Hoke, A.; Butler, R.; Hambrick, J.; Kroposki, B. "Steady-State Analysis of Maximum Photovoltaic Penetration Levels on Typical Distribution Feeders." *IEEE Transactions on Sustainable Energy* (4), 2013; pp. 350–357.

8. "Dynamic Maps, GIS Data, and Analysis Tools—Wind Maps." National Renewable Energy Laboratory, 2014. Accessed August 14, 2014: http://www.nrel.gov/gis/wind.html.

9. Barker, P.P.; de Mello, R.W. "Determining the Impact of Distributed Generation on Power Systems. I. Radial Distribution Systems." *IEEE Power Engineering Society Summer Meeting Proceedings*; 2000; pp. 1,645–1,656.

10. McDermott, T.E.; Dugan, R.C. "Distributed Generation Impact on Reliability and Power Quality Indices." *IEEE Rural Electric Power Conference Proceedings*; 2002; pp. D3–D3_7.

11. Ochoa, L.F.; Padilha-Feltrin, A.; Harrison, G.P. "Evaluating Distributed Generation Impacts with a Multiobjective Index." *IEEE Transactions on Power Delivery* (21), 2006; pp. 1,452–1458.

12. McDermott, T.E.; Manwell, J.F.; McGowan, J.G. "A Checklist Approach to DR Interconnection and Impact Studies." *IEEE Power and Energy Society General Meeting Proceedings*; 2009; pp. 1–4.

13. Bollen, M.H.; Hassan, F. *Integration of Distributed Generation in the Power System.* Vol. 80. New York: John Wiley & Sons, 2011.

14. Zhang, J.; Fan, H.; Tang, W.; Wang, M.; Cheng, H.; Yao, L. "Planning for Distributed Wind Generation Under Active Management Mode." *International Journal of Electrical Power & Energy Systems* (47), 2013; pp. 140–146.

15. Brown, R.E.; Pan, J.; Feng, X.; Koutlev, K. "Siting Distributed Generation to Defer T&D Expansion." *IEEE Transmission and Distribution Conference and Exposition Proceedings*; 2001; pp. 622–627.

16. Hemdan, N.G.; Kurrat, M. "Effect of Integration of Distributed Wind Generation into a Real MV Distribution Network: A Case Study Using Measured Wind Data and Simulated Load Profiles." *IEEE Power and Energy Society General Meeting Proceedings*; 2010; pp. 1–8.

17. Su, S.-Y.; Lu, C.-N.; Chang, R.-F.; Gutierrez-Alcaraz, G. "Distributed Generation Interconnection Planning: A Wind Power Case Study." *IEEE Transactions on Smart Grid* (2), 2011; pp. 181–189.

18. Cleary, J.G.; McDermott, T.E.; Fitch, J.; Colombo, D.J.; Ndubah, J. "Case Studies: Interconnection of Wind Turbines on Distribution Circuits." *IEEE Conference on Innovative Technologies for an Efficient and Reliable Electricity Supply (CITRES) Proceedings*; 2010; pp. 396–400.

19. Miranda, V. "Wind Power, Distributed Generation: New Challenges, New Ssolutions." *Turkish Journal of Electrical Engineering & Computer Sciences* (14), 2007; pp. 455–473.

20. Zong, Y.; Kullmann, D.; Thavlov, A.; Gehrke, O.; Bindner, H. "Model Predictive Control Strategy for a Load Management Research Facility in the Distributed Power System with High Wind Penetration—Towards a Danish Power System with 50% Wind Penetration." *Asia-Pacific Power and Energy Engineering Conference (APPEEC) Proceedings*; 2011; pp. 1–4.

21. Ochoa, L.F.; Padilha-Feltrin, A.; Harrison, G.P. "Time-Series-Based Maximization of Distributed Wind Power Generation Integration." *IEEE Transactions on Energy Conversion* (23), 2008; pp. 968–974.

22. Schneider, K.P.; Chen, Y.; Chassin, D.P.; Pratt, R.G.; Engel, D.W.; Thompson, S. *Modern Grid Initiative: Distribution Taxonomy Final Report.* Richland, WA: Pacific Northwest National Laboratory, 2008.

23. Mu, W.; Zhe, C. "A Study of Protective Operation Strategy for a Distributed Generation System with Wind Turbines." *International Conference on Advanced Power System Automation and Protection (APAP) Proceedings*; 2011; pp. 812–817.

24. Maki, K.; Repo, S.; Jarventausta, P. "Effect of Wind Power Based Distributed Generation on Protection of Distribution Network." *Eighth IEE International Conference on Developments in Power System Protection Proceedings*. Vol. I; 2004; pp. 327–330.

25. Milanovic, J.; Ali, H.; Aung, M. "Influence of Distributed Wind Generation and Load Composition on Voltage Sags." *IET Generation, Transmission & Distribution* (1), 2007; pp. 13–22.

26. Yang, Y.; Bollen, M. *Power Quality and Reliability in Distribution Networks with Increased Levels of Distributed Generation.* Stockholm, Sweden: Elforsk, 2008.

27. Fakham, H.; Ahmidi, A.; Colas, F.; Guillaud, X. "Multi-Agent System for Distributed Voltage Regulation of Wind Generators Connected to Distribution Network." *IEEE PES Innovative Smart Grid Technologies Conference Europe (ISGT Europe)*; 2010; pp. 1–6.

28. Gnativ, R.; Milanovi, J. "Voltage Sag Propagation in Systems with Embedded Generation and Induction Motors." *IEEE Power Engineering Society Summer Meeting Proceedings*; 2001; pp. 474–479.

29. Gnativ, R.; Milanović, J. "Qualitative and Quantitative Analysis of Voltage Sags in Networks with Significant Penetration of Embedded Generation." *European Transactions on Electrical Power* (15), 2005; pp. 77–93.

30. Milanovic, J.; Gnativ, R.; Chow, K. "The Influence of Loading Conditions and Network Topology on Voltage Sags." *Ninth International Conference on Harmonics and Quality of Power Proceedings*; 2000; pp. 757–762.

31. Nourbakhsh, G.; Thomas, B.; Mokhtari, G.; Ghosh, A.; Ledwich, G. "Distribution Tap Changer Adjustment to Improve Small-Scale Embedded Generator Penetration and Mitigate Voltage Rise." *Australasian Universities Power Engineering Conference (AUPEC) Proceedings*; 2013; pp. 1–5.

32. Carvalho, P.M.S.; Correia, P.F.; Ferreira, L.A. "Distributed Reactive Power Generation Control for Voltage Rise Mitigation in Distribution Networks." *IEEE Transactions on Power Systems* (23), 2008; pp. 766–772.

33. Mekhilef, S.; Chard, T.R.; Ramachandramurthy, V.K. "Voltage Rise Due to Inter-Connection of Embedded Generators to Distribution Network on Weak Feeder." *IEEE Symposium on Industrial Electronics and Applications (ISIEA) Proceedings*; 2009; pp. 1,028–1,033.

34. Repo, S.; Laaksonen, H.; Jarventausta, P.; Huhtala, O.; Mickelsson, M. "A Case Study of a Voltage Rise Problem Due to a Large Amount of Distributed Generation on a Weak Distribution Network." *IEEE Power Tech Conference Proceedings*. Vol. 4; 2003; Bologna; 6 pp.

35. Caples, D.; Boljevic, S.; Conlon, M.F. "Impact of Distributed Generation on Voltage Profile in 38kV Distribution System." *Eighth International Conference on the European Energy Market (EEM) Proceedings*; 2011; pp. 532–536.

36. Smith, J.W.; Brooks, D.L. "Voltage Impacts of Distributed Wind Generation on Rural Distribution Feeders." *IEEE Power Engineering Society Transmission and Distribution Conference and Exposition Proceedings.* Vol. 1; 2001; pp. 492–497.

37. Dugan, R.C.; McDermott, T.E. "An Open Source Platform for Collaborating on Smart Grid Research." *IEEE Power and Energy Society General Meeting*; 2011; pp. 1–7.

38. MathWorks. *MATLAB: The Language of Technical Computing—Desktop Tools and Development Environment.* Version 7. Vol. 9. MathWorks, 2005.

39. Dugan, R. "OpenDSS Training: Level 2." Palo Alto, CA: Electric Power Research Institute, 2009.

40. Chassin, D.P.; Schneider, K.; Gerkensmeyer, C. "GridLAB-D: An Open-Source Power Systems Modeling and Simulation Environment." *IEEE Power Engineering Society Transmission and Distribution Conference and Exposition Proceedings*; 2008; pp. 1–5.

41. Cohen, M.A. "GridLAB-D Taxonomy Feeder Graphs." 2014.

42. W. W. G. M. Group. *WECC Wind Power Plant Power Flow Modeling Guide.* Salt Lake City, UT: Western Electricity Coordinating Council, 2008.

43. American National Standards Institute. *ANSI C84. 1-2011: American National Standard for Electric Power System and Equipment–Voltage Ratings (60 Hertz).* Rosslyn, VA: National Electrical Manufacturers Association, 2011. Accessed August 15, 2014: https://www.nema.org/Standards/ComplimentaryDocuments/Contents-and-Scope-ANSI-C84-1-2011.pdf.

44. Clarke, C.R. "Distribution System Modeling." Vol. 2014. SunShot Initiative High Penetration Solar Portal, 2012.

45. Schneider, K.P.; Chen, Y.; Chassin, D.P.; Pratt, R.; Engel, D.; Thompson, S. *Modern Grid Initiative Taxonomy Feeder Report.* Work performed by Pacific Northwest National Laboratory, Richland, WA. Washington, DC: 2008. Accessed August 26, 2014: http://www.gridlabd.org/models/feeders/taxonomy_of_prototypical_feeders.pdf

46. Allen, A.; Zhang, Y.; Hodge, B.-M. "Impact of Increasing Distributed Wind Power and Wind Turbine Siting on Rural Distribution Feeder Voltage Profiles." *International Workshop on Large-Scale Integration of Wind Power into Power Systems as Well as on Transmission Networks for Offshore Wind Power Plants Proceedings*; 2013.

47. Moisy, F. "Ezyfit: A Free Curve Fitting Toolbox for Matlab." *U. Paris Sud. Version,* vol. 2, 2011.

48. Schneider, K.C.; Hoad, R.F. "Initial Transformer Sizing for Single-Phase Residential Load." *IEEE Transactions on Power Delivery* (7), 1992; pp. 2,074–2,081.

Appendix A

All of the figures in Appendix A are of taxonomy feeder R1-12.47-2. These figures show the results for Phase B and Phase C. Figure 127 uses a heat map to show the per-unit bus voltages in the feeder. The voltage profiles shown in Figure 130 and Figure 131 indicate that the voltage along the feeder changes when wind turbines are added to the feeder. The voltage profiles for two wind turbine locations are provided: one wind turbine location is near the feeder substation, and the second wind turbine location is farther from the feeder substation. The wind turbine power output is 3,000 kW. The change in voltage for each Phase B bus in the feeder is provided in Figure 132 and Figure 133. Figure 134 to Figure 140 show the results for Phase C. The highest change in voltage occurs when the wind turbine is located farther from the substation. The results for Phase A and the feeder voltage analysis are described in more detail in Section 3.2.3.1.

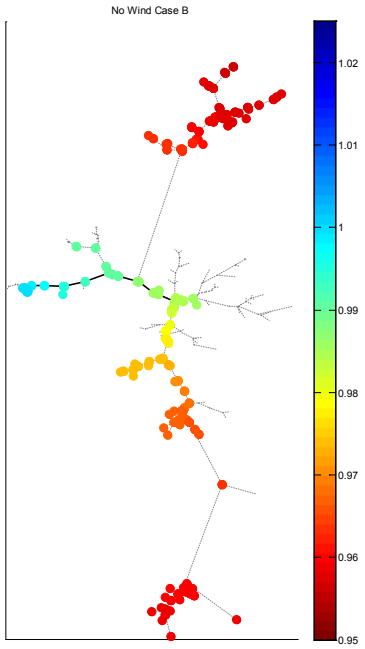

Figure 126.
Feeder R1-12.47-2. Heat map of Phase B per-unit bus voltages with 0 kW of wind power

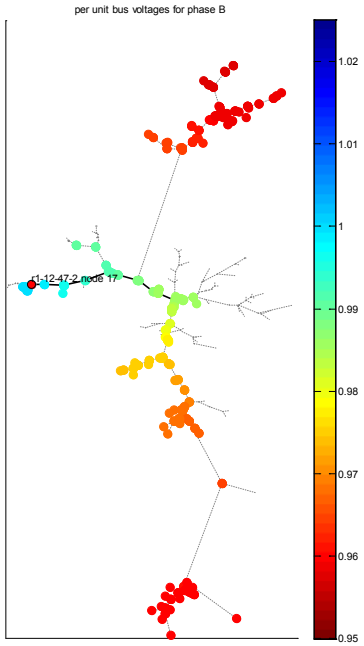

Figure 127.
Feeder R1-12.47-2. Heat map of Phase B per-unit bus voltages with 3,000 kW of wind power connected to Bus 17

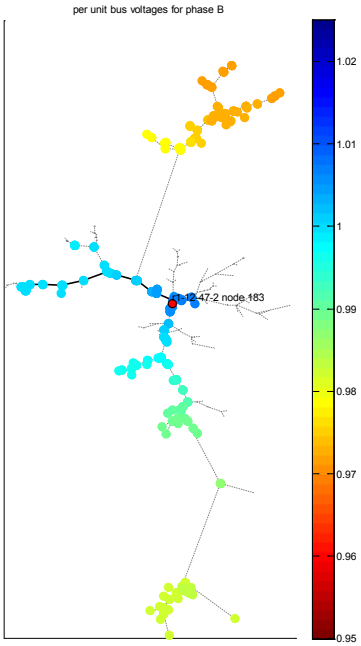

Figure 128.
Feeder R1-12.47-2. Heat map of Phase B per-unit bus voltages with 3,000 kW of wind power connected to Bus 183

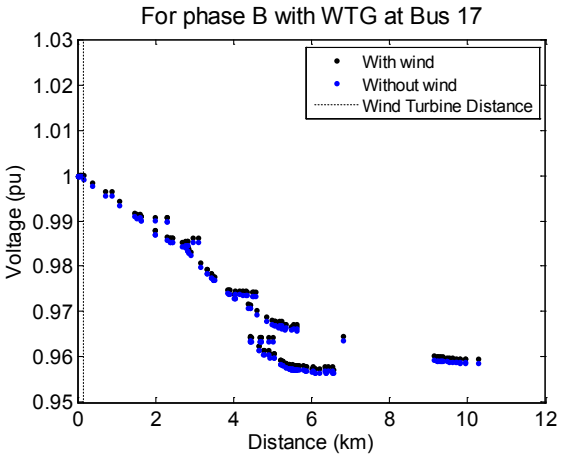

Figure 129.
Feeder R1-12.47-2. Phase B voltage profiles without wind and with 3,000 kW of wind power connected to Bus 17

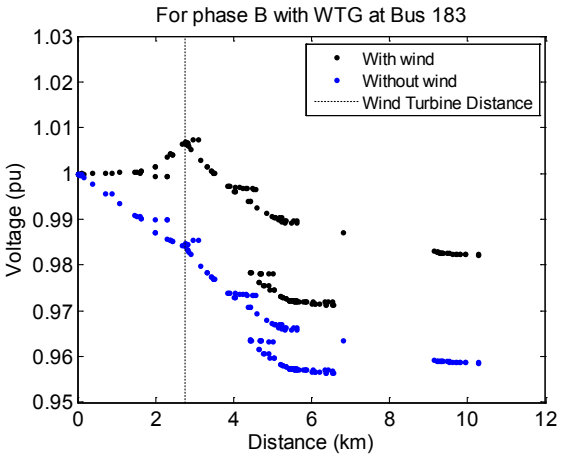

Figure 130.
Feeder R1-12.47-2. Phase B voltage profiles without wind and with 3,000 kW of wind power connected to Bus 183

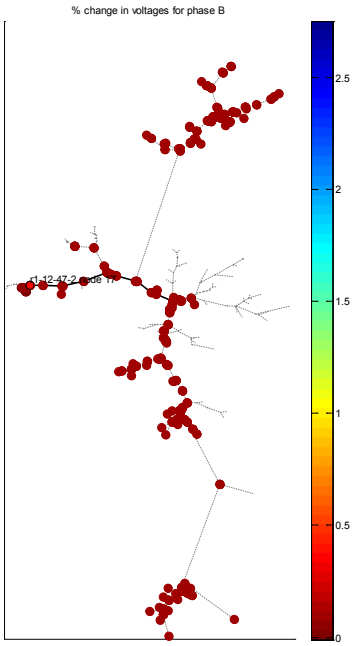

Figure 131.
Feeder R1-12.47-2. Heat map of Phase B change in bus voltage with 3,000 kW of wind power connected to Bus 17

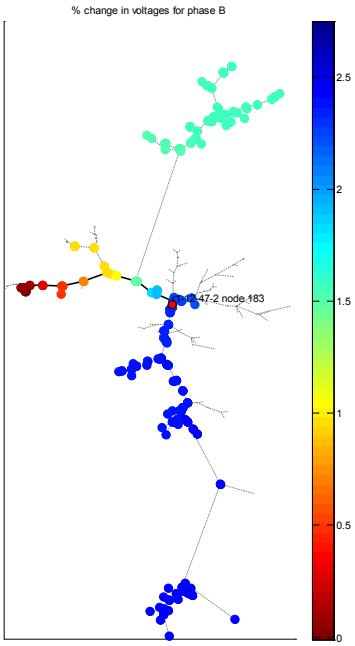

Figure 132.
Feeder R1-12.47-2. Heat map of Phase B change in bus voltage with 3,000 kW of wind power connected to Bus 183

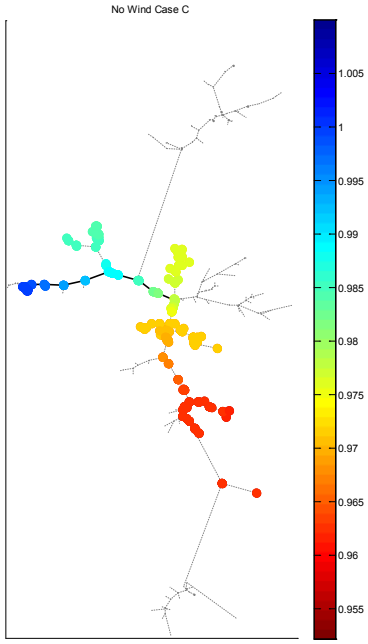

Figure 133.
Feeder R1-12.47-2. Heat map of Phase C per-unit bus voltages with 0 kW of wind power

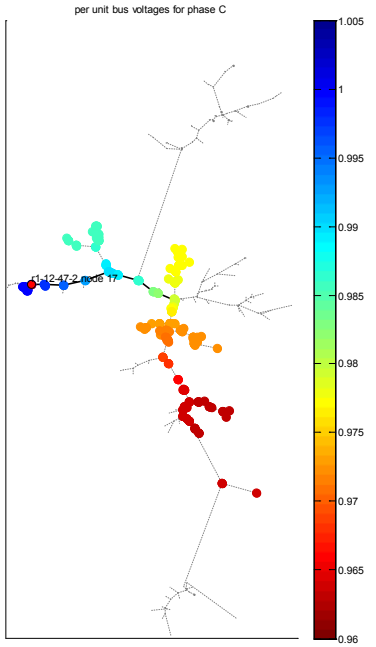

Figure 134.
Feeder R1-12.47-2. Heat map of Phase C per-unit bus voltages with 3,000 kW of wind power connected to Bus 17

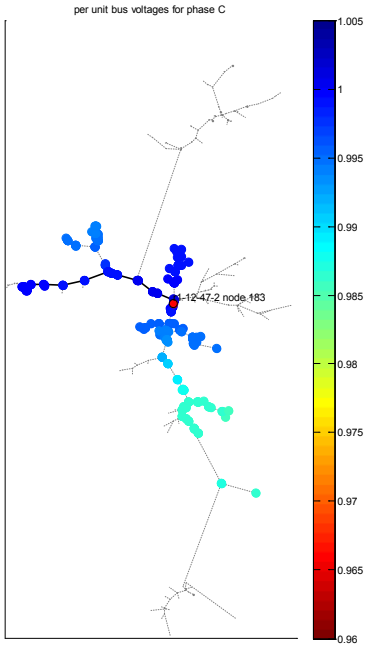

Figure 135.
Feeder R1-12.47-2. Heat map of Phase C per-unit bus voltages with 3,000 kW of wind power connected to Bus 183

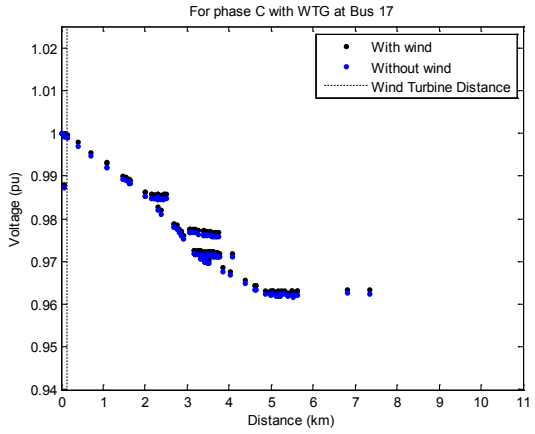

Figure 136.
Feeder R1-12.47-2. Phase C voltage profiles without wind and with 3,000 kW of wind power connected to Bus 17

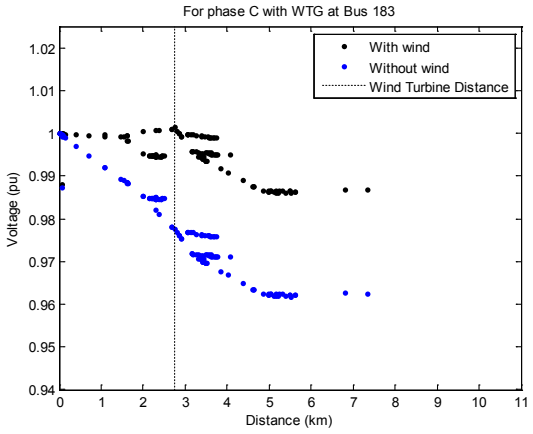

Figure 137.
Feeder R1-12.47-2. Phase C voltage profiles without wind and with 3,000 kW of wind power connected to Bus 17

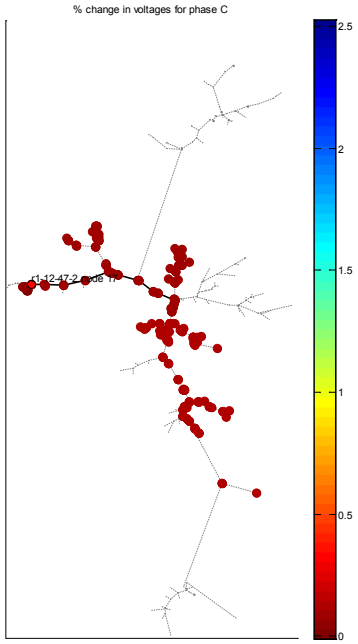

Figure 138.
Feeder R1-12.47-2. Heat map of Phase C change in bus voltage with 3,000 kW of wind power connected to Bus 17

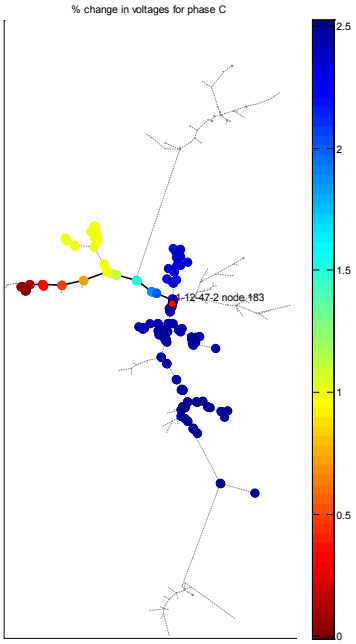

Figure 139.
Feeder R1-12.47-2. Heat map of Phase C change in bus voltage with 3,000 kW of wind power connected to Bus 183

The same analysis is applied to feeder R1-12.47-2, but the total load is uniformly reduced to 33% of full load. The results for Phase B and Phase C are shown in Figure 147 to Figure 154.

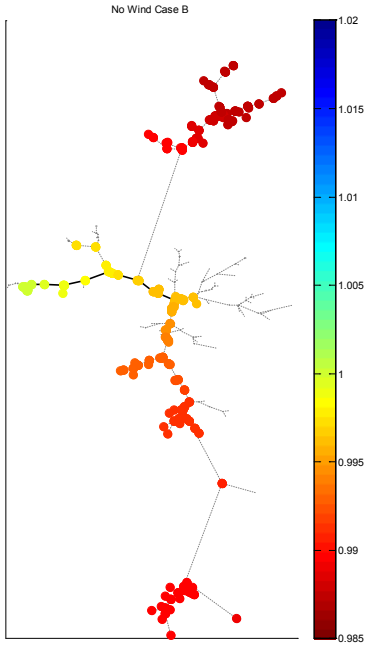

Figure 140.
Feeder R1-12.47-2. Heat map of Phase B per-unit bus voltages with 33% of full load and 0 kW of wind power

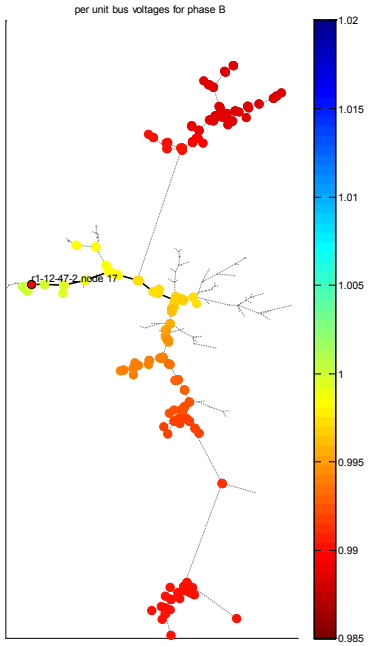

Figure 141.
Feeder R1-12.47-2. Heat map of Phase B per-unit bus voltages with 33% of full load and 3,000 kW of wind power connected to Bus 17

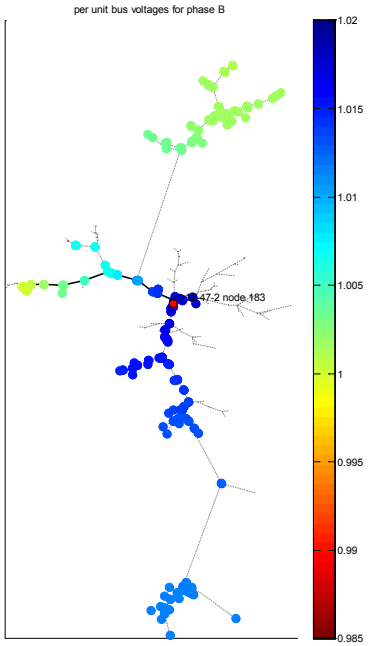

Figure 142.
Feeder R1-12.47-2. Heat map of Phase B per-unit bus voltages with 33% of full load 3,000 kW of wind power connected to Bus 183

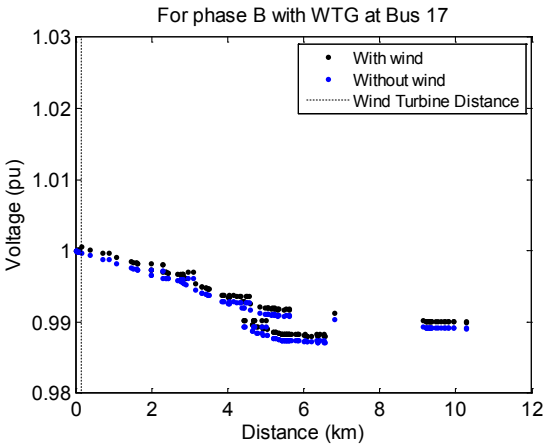

Figure 143.
Feeder R1-12.47-2. Phase B voltage profiles with 33% of full load without wind and 3,000 kW of wind power connected to Bus 17

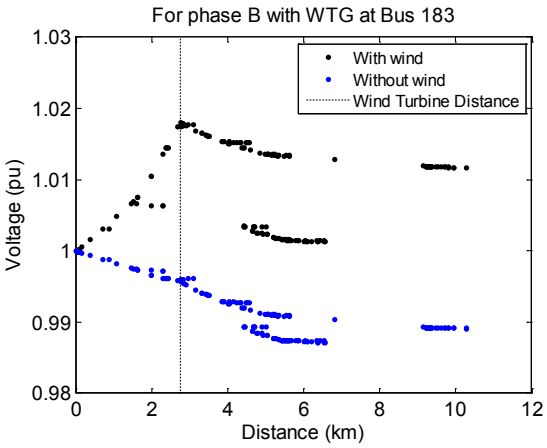

Figure 144.
Feeder R1-12.47-2. Phase B voltage profiles with 33% of full load without wind and 3,000 kW of wind power connected to Bus 183

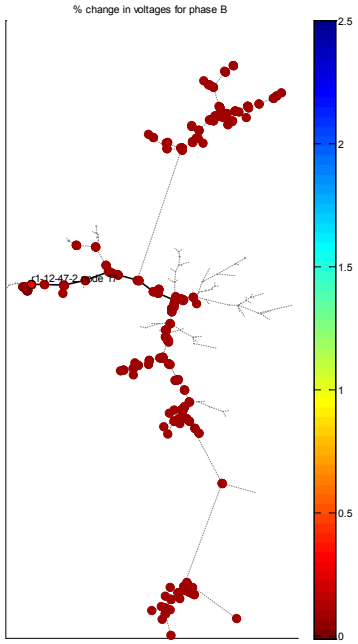

Figure 145.
Feeder R1-12.47-2. Heat map of Phase B change in bus voltage with 33% of full load and 3,000 kW of wind power connected to Bus 17

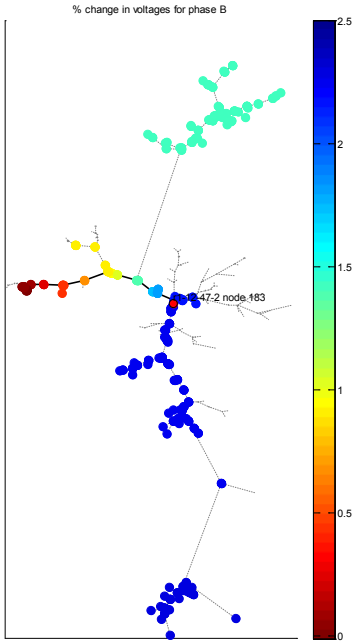

Figure 146.
Feeder R1-12.47-2. Heat map of Phase B change in bus voltage with 33% of full load and 3,000 kW of wind power connected to Bus 183

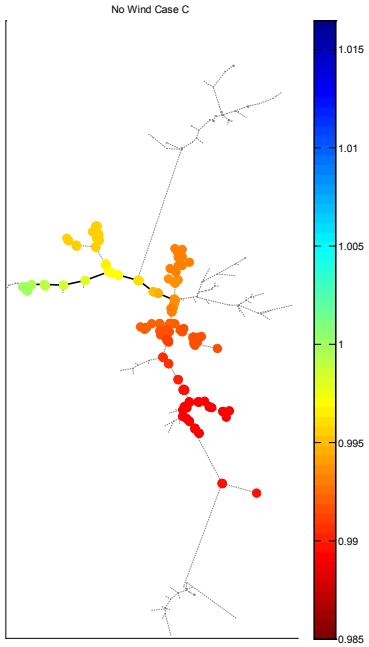

Figure 147.
Feeder R1-12.47-2. Heat map of Phase C per-unit bus voltages with 33% of full load and 0 kW of wind power

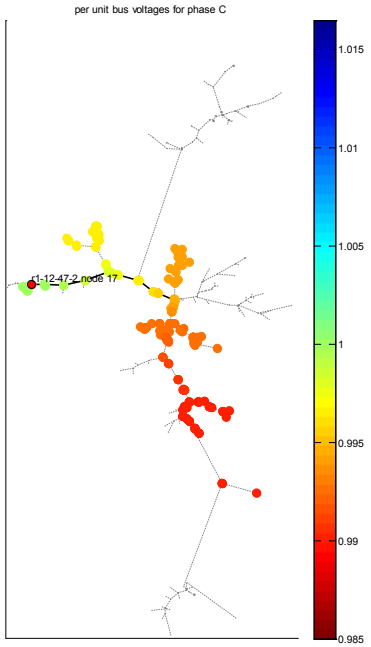

Figure 148.
Feeder R1-12.47-2. Heat map of Phase C per-unit bus voltages with 33% of full load and 3,000 kW of wind power connected to Bus 17

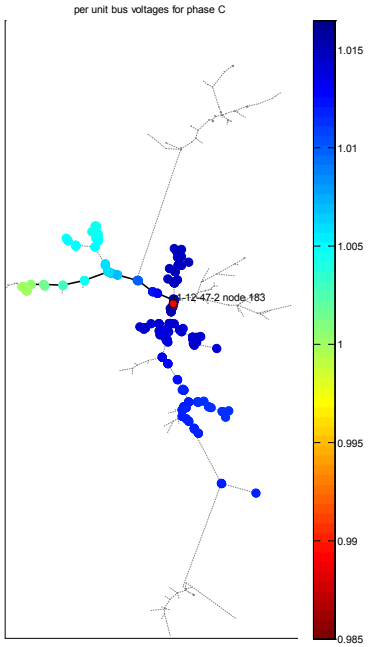

Figure 149.
Feeder R1-12.47-2. Heat map of Phase C per-unit bus voltages with 33% of full load and 3,000 kW of wind power connected to Bus 183

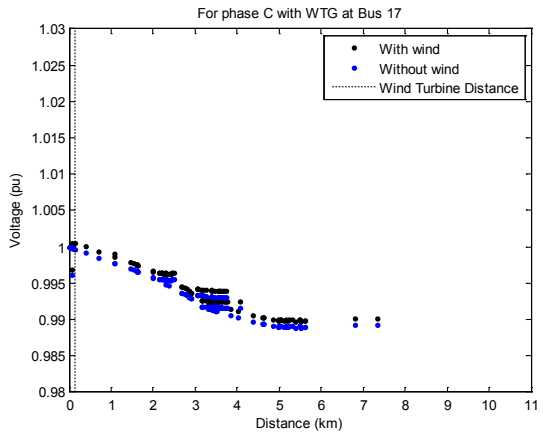

Figure 150.
Feeder R1-12.47-2. Phase C voltage profiles with 33% of full load without wind and with 3,000 kW of wind power connected to Bus 17

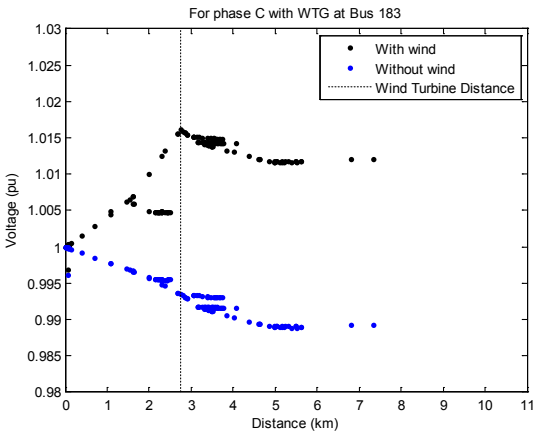

Figure 151.
Feeder R1-12.47-2. Phase C voltage profiles with 33% of full load without wind and with 3,000 kW of wind power connected to Bus 183

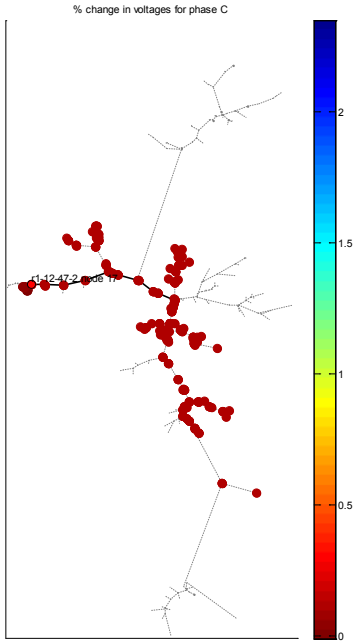

Figure 152.
Feeder R1-12.47-2. Heat map of Phase C change in bus voltage with 33% of full load and 3,000 kW of wind power connected to Bus 17

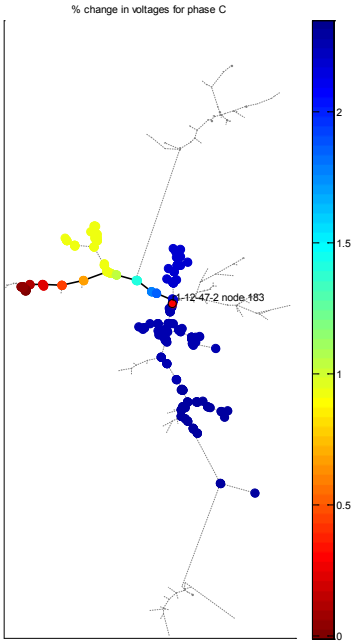

Figure 153.
Feeder R1-12.47-2. Heat map of Phase C change in bus voltage with 33% of full load and 3,000 kW of wind power connected to Bus 183

Appendix B

Table 16 shows the maximum wind power for each phase that can be added to the three-phase buses in feeder R4-12.47-1 without exceeding ANSI Range A overvoltage limits. The last column shows the maximum allowable wind power that can be added to the circuit. The analysis for this feeder is described in Section 3.4.

Table 16. Maximum Wind Power for Buses in Feeder R4-12.47-1

		Wind Power (kW)			
Bus Name	Bus Resistance	Phase A	Phase B	Phase C	Max Allowable (kW)
396	2.896	4,500	4,500	6,000	4,500
11	2.928	4,500	4,500	6,000	4,500
22	2.862	4,500	6,000	6,000	4,500
19	2.869	4,500	6,000	6,000	4,500
194	2.831	4,500	6,000	6,000	4,500
21	2.849	4,500	6,000	6,000	4,500
23	2.853	4,500	6,000	6,000	4,500
394	3.295	4,500	4,500	6,000	4,500
45	3.369	4,500	4,500	6,000	4,500
121	2.945	4,500	4,500	6,000	4,500
193	3.153	4,500	4,500	6,000	4,500
191	3.284	4,500	4,500	6,000	4,500
395	3.013	4,500	4,500	6,000	4,500
46	3.369	4,500	4,500	6,000	4,500
196	2.819	6,000	6,000	6,000	6,000
203	2.783	6,000	6,000	6,000	6,000
404	2.679	6,000	6,000	6,000	6,000
209	2.554	6,000	6,000	7,500	6,000
205	2.590	6,000	6,000	6,000	6,000
211	2.408	6,000	6,000	7,500	6,000
407	2.307	6,000	6,000	7,500	6,000
217	2.173	6,000	6,000	7,500	6,000
215	2.247	6,000	6,000	7,500	6,000
542	2.262	6,000	6,000	7,500	6,000
532	2.650	6,000	6,000	6,000	6,000
408	2.278	6,000	6,000	7,500	6,000
227	1.766	7,500	7,500	9,000	7,500
139	1.787	7,500	7,500	9,000	7,500
501	2.154	7,500	7,500	7,500	7,500
222	2.074	7,500	7,500	9,000	7,500
219	2.154	7,500	7,500	7,500	7,500
225	1.863	7,500	7,500	9,000	7,500
226	1.823	7,500	7,500	9,000	7,500
228	1.761	7,500	7,500	9,000	7,500
229	1.748	7,500	7,500	9,000	7,500
410	1.708	7,500	7,500	9,000	7,500
230	1.700	7,500	7,500	9,000	7,500
503	2.077	7,500	7,500	9,000	7,500
223	2.078	7,500	7,500	9,000	7,500
551	1.467	9,000	9,000	10,500	9,000
17	1.530	9,000	9,000	10,500	9,000

231	1.654	9,000	7,500	10,500	7,500
233	1.644	9,000	7,500	10,500	7,500
235	1.618	9,000	9,000	10,500	9,000
546	1.549	9,000	9,000	10,500	9,000
241	1.419	9,000	9,000	10,500	9,000
239	1.439	9,000	9,000	10,500	9,000
242	1.226	10,500	10,500	13,500	10,500
251	1.174	12,000	12,000	13,500	12,000
252	1.150	12,000	12,000	13,500	12,000
414	1.104	12,000	12,000	15,000	12,000
517	1.084	12,000	12,000	13,500	12,000
537	1.084	12,000	12,000	13,500	12,000
561	1.112	12,000	12,000	13,500	12,000
271	1.003	13,500	13,500	15,000	13,500
5	0.949	15,000	15,000	-	15,000
8	0.990	15,000	13,500	16,500	13,500
272	0.946	15,000	15,000	16,500	15,000
14	0.960	15,000	15,000	16,500	15,000
9	0.990	15,000	13,500	16,500	13,500
273	0.912	16,500	15,000	-	15,000
518	0.908	16,500	15,000	-	15,000
276	0.894	16,500	16,500	-	16,500
275	0.908	16,500	15,000	-	15,000
278	0.876	16,500	16,500	-	16,500

Table 17 shows the maximum wind power for each phase that can be added to the three-phase buses in feeder R4-12.47-1 without exceeding ANSI Range A overvoltage limits. The last column shows the maximum allowable wind power that can be added to the circuit. The analysis for this feeder is described in Section 3.5.

Table 17. Maximum Wind Power for Buses in Feeder R5-12.47-3

		Wind Power (kW)			
Bus Name	Bus Resistance	Phase A	Phase B	Phase C	Max Allowable (kW)
265	7.525	1,500	1,500	1,500	1,500
203	7.592	1,500	1,500	1,500	1,500
264	6.659	1,500	3,000	1,500	1,500
247	7.072	1,500	3,000	1,500	1,500
266	6.534	1,500	3,000	1,500	1,500
267	6.258	1,500	3,000	1,500	1,500
272	6.166	1,500	3,000	1,500	1,500
878	5.824	1,500	3,000	1,500	1,500
873	4.868	1,500	4,500	3,000	1,500
874	5.073	1,500	3,000	3,000	1,500
883	5.301	1,500	3,000	3,000	1,500
877	5.472	1,500	3,000	3,000	1,500
1,414	5.686	1,500	3,000	1,500	1,500
879	5.130	1,500	3,000	3,000	1,500
882	5.213	1,500	3,000	3,000	1,500
881	5.269	1,500	3,000	3,000	1,500
1,054	7.799	1,500	1,500	1,500	1,500
749	3.097	3,000	4,500	4,500	3,000

220	3.163	3,000	4,500	4,500	3,000
648	4.018	3,000	4,500	3,000	3,000
649	4.107	3,000	4,500	3,000	3,000
659	4.267	3,000	4,500	3,000	3,000
756	3.498	3,000	4,500	4,500	3,000
731	3.809	3,000	4,500	3,000	3,000
742	2.978	3,000	6,000	4,500	3,000
744	3.048	3,000	4,500	4,500	3,000
752	3.314	3,000	4,500	4,500	3,000
754	3.420	3,000	4,500	4,500	3,000
872	4.445	3,000	4,500	3,000	3,000
876	4.708	3,000	4,500	3,000	3,000
889	4.545	3,000	4,500	3,000	3,000
89	2.459	3,000	4,500	4,500	3,000
90	2.461	3,000	4,500	4,500	3,000
93	2.503	3,000	4,500	4,500	3,000
741	2.814	4,500	6,000	4,500	4,500
2	2.857	4,500	6,000	4,500	4,500
1,080	2.032	4,500	4,500	4,500	4,500
161	2.032	4,500	4,500	4,500	4,500
374	1.954	4,500	6,000	4,500	4,500
376	1.969	4,500	6,000	4,500	4,500
377	1.981	4,500	6,000	4,500	4,500
379	2.018	4,500	4,500	4,500	4,500
651	3.534	4,500	6,000	4,500	4,500
703	3.145	4,500	7,500	6,000	4,500
1,411	2.693	4,500	6,000	6,000	4,500
844	2.491	4,500	7,500	6,000	4,500
841	2.648	4,500	6,000	6,000	4,500
162	2.033	4,500	4,500	4,500	4,500
17	2.117	4,500	4,500	4,500	4,500
18	2.281	4,500	4,500	4,500	4,500
138	1.600	6,000	7,500	6,000	6,000
9	1.687	6,000	6,000	6,000	6,000
27	1.769	6,000	6,000	6,000	6,000
1,371	2.752	6,000	-	9,000	6,000
842	2.245	6,000	7,500	7,500	6,000
840	2.355	6,000	7,500	7,500	6,000
1,408	2.360	6,000	7,500	7,500	6,000
913	2.057	6,000	9,000	9,000	6,000
914	2.245	6,000	7,500	7,500	6,000
1,151	1.494	7,500	7,500	7,500	7,500
185	1.357	7,500	9,000	7,500	7,500
1,141	1.417	7,500	9,000	7,500	7,500
1,372	2.586	7,500	-	-	7,500
514	1.788	9,000	-	12,000	9,000
513	1.703	10,500	-	-	10,500
35	0.996	12,000	-	13,500	12,000